EXPRESSION PATTERN AND FUNCTIONS OF DIHYDROPYRIMIDINASE LIKE-3 IN THE RODENT MICROGLIA

JANANI MANIVANNAN

NATIONAL UNIVERSITY OF SINGAPORE

2013

EXPRESSION PATTERN AND FUNCTIONS OF DIHYDROPYRIMIDINASE LIKE-3 IN THE RODENT MICROGLIA

JANANI MANIVANNAN, *M.Sc.*

A THESIS SUBMITTED FOR THE DEGREE OF DOCTOR OF PHILOSOPHY

DEPARTMENT OF ANATOMY

YONG LOO LIN SCHOOL OF MEDICINE

NATIONAL UNIVERSITY OF SINGAPORE

2013

DECLARATION

I hereby declare that the thesis is my original work and it has been written by me in its entirety. I have duly acknowledged all the sources of information which have been used in the thesis.

This thesis has also not been submitted for any degree in any university previously.

_____

Janani Manivannan

ACKNOWLEDGEMENTS

First, I would like to express my deepest appreciation to my supervisor **Associate Professor S.Thameem Dheen**, Department of Anatomy, National University of Singapore for his unstinted guidance and persistent support throughout my work. He has been instrumental in both professional and scientific development of my research career.

I would like to extend my warm thanks to **Professor Bay Boon Huat,** Head, Department of Anatomy, for providing me an opportunity to pursue research at this Department and also for his expert advice and suggestions during my study.

I am greatly indebted to **Emeritus Professor Ling Eng-Ang**, former Head, and **Associate Professor Samuel S.W. Tay**, Deputy Head, Department of Anatomy, National University of Singapore for their valuable advice and suggestions to my research during the candidature.

I would like to thank **Mrs. Ng Geok Lan, Mrs. Yong Eng Siang and Ms. Chan Yee Gek** for their technical assistance, **Mdm. Ang Carolyne Lye Geck, Ms. Teo Li Ching Violet** and **Mdm. Diljit Kaur** for their secretarial assistance.

I must thank my labmates, **Mr. Parakalan Rangarajan**, **Ms. Nimmi Baby, Ms. Sukanya Shyamasundar** and **Ms. Shweta Jadhav** for their help and valuable suggestions during lab meetings. I had an opportunity to train **Ms. Lina Farhana** (Honors student, NUS) for her final year project experiments and would like to thank her for some contribution to the preliminary analysis of this project. I would

also like to take this opportunity to thank **Late Mr. Dhayaparan Devaraj** for his support and friendship.

I wish to thank the Yong Loo Lin School of Medicine, National University of Singapore for the financial support by means of Research Scholarship. Research grant support from National Medical Research Council (NMRC/EDG/1039/2011; R-181-000-139-275) to A/P Dheen to carry out this present study, is gratefully acknowledged.

Lastly, and most importantly, I thank my family (my parents, my brother and my husband) for their love, care and support.

Dedicated to my beloved family

TABLE OF CONTENTS

PUBLICATIONS

International Journals:

1. **Manivannan Janani**, Samuel SW Tay, Eng-Ang Ling, and *S.Thameem Dheen (2013). Dihydropyrimidinase like 3 regulates the inflammatory response of microglia. Neuroscience 253:40-54.

2. Rangarajan Parakalan, Boran Jiang, Baby Nimmi, **Manivannan Janani**, Manikandan Jayapal, Jia Lu, Samuel SW Tay, Eng-Ang Ling and S. Thameem Dheen (2012). Transcriptome analysis of amoeboid and ramified microglia isolated from the corpus callosum of rat brain. BMC Neuroscience 13:64.

Conference presentations:

I. Oral presentation

1. **J.Manivannan**, E.A.Ling, S.S.W.Tay and *T. Dheen. Role of Dihydropyrimidinase like 3 in regulating the inflammatory response of activated microglia in "Society for Neuroscience Conference 2012", 13th -17thOct 2012, New Orleans, USA.

II. Poster Presentations

1. **Janani Manivannan,** Eng-Ang Ling and S. Thameem Dheen. Dihydropyrimidinase like 3 regulates the inflammatory response of activated microglia, Singapore Neuroscience Association (SNA) Symposium 2013, 26th April 2013, Centre for Life Science, National University of Singapore, Singapore.

2. **Janani Manivannan,** Eng-Ang Ling and S. Thameem Dheen. Dihydropyrimidinase like 3 in regulating the inflammatory response of activated microglia, Yong Loo Lin School of Medicine 3rd Annual

Graduate Scientific Congress, 30th January 2013, National University of Singapore, Singapore.

3. **Janani Manivannan,** Eng-Ang Ling and S. Thameem Dheen. Role of Dihydropyrimidinase like 3 in regulating the inflammatory response of activated microglia", Singapore Neuroscience Association (SNA) Symposium 2012, 19th April 2012, National University of Singapore, Singapore.

4. Eng-Ang Ling, **Janani Manivannan,** Lu Jia and S. Thameem Dheen. Expression of Dihydropyrimidinase-like 3 in Amoeboid Microglia in Postnatal Rat Brain and in the Activated Microglia in Traumatic Brain Injury", Ninth World Congress on Brain Injury, 21st-25th March 2012, Edinburgh, Scotland, UK

5. **Janani Manivannan,** Eng-Ang Ling and S. Thameem Dheen. "A study on the expression and function of Dihydropyrimidinase like 3 in activated microglia", Yong Loo Lin School of Medicine 2nd Annual Graduate Scientific Congress, 15th February 2012, National University of Singapore, Singapore.

III. Award

Best graduate overseas oral presentation award by the Yong Loo Lin School of Medicine on 30th January 2013 at Annual Scientific Graduate Congress, Centre for Life Science, National University of Singapore, Singapore.

SUMMARY

Microglia, which are the resident immune cells of the central nervous system, become activated in response to stress, injury, infection and inflammation. Activation of microglia results in excessive production of proinflammatory cytokines and neurotoxic factors that underlie several neuropathological conditions. Further, the activated microglia undergo morphological transformation, rapid proliferation, and directed migration (to the affected region) which are regulated by the actin cytoskeleton organization. It was hypothesized that genes controlling cytoskeleton organization are involved in microglial activation. Determination of factors that inhibit microglial activation has been considered to be an important therapeutic strategy for various inflammatory and neurodegenerative diseases.

Dihydropyrimidinase-like 3 (*Dpysl3*), a member of collapsin response mediator protein family, is known to directly regulate the F-actin cytoskeleton. In this study, the roles of Dpsyl3 on the inflammatory reaction of activated microglia have been investigated. Microarray analysis comparing the global gene expression profile of amoeboid and ramified microglia has shown that Dpysl3 is mainly expressed in amoeboid microglia in the 5-day postnatal rat brain**.** Immunohistochemical analysis revealed that Dpysl3 was intensely expressed in amoeboid microglial cells until postnatal day 7, and then gradually diminished in ramified microglia (postnatal day 14). Further, *in vitro* analysis confirmed that the expression of Dpysl3 was induced in activated BV-2 microglial cells by LPS. It is well documented that microglial activation increases the expression of iNOS and

proinflammatory cytokines through activation of NF-κB activity. In the present study, siRNA-mediated knockdown of Dpysl3 prevented the LPS-induced expression of iNOS and cytokines including IL-1β, and TNF-α as well as nuclear translocation of NF-κB in microglia, indicating that Dpysl3 promotes the proinflammatory response of activated microglia.

Dpysl3 was found to be localized with F-actin cytoskeleton which is essential for cell motility and phagocytosis. Knockdown of Dpysl3 inhibited the migration and the phagocytic ability of activated microglia coupled with deranged actin filament configuration, suggesting that Dpysl3 regulates the microglial activation by altering their migration and phagocytic ability through the actin cytoskeleton rearrangement. This was further confirmed since the knockdown of Dpysl3 attenuated the expression of Rho GTPase cytoskeletal proteins such as RhoA and Rac1, which have been shown to regulate inflammatory and oxidative responses in activated microglia.

In summary, the present study demonstrated the mechanism by which Dpysl3 regulates the inflammatory response of activated microglia. Dpysl3 is developmentally regulated in amoeboid microglia and its expression is increased in activated microglial cells. Further, Dpysl3 knockdown in activated microglia altered the expression of proinflammatory cytokines such as TNF-α and IL-1β and inflammatory mediators including iNOS and NO and the migratory and phagocytic ability of activated microglia, possibly by regulating NF-κB and Rho GTPase signaling pathways.

Overall, this study describes that Dpysl3 not only functions as a cytoskeletal gene but also acts as a novel regulator for inflammatory response, migration and phagocytosis of activated microglia. Although this study demonstrates the potential function of Dpysl3 in activated microglia, further studies using *in vivo* animal models such as Dpysl3 knockout mice and Alzheimer's disease mice, would be required to understand its functions in neuropathological conditions.

LIST OF TABLES

LIST OF ILLUSTRATION/TEXT FIGURES

LIST OF SYMBOLS/ABBREVIATION

AMC: Amoeboid microglial cells

Aβ: β-Amyloid

BrdU: 5-Bromo-2’-deoxyuridine

CNS: Central nervous system

Co-IP: Co-Immunoprecipitation

CRMPs: Collapsin response mediator proteins

DAPI: 4', 6-diamidino-2-phenylindol

DMEM: Dulbecco's Modified Eagle Medium

DMS: N, N-dimethylsphingosine

Dpysl3: Dihydropyrimidinase like-3

F-actin: Filamentous actin

FBS: Fetal bovine serum

HRP: Horseradish peroxidase

IF: Immunofluorescence

IHC: Immunohistochemistry

IL-1β: Interleukin-1 beta

iNOS: Inducible nitric oxide synthase

LPS: Lipopolysaccharide

MS: Multiple sclerosis

NF-κB: Nuclear factor kappa-light-chain-enhancer of activated B cells

NO: Nitric oxide

PBS: Phosphate-buffered saline

PD: Parkinson’s disease

PF: Paraformaldehyde

PVDF: Polyvinylidene fluoride

Rac1: Ras-related C3 botulinum toxin substrate 1

RhoA: Ras homolog gene family, member A

RMC: Ramified microglial cells

ROS: Reactive oxygen species

RT: Room temperature

RT-PCR: Reverse transcription-polymerase chain reaction

SDS-PAGE: Sodium dodecyl sulphate- polyacrylamide gel electrophoresis

SDS: Sodium dodecyl sulphate

TBI: Traumatic brain injury

TBS: Tris buffered saline

TBST: TBS with 0.1% tween- 20

TEMED: Tetramethylethylenediamine

TNF-α: Tumor necrosis factor-alpha

Chapter 1

Introduction

1.1 Central nervous system and its cell types

The central nervous system (CNS) comprises of the brain and spinal cord which contain two main cell types, neurons and the glial cells (Carnevale et al., 2007). Glial cells mainly provide support and protection to the neurons. In addition, glial cells play essential roles in neuronal development, plasticity and recovery from injury (Brown and Neher, 2010).The three main Glial cell types in the central nervous system includes microglia, astrocytes and oligodendrocytes (Jessen and Mirsky, 1980).

1.2 Microglia

Microglia were described as the macrophage-like cells in 1919 by Spanish neuroscientist Rio-Hortega (Pessac et al., 2001; Kettenmann et al., 2011). Microglia are the resident immune cells of the CNS, represent approximately 5-10% of total Glial cell population in the CNS. They respond to injuries and infections in the CNS, by producing proinflammatory cytokines and performing phagocytosis of cellular debris and pathogens (Guillemin and Brew, 2004; Kettenmann et al., 2011).

Inflammatory response to injury or stimulation (by a chemical or biological agent) in the CNS is a complex process, which initiates a series of signaling events. The inflammatory response occurs mainly to remove the invading microorganisms as well as the toxic agents thereby resulting in repair and healing (Wyss-Coray and Mucke, 2002; Wyss-Coray, 2006). The process of neuroinflammation is instigated primarily by microglia (Kettenmann et al.,

2011). Microglia have been shown to be ubiquitously distributed throughout the CNS and participate in the maintenance of tissue homeostasis by screening the brain microenvironment under normal physiological condition (Perry and Teeling, 2013). In response to pathological conditions, they undergo rapid proliferation resulting in microglosis. Microglia are considered to be both detrimental and beneficial in the healthy and diseased CNS (Hanisch and Kettenmann, 2007).

1.3 Morphology of microglia

Morphologically microglia are classified into 3 phenotypes: amoeboid, ramified and reactive. The amoeboid microglia are predominantly found in the developing brain and transform into ramified microglia with age. In response to injury or inflammation, the ramified microglia transform into reactive which are amoeboid in shape (Figure I) (Tambuyzer et al., 2009).

1.3.1 Amoeboid microglia

There are several theories on the origin of microglia, the most widely accepted theory is that microglia are derived from circulating mesodermal hematopoietic cells which originate from the yolk sac in mammals (Ling et al., 1991; Kaur et al., 2001; Chan et al., 2007). Apart from this theory, studies have also shown that blood monocytes enter into the early postnatal brain and transform into the amoeboid microglia (Ling and Wong, 1993). Amoeboid microglia are spherical in appearance and function as brain macrophages. They are predominantly distributed in the corpus callosum of the developing brain (Ling et al., 2001).

Amoeboid microglia have been shown to have lamellipodia projections (grooves) radiating from its cells body coordinating the direction of migration during development (Marin-Teva et al., 1998). In addition, amoeboid microglia are involved in phagocytosis of cellular debris/apoptotic cells and also perform synaptic pruning during its development (Zabel and Kirsch, 2013).

1.3.2 Ramified microglia

Amoeboid microglia gradually transform into ramified microglia during third week of postnatal brain development (Ling and Wong, 1993). Morphologically, ramified microglia possess flattened cell bodies and highly branched and long processes. They are known to be resting or inactive, while their branches survey the microenvironment of the brain (Nimmerjahn et al., 2005). Ramified microglia constitute the resident microglial cells that are involved in surveillance of brain parenchyma (Aloisi, 2001).

1.3.3 Activated microglia

In response to injury or inflammation, the ramified microglia retract its processes and transform into activated/reactive microglia. Activated microglia appear as large amoeboid shaped cells with enlarged soma and numerous lamellipodia which migrate to the site of injury and proliferates to perform strong phagocytic activity (Streit et al., 1999; Monif et al., 2009). The function of activated/reactive microglia in the brain can be both protective and detrimental. In initial stages of neurodegeneration, activated/reactive microglia migrate to the injured site where they are involved in phagocytosis of debris and mediates the release of

proinflammatory cytokines and nitric oxide factors (Aloisi, 2001). However, prolonged microglial activation causes excessive release of proinflammatory cytokines and nitric oxide intermediates leading to neuronal death (Kaur and Ling, 2009) .

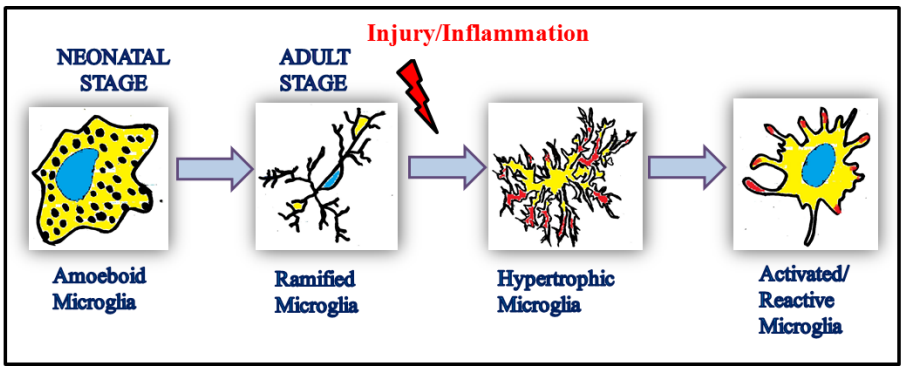

Figure I: *Diagrammatic representation of different morphology of microglia. During brain development, amoeboid microglia transform into ramified microglia. In the adult brain, microglia exists in a ramified state. Upon stimuli by inflammation or injury, the ramified microglia become hypertrophic and transform into a rounded activated phenotype. Adapted and modified from (Streit and Xue, 2009; Gomez-Gonzalez and Escobar, 2010).*

1.4 Functions of microglia

1.4.1 Chemotaxis and migration of microglia

Activated microglia migrate to the injured site and are involved in phagocytosis of cellular debris upon injury in CNS. In addition, microglial migration has also been reported during CNS development (Eyo and Dailey, 2013). Studies have shown that migration of microglia towards the injured site in the CNS is regulated by Chemokines (Barcia et al., 2012), Rho-family GTPases namely Rho, Rac1, and Cdc42 (Saraswathy et al., 2006) and two cytoskeletal proteins namely, actin and tubulin. The cytoskeletal proteins namely actin and tubulin are closely associated with migration and cell morphology (Eugenin et al., 2005). Under physiological

resting condition *in vitro*, actin and tubulin proteins are confined in the perinuclear region. However upon activation by stimulus, the cytoskeletal proteins are rearranged to undergo the process of attachment and protrusion contributing to microglial migration (abd-el-Basset and Fedoroff, 1995; Eugenin et al., 2005). In addition, several factors such as complement proteins, and chemokines such as monocyte chemoattractant protein (MCP-1) have been shown to stimulate the microglial chemotaxis (Akiyama et al., 1994; Biber et al., 2008; Deng et al., 2009).

1.4.2 Phagocytosis

Microglia are involved in phagocytosis of apoptotic cells, infectious agents and degenerating axons during CNS development and injury (Neumann et al., 2009). Light and electron microscopy observations revealed that microglia are characterized by cytoplasmic vacuoles and lysosomal bodies that are similar to the characteristics of phagocytic cells (Murabe and Sano, 1982; Kaur and You, 2000). It has been shown that microglia have specific receptor molecules namely CR3, immunoglobulin (FcR) and glycation endproducts to facilitate phagocytosis (Rotshenker, 2003).

1.4.3 Proliferation

Microglial cells undergo rapid proliferation in response to brain injury and infection (Kettenmann et al., 2011). Microglial proliferation helps in the repair of brain damage and phagocytosis of cellular debris. Microglial proliferation has been reported in various CNS pathologies namely Parkinson's disease,

Alzheimer's disease, and traumatic brain injury (Gomez-Nicola et al., 2013). Microglia are induced to proliferate *in vitro* by several potent molecules like interleukin-3 (IL-3), interleukin-6 (IL-6), macrophage colony stimulating factor (M-CSF) and granulocyte-macrophage colony stimulating factor granulocyte-macrophage colony stimulating factor (GM-CSF) (Lee et al., 1994; Streit et al., 2000).

1.4.4 Release of cytokines and reactive oxygen intermediates

Microglia mediate immune response through the release of cytokines (Hanisch, 2002). In pathological conditions, the microglia secrete a plethora of cytokines that modulate innate defense mechanisms namely nitric oxide (NO) and reactive oxygen species (ROS) which are known to be neurotoxic (Smith et al., 2012; di Penta et al., 2013).The cytokines secreted by microglia includes proinflammatory mediators (namely TNF-α, IL-1β, IL-6) and immunosuppressive cytokine (IL-10). In addition, these cytokines modulate the recruitment of leukocytes to CNS and involved in tissue repair mechanism (Hanisch, 2002).

1.4.4.1 Tumor Necrosis Factor-alpha (TNF-α)

TNF-α is a proinflammatory mediator produced by activated microglia (Figiel, 2008). TNF-α has been shown to be involved in cell growth, inflammation, differentiation and tumorigenesis (Aggarwal et al., 2000). The level of TNF-α expression increases rapidly in microglia upon acute insults to the brain and also in neurodegenerative disorders namely Parkinson's disease and Alzheimer's disease. TNF- α mediates its biological activity by two receptors: TNF-R1 and

TNF-R2 (Wilt et al., 1995; Cacci et al., 2005). The two receptors differ in their expression profiles and downstream signaling. The TNF-R1 contains the death domain and this domain is not present in TNF-R2. Binding of TNF-α to TNF-R1 is responsible for initiation of intracellular signaling namely (MAPK and NF-κB) and programmed cell death signaling (Aggarwal et al., 2000; Syed et al., 2007). TNF-R2 regulates the expression of anti-inflammatory molecules namely granulocyte colony-stimulating factor and IL-10 in microglia (Aggarwal et al., 2000; Veroni et al., 2010). In addition to this, high levels of TNF-α has been shown to produce toxic effects on neurons (Couch et al., 2013). In contrast, low levels of TNF-α has been shown to be neuroprotective by promoting neural cell survival and proliferation (Sriram et al., 2006; Figiel, 2008).

1.4.4.2 Interleukin 1 beta (IL-1β)

IL-1β, a member of Interleukin 1 family, is an important cytokine produced by the activated microglia (Kim et al., 2006b). IL-1β has been shown to be involved in several physiological activities such as cell proliferation, differentiation, apoptosis (Sebire et al., 1993), innate defense and immune responses (Netea et al., 2010). The expression of IL-1β is upregulated in the activated microglia in response to infection, injury or ischemia in the brain and has been linked to the process of neuroinflammation and neurodegeneration (Shaftel et al., 2008). IL-1β has been reported to bind to type I IL-1 receptor/IL-1 accessory protein complex, leading to NFkB-dependent transcription of pro-inflammatory cytokines (TNF-α and IL-6) and neutrophil-recruiting chemokines (CXCL1 and CXCL2) in glial cells (Moynagh, 2005). Further, IL-1β acts as an apoptosis signal thereby mediating the

phosphorylation of p38 mitogen activated protein kinase (MAPK). This leads to the activation of caspase-3 (Kim et al., 2004; Kim et al., 2006b). Hence, suppression of IL-1β has been shown to have neuroprotective effects.

1.4.4.3 Inducible nitric oxide synthase (iNOS) and Nitric oxide (NO)

Nitric oxide synthases (NOS) catalyzes the production of nitric oxide (NO) which has been shown to modulate microglial activation (Stefano et al., 2004). The NOS family consists of 3 isoenzymes namely, neuronal NOS (nNOS), endothelial NOS (eNOS), and inducible NOS (iNOS) (Qu et al., 2001). iNOS catalyzes NO production in microglia in response to stress (Tran et al., 1997). Activation of microglia with LPS *in vitro* shown to increase the level of iNOS resulting in significant amount of NO production (Boje and Arora, 1992). The continuous release of NO by activated microglia mediates mitochondrial dysfunction, DNA damage and cell death that contribute to neurodegenerative disorders namely Alzheimer's disease, ischemia and Parkinson's disease (Wyss-Coray, 2006; Klegeris et al., 2007). NO reacts with superoxide and forms peroxynitrite that causes cell toxicity (Beckman and Koppenol, 1996).The superoxide is produced from mitochondria respiratory chain using variety of enzymes namely, NADPH oxidase, cytochromes and P-450 enzymes, xanthine oxidase and iNOS (Wilkinson and Landreth, 2006). The activated microglia exhibit increased expression of iNOS and NADPH oxidase which are involved in inflammatory processes by oxidative stress contributes to the pathogenesis of neurodegenerative diseases (Brown, 2007; Brown and Neher, 2010). Combination of NADPH oxidase with iNOS results in apoptosis via peroxynitirite production (Brown and Neher, 2010).

NO from iNOS expression synergizes with hypoxia and induces neuronal death (Park et al., 2002). Further, the NO inhibits cytochrome oxidase resulting in glutamate release and excitotoxicity of neurons (Brown and Cooper, 1994; Brown and Neher, 2010). This excitotoxicity may be potentiated by a second mechanism as NO from iNOS results in glutamate release from astrocytes (Brown and Cooper, 1994; Bal-Price and Brown, 2001; Golde et al., 2002). In addition, NO secreted by activated microglia leads to the death of oligodendrocytes and impairs myelin formation (Miller et al., 2007; Pang et al., 2010). Recently, molecules like prostaglandins, FGF, sodium salicylates, glucocorticoids, have been shown to attenuate the expression of iNOS thereby controlling amount of NO produced by microglia (Kim et al., 1998; Petrova et al., 1999; Arimoto and Bing, 2003).

1.4.4.4 Generation of Reactive Oxygen Species (ROS)

Reactive oxygen species (ROS) includes hydroxyl radical (OH•), superoxide (O2−), peroxynitrite (ONOO−) and hydrogen peroxide (H2O2), are generated by mitochondrial electron transport chain (Inoue et al., 2003) and play important role in microglia-mediated neurotoxicity in the neurodegenerative disorders (Uttara et al., 2009). Activated microglia produces excessive amount of NADPH oxidase. The NADPH oxidase enzyme is a multi-subunit protein complex that reduces molecular oxygen to superoxide resulting in generation of ROS. Overproduction of ROS leads to oxidative stress to healthy neurons in the vicinity, forming the basis for neurodegeneration (Huo et al., 2011; Qin and Crews, 2012). In addition, excessive intracellular ROS might result in microglial apoptosis (Block and Hong, 2005). Further, the dysregulation of intracellular ROS in microglia has been

shown to amplify the secretion of proinflammatory cytokines which trigger the activation of several transcription factors (NF-κB) and kinase cascades in age related neurodegenerative disorders such as Alzheimer's disease (Block and Hong, 2007).

1.5 Activation of microglia

Several studies have described that microglia can be activated *in vitro* by various inflammatory stimuli, such as LPS, beta amyloid (Aβ) to understand the molecular mechanisms by which activated microglia mediate neurotoxicity in neuropathological conditions.

1.5.1 Lipopolysaccharide (LPS)

LPS is a bacterial endotoxin produced from the cell wall of Gram-negative bacteria, and has been widely used for microglia activation both *in vitro* and *in vivo* models (Lund et al., 2006b). Toll-like receptor (TLR)-4 is a receptor/ligand for LPS and is expressed by microglial cells (Hines et al., 2013). LPS forms a complex with LPS binding protein (LBP) and receptor CD14 for the activation of TLR4 signaling. TLR activation is important for mediating immune response upon infection. This activation mediates molecular signaling mechanisms namely NF-κB, MAPK pathways (Lee et al., 2006) thereby also triggers inflammatory reaction resulting in the secretion of proinflammatory cytokines, chemokines and neurotoxic mediators.

1.5.2 Beta –Amyloid (Aβ)

Aβ is the principle constituent of amyloid plaques, a characteristic feature of Alzheimer's disease (AD). Aβ is commonly used to activate microglial cells *in vitro* (Dheen et al., 2005; Lee and Landreth, 2010; Solito and Sastre, 2012).Specifically Aβ fragments, $A\beta_{25–35}$ and $A\beta_{1–42}$ are used for microglia activation (Silei et al., 1999). Microglia interact with Aβ with the help of cell surface receptors (namely complement receptors, Fc receptors, toll-like receptors) and elicits the activation of signaling cascades thereby resulting in microglial activation (Bamberger and Landreth, 2001; Doens and Fernandez, 2014). Excessive secretion of proinflammatory cytokines and other molecules, namely prostaglandins and chemokines by activated microglia (Fleisher-Berkovich et al., 2010) contributes to loss of neurons and cognitive deficits in AD patients (Mrak, 2012; Rubio-Perez and Morillas-Ruiz, 2012).

1.6 Signaling pathways involved in microglial activation

1.6.1 Nuclear factor-κB pathway (NF-κB)

NF-κB is a key transcription factor that mediates inflammatory response of microglia in the CNS (Heese et al., 1998; Caamano and Hunter, 2002; Ghosh and Hayden, 2008). NF-κB has been shown to perform various functions in the central nervous system. Further, animal models of systemic inflammation have revealed the activation of NF-κB in brain tissues (de Mos et al., 2009). In unstimulated microglial cells, NF-κB is expressed only in the cytoplasm. Upon activation of microglia, NF-κB translocates from cytoplasm to the nucleus, thereby regulating

the transcription of pro-inflammatory cytokines (TNF-α , IL-1β and IL-6) and iNOS (Block and Hong, 2005).

1.6.2 Mitogen-activated protein kinase pathways (MAPKs)

MAPKs belong to a highly conserved family serine/threonine that directs cellular responses such as osmotic stress, cell survival, proliferation, apoptosis and differentiation (Bachstetter et al., 2011). The MAPK signaling pathway comprises of 3 major pathways: (i) p38 MAPK, (ii) extracellular-signal-regulated kinases, ERK, (iii) c-Jun N-terminal kinases (JNK). Studies have reported that the MAPK pathway is important for microglial activation and mediates the release of the proinflammatory cytokines and neurotoxic molecules (Kim et al., 2004; Bachstetter et al., 2013).

Recently, the inhibitors of ERK, p38 MAPK and JNK have been reported to inhibit the microglia activation by reducing the production of a proinflammatory cytokines thereby attenuating neuronal cell death (Zhou et al., 2007; Wilms et al., 2009; Huo et al., 2011).

1.6.3 Rho family of guanosine triphosphatases GTPases (Rho GTPases)

Rho GTPases, a small family of signaling G-proteins, mediate intracellular signaling cascades such as cell proliferation , apoptosis, actin dynamics and gene transcription (Bustelo et al., 2007). The process of cells migration is divided into four steps: lamellipodium extension, formation of new adhesions, cell body contraction, and tail detachment (Ridley, 2001). The members of Rho GTPases include RhoA, Rac1, and Cdc42. They are key regulators involved in remodeling

of cytoskeleton and causes changes in cell polarity, motility and morphology in various cell types including macrophages and neurons (Barcia et al., 2012). The activation of these GTPases induces lamellipodia formation by Rac1, filopodia formation by Cdc42, actin stress fiber formation by RhoA and focal adhesion complex formation by Rac1 and RhoA (Ridley, 2001).Studies have described that RhoA pathway has been involved in mediating the inflammatory and oxidative responses in microglia (Villar-Cheda et al., 2012). RhoA has been shown to regulate phagocytosis, cytokine release, and production of ROS in leukocytes (Kitano et al., 2014). Rac1 has been shown to mediate the generation of radicals, activation of transcription factors and also induce NADPH oxidase for the formation of ROS. Rac1 also seem to be involved in reorganization of actin cytoskeleton and phagocytosis plays a key role in microglial activation (Chung et al., 2000; Roepstorff et al., 2008). It has been shown that activated Cdc42 and Rac1 are localized in the motile cells and initiate the formation of filopodial protrusions and lamellipodial extension along the membrane ruffling (Ohsawa et al., 2000; Bustelo et al., 2007; Apolloni et al., 2013). Further, the GTPase Rho has shown to initiate the formation of actin-myosin filament bundles and focal adhesion complexes thereby allowing the attachment of cells to extracellular substrates. In neurons and other cell types, Rho GTPases has been shown to trigger retraction of neurites and cell rounding (Vincent et al., 2012).

1.7 Cytoskeleton organization in microglia

Microglia undergo cellular modeling during migration and phagocytosis (Gitik et al., 2010). These processes are regulated by changes in the organization of actin

cytoskeleton and the assembly and disassembly of focal adhesions (Stuart et al., 2007). Focal adhesions provide structural tethers linking the actin cytoskeleton to the extracellular matrix and also serve as a convergence point for signaling pathways regulating numerous cellular processes, including migration, proliferation, transformation, and apoptosis (Defilippi et al., 2006). For example, the scaffolding protein p130Cas is localized in focal adhesions and through its multiple interaction domains induces sequential kinase phosphorylation, rearrangement of the actin cytoskeleton, and induction of cell migration and phagocytosis in microglia (Defilippi et al., 2006; Stuart et al., 2007) .

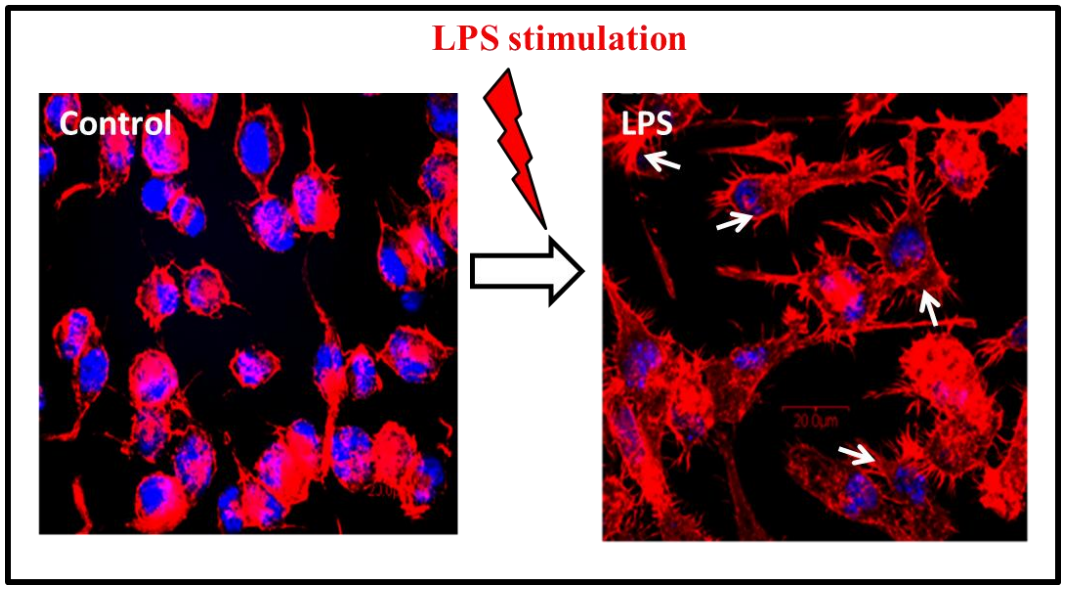

Figure II: *Confocal image show the immunoexpression of F-Actin (red) in control and LPS-treated BV-2 microglia. In control BV-2 microglia, F-actin filaments are granular in appearance and distributed throughout the cell body. Upon activation of microglia (with LPS), the F-actin filaments are organized into long microspike projections.*

Microglia comprise of three major cytoskeletal elements: (i) f-actin filaments, (ii) intermediate filaments and (iii) microtubules. The f-actin filaments originate in

the periphery of lamellipodia and they are distributed unevenly throughout the cytoplasm of the cell body. The intermediate filaments and microtubules forms dense network which radiates to the periphery (Graeber et al., 1988). Activation of microglia has been shown to alter the organization of microglial cytoskeleton causing F-actin network to reorganize as microspike projections (Figure II) (abd-el-Basset and Fedoroff, 1995). Thus the polymerization and depolymerization of actin filaments is essential for microglial migration and phagocytosis.

1.8 Microglial activation in neuropathologies

Microglial activation is considered as the hallmark of several neurodegenerative diseases.

1.8.1 Microglial activation in Alzheimer's disease

Alzheimer's disease is one of the age-related neurodegenerative disorder characterized by memory loss and impairments in cognitive functions (Salawu et al., 2011). This disease is characterized by the accumulation of β-amyloid (Aβ) and neurofibrillary tangles (NFTs) in the brains thereby resulting in loss of neurons and synapses in cortical and subcortical regions (Rogers et al., 2007). Studies have shown that microglia play a vital role in clearing the degenerated neurons and Aβ plaques in AD (Hickman et al., 2008). However, the continuous signals from Aβ peptides and NFTs overactivate microglia which release excessive amount of proinflammatory cytokines and neurotoxic molecules, thereby resulting in disease progression (Hickman et al., 2008; Crehan et al., 2012; Solito and Sastre, 2012).

1.8.2 Microglial activation in Parkinson's disease

Parkinson's disease is a neurological disorder marked by rigidity, tremor and loss of postural reflexes. Pathophysiologically, this disease is characterized by loss of dopaminergic neurons in the substania nigra pars compacta (SN) with the presence of α-synuclein positive lewy bodies within pigmented neurons of substania nigra and other parts of brain. α-synuclein is a synaptic vesicle protein, a principle element required for the formation of lewy bodies that play essential role in both onset and progression of PD (Rogers et al., 2007). Extracellular aggregation of α-synuclein induces microglial activation which augments neuroinflammation by releasing excessive amount of proinflammatory cytokines and neurotoxic molecules, thereby leading to progression of PD (Liu and Hong, 2003; Croisier et al., 2005; Zhang et al., 2005; Su et al., 2008). This microglial activation is characterized by increase in number and changes its morphology to an irregular and elongated body and short processes (Richardson and Hossain, 2013). Increased expression of inducible nitric oxide synthase (iNOS) within the SN has been reported in PD patients. Thus, progressive PD is driven by the inflammatory response and production of ROS by activated microglia, are responsible for loss of dopaminergic neurons in the SN which may play a key role in the neurodegeneration (Peterson and Flood, 2012).

1.8.3 Microglial activation in traumatic brain injury

Traumatic brain injury (TBI) is an insult to the brain caused by mechanical force leading to cognitive impairment (Dikmen et al., 2009).TBI leads to tissue

disruption and the molecules released from injured sites elicit microglial activation (Mannix and Whalen, 2012). The activated microglia migrates to the injury site and release of proinflammatory cytokines and neurotoxic mediators leading to neurotoxicity and neuroinflammation (Ramlackhansingh et al., 2011).

1.9 Current approaches for controlling microglia activation

Microglia have been shown to exhibit neuroprotective and neurotoxic functions in the CNS (Sawada et al., 2010). Chronic activation of microglia in neurodegenerative diseases leads to release of excessive amount of proinflammatory mediators and neurotoxic molecules, which further exacerbate the neurodegeneration (Kraft and Harry, 2011). Therefore inhibition of microglial activation could slow down the process of neurodegeneration and facilitate tissue repair aiding in neuron survival and axon regrowth. Recent studies have identified several inhibitors/drugs (such as dexamethasone, retinoic acid etc.) to control the activation of microglia (Dheen et al., 2005; Hinkerohe et al., 2010). Although these drugs help alleviate the symptoms, their chronic usage leads to various side effects. Therefore, identification of novel targets to develop better therapeutic strategies for neurodegenerative diseases is required.

1.10 BV-2 microglial cells for *in vitro* experimental study

BV-2 cells are immortalized murine microglial cell line. BV-2 cells have been shown to express similar inflammatory gene profile as *in vivo* microglia upon activation. In addition, BV-2 cells also produce factors and express receptors that are essential for its communication with neurons and other glial cells (Henn et al.,

2009). BV-2 cells show distinct morphological phenotypes: amoeboid and ramified under different culture conditions *in vitro* (Pottler et al., 2006). The primary microglia is more vulnerable to cell toxicity during transfection process which led to the replacement with BV-2 microglial cell line for further gene functional studies.

1.11 Global gene expression profiling of microglia

Global gene expression profiling of amoeboid and ramified microglia were performed by isolating the amoeboid and ramified microglia from the corpus callosum of 5 days and 28 days rat brains using laser capture microdissection (Parakalan et al., 2012). It revealed ~800 genes that were differentially expressed between these two groups. The top 25 genes that were highly expressed in amoeboid and ramified microglia were obtained based on fold change. Among these, Dihydropyrimidinase like 3 (Dpysl3) was found to be highly expressed with a fold change of 31.01 in amoeboid microglia when compared to the ramified microglia (Figure III).

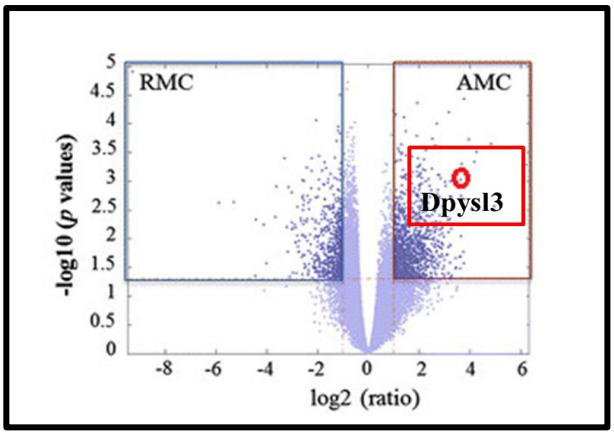

Figure III: *Volcano plot represents the differential expression of Dpysl3 in amoeboid and ramified microglia. Dpysl3 is expressed only in amoeboid*

microglia and not in ramified microglia. Adapted and modified from (Parakalan et al., 2012).

Dpysl3, also known as Collapsin Response Mediator Protein 4 (Crmp4) shown to play significant roles in cytoskeletal rearrangement, axon guidance and in semaphorin signaling (Goshima et al., 1995; Quinn et al., 1999). Dpysl3 are shown to be expressed in neurons and other glial cells in the brain. However, its expression pattern and functional significance in microglia had not been elucidated and hence this gene was the focus of this present study.

1.12 Collapsin Response Mediator Proteins (CRMPs)

Collapsin Response Mediator Proteins (CRMPs) are cytosolic phosphoproteins shown to be widely expressed in the nervous system, and involved in axon extension and guidance. CRMPs were first demonstrated as a protein component essential for the extracellular Semaphorin signaling (Goshima et al., 1995; Quinn et al., 2003). The CRMPs are also termed as the Dihydropyrimidinase related proteins (DRPs), turned on after division 64kDa (TOAD64), UNC-33 like proteins (Ulip) and TOAD-64/Ulip/CRMP (TUC) proteins (Goshima et al., 1995; Minturn et al., 1995b; Wang and Strittmatter, 1996). CRMPs are composed of five members (CRMPs 1-5), among which CRMPs 1-4 share nearly 80% homology whereas, CRMP5 shares only 50% homology with the other CRMPs in vertebrates (Goshima et al., 1995; Minturn et al., 1995b; Byk et al., 1996; Wang and Strittmatter, 1996). Each CRMP gene is made of 2 isoforms: long CRMP and short CRMP transcripts that differ in their amino terminal domains (Quinn et al.,

2003; Alabed et al., 2007). In spite of their homology, the physiological roles of CRMPs are often diverse in different biological processes.

1.12.1 Dihydropyrimidinase like-3 (Dpysl3) or Collapsin response mediator protein-4 (CRMP4) - Gene Ontology predictions

The molecular function of Dpysl3 includes SH3 binding domain, chondroitin sulfate binding domain (Franken et al., 2003), phosphoprotein binding domain and hydrolase activity. In the biological process, Dpysl3 is involved in axon guidance for nervous system development (Goshima et al., 1995) and actin filament bundle assembly (Rosslenbroich et al., 2005), respond to axon injury (Alabed et al., 2007) and pyrimidine nucleobase catabolic process.

1.13 Expression of Dpysl3 in different cell types

1.13.1 Dpysl3 in the developing nervous system

The expression of all Crmps is shown to be differentially regulated in the developing rat brain, where the expressions of these genes are high in the first postnatal week and then gradually decreased with age (Wang and Strittmatter, 1996). The expression of Dpysl3/Crmp4 was increased in post mitotic neurons of the ventricular zone during corticogenesis and it has been used as a marker for cells that undergo neuronal cell fate (Minturn et al., 1995a). In addition, Dpysl3/Crmp4 is shown to be expressed also in oligodendrocytes (Ricard et al., 2000).

1.13.2 Dpysl3 in adult nervous system

In the adult brain, the expression level of CRMPs is much lower as compared to the developing brain except for CRMP2 and CRMP3. The expression level of Dpysl3/Crmp4is shown to be increased during neurogenesis in different regions of the brain such as hypothalamus, interpeduncular nucleus, cerebral cortex, granule cell layer of the cerebellum and visual cortex (Nacher et al., 2000; Liu et al., 2003). These regions are important for synaptic rearrangement and axonal outgrowth in the adult brain (Nacher et al., 2000). In addition Crmp1, Crmp2, Crmp3 and Crmp4/Dpysl3have been shown to be expressed by oligodendrocytes of the adult rat brain (Ricard et al., 2000).

1.13.3 Dpysl3 in the peripheral nervous system

Apart from the CNS, CRMPs are also highly expressed in neurons of the dorsal root ganglion in the peripheral nervous system. Further, Dpysl3/Crmp4 is expressed in neuronal cell lines in response to nerve growth factor (NGF) and also in dorsal root ganglion by ciliary neurotrophic factor (CNTF) (Byk et al., 1996; Jang et al., 2010).

1.14 Function of CRMPs

1.14.1 CRMPs in neuronal development

The CRMPs play functional roles in neuronal migration, neuronal development and axonal growth (Charrier et al., 2003). CRMPs help in facilitating the Semaphorin signaling, thereby mediating axon guidance and extension by

inhibiting the collapse of growth cones (Goshima et al., 1995). The Sema3A induces the neuronal receptor, Plexin A1 to form a complex with Crmp1 and facilitate axonal guidance (Deo et al., 2004). In addition, Crmp2 promotes axon formation (Inagaki et al., 2001; Yoshimura et al., 2005) whereas, long transcript of L-Dpysl3/Crmp4 promotes neurite outgrowth and branching in developing cortical neurons and short transcript of S-Dpysl3/Crmp4 promotes axon elongation (Quinn et al., 2003; Alabed et al., 2007). Conversely, overexpression of Crmp3 and Crmp5 prevents neurite outgrowth (Aylsworth et al., 2009; Brot et al., 2010).

Crmp1 gene is shown to promote neuronal migration in the cerebral cortex (Charrier et al., 2003). Disruption of Crmp1 impairs long-term potentiation (LTP), spatial learning and memory that is associated with improper neurite outgrowth (Su et al., 2007). Similarly, deletion of Crmp3 leads to abnormal morphogenesis of spine and dendrites in the hippocampal neurons resulting in impairment of LTP (Quach et al., 2008).

Further, the CRMPs are also shown to be expressed in oligodendrocytes which help in oligodendrocytes outgrowth during the myelination and remyelination process (Ricard et al., 2000).

1.14.2 CRMPs in pathological conditions

The expression of CRMPs is shown to be highly increased in neuropathological conditions such as epilepsy, Huntington's disease and Alzheimer's disease (Czech et al., 2004; Good et al., 2004; Cole et al., 2007). Recent findings show that the

antidepressant drugs like tianeptine increases the expression of CRMP-2, while other molecules like the epilepsy drug lacosamide and the natural brain metabolite lanthionine ketimine bind to CRMP-2 directly and increase its neuroprotective effects (Doty et al., 2007; Hensley et al., 2013). These results show that altering CRMP expression through pharmaceuticals is possible and might help in the protection against various neurological diseases. The implication of CRMPs in neuropathological diseases are quite minimal but its dysregulation has been widely discussed in cancerous conditions (Gao et al., 2010b). The implication of CRMPs in these pathological conditions indicates that CRMPs are not only involved in the nervous system development (Vuaillat et al., 2008) and also play wider roles in diverse physiological processes like in cancerous events.

1.15 Signaling pathways involving Dpysl3

1.15.1 F-actin cytoskeletal bundling

The interesting feature of CRMPs is their ability to bind with F-actin cytoskeleton (Charrier et al., 2003).The interaction of Crmp4 with cytoskeletal proteins like tubulin and actin indicates its importance in cell assembly. Among the CRMPs, Crmp2 and Crmp4/Dpysl3 are known to directly interact with F-actin cytoskeleton and to reorganize the F-actin into tight bundles (Goshima et al., 1995; Arimura et al., 2005; Rosslenbroich et al., 2005) that are important for mediating cell migration. Crmp4/Dpysl3 is shown to localize with F-actin in lamellipodia of B35neuroblastoma cells and growth cones of sensory neurons in

the dorsal root ganglion (Rosslenbroich et al., 2005). Crmp4/Dpysl3 has also been shown to colocalized with synaptic vesicle protein2 (SV2) and Intersectin and regulate actin dynamics in growth cones (Fulga et al., 2007). Further overexpression of Crmp4/Dpysl3 increases the filopodial length and branch in neuronal growth cones (Quinn et al., 2003).Thus it is evident that Crmp4/Dpysl3 can regulate F-actin cytoskeleton and has a broader role in cytoskeletal signaling.

1.15.2 Rho GTPase Regulators

The Rho family of guanosine triphosphatases GTPases are small signaling G-proteins that act as molecular switches and play important role in signaling processes such as actin dynamics, cell proliferation, gene transcription and apoptosis (Van Aelst and D'Souza-Schorey, 1997). The most widely described members of Rho GTPases are Cdc42, Rac1 and RhoA that regulate cytoskeleton mechanism (Van Aelst and D'Souza-Schorey, 1997). Studies in non-neuronal cells have shown that activation of RhoA, Rac1 or Cdc42 induce the formation of lamellipodia and actin stress fibers (Ridley et al., 1992). Indeed, it also regulates the cytoskeletal reorganization of growth cone and thereby affects the growth cone motility. Further, studies have reported that Rho GTPase regulate several physiological processes that are associated with actin cytoskeleton including cell migration, wound healing, axon extension, cytokinesis and nerve regeneration (Ellezam et al., 2002). The interaction of Crmp4/Dpysl3 with RhoA is shown to mediate neurite outgrowth inhibition. This interaction with Rho GTPase activity can induce formation of focal adhesion and actin contractility (Alabed et al., 2007).

1.16 Role of Dpysl3 in nerve regeneration

Upon injury in the CNS, the injured axon inhibits regeneration by inhibitory signaling molecules. This inhibitory signaling affects the cytoskeleton structure, thereby inhibiting growth cone formation and axonal outgrowth (Kalil and Dent, 2005). CRMPs are shown to be important regulators in mediating nerve regeneration. It is shown that RhoA signals through Crmp4/Dpysl3 to inhibit neurite outgrowth. Further, blocking the interaction of RhoA-Crmp4/Dpysl3 with a C4RIP-V5 construct (CRMP4b (residues 1-126)–RhoA inhibitory peptide fused to a V5 epitope tag) has shown to decrease inhibition of neurite outgrowth (Alabed et al., 2007; Jang et al., 2010). Overall, it is evident that RhoA-Crmp4/Dpysl3 interaction pathway is important for cytoskeletal rearrangement and Crmp4/Dpysl3 is a critical regulator of axonal outgrowth.

1.16 Aim of the study

Microglia transforms into activated state in response to stress, injury, infection and cause neurodegeneration in the CNS. The activated microglia undergoes morphological transformation, rapid proliferation and directed migration (to the affected region) which are related to rearrangements of the actin cytoskeleton. It was hypothesized that genes controlling cytoskeleton rearrangement are involved in microglial activation.

Dpysl3 is shown to be directly involved in F-actin bundling (Rosslenbroich et al., 2005) and might play an important role in rearrangement of microglial actin cytoskeleton during development and activation. The present study was aimed at understanding the function of Dpysl3 in microglial activation and function. The main objectives of this study are:

1.16.1 To investigate the expression pattern and function of Dpysl3 in the normal or resting and activated microglia

- The temporal expression pattern of Dpysl3 in microglia in rat brain's corpus collasum *in vivo* was investigated.
- The expression pattern of Dpysl3 in activated microglia (by LPS) *in vivo* and *in vitro* was investigated.
- The role of Dpysl3 in the production of proinflammatory cytokines by activated microglia was studied. Specifically, effects of siRNA-mediated knockdown of Dpysl3 in control and activated BV-2 microglia on the expression and production of proinflammatory cytokines were examined.

1.16.2 To examine the role of Dpysl3 in microglial migration, phagocytosis and proliferation

The transformation from resting to activated state of microglia induces changes in their morphology, migratory behavior, cytoplasmic motility, phagocytic ability. It has been studied that the changes in cell morphology and activity are accompanied by the changes involved in organization of cytoskeleton and also the expression of different cytoskeletal proteins in microglia. It was hypothesized that Dpysl3, known to regulate F-actin (Rosslenbroich et al., 2005), cytokinesis and cytoskeleton formation during development, may regulate microglial activation. To address this,

- Effects of siRNA-mediated knockdown of Dpysl3 on migration, phagocytosis and proliferation of activated BV-2 microglia were examined.

1.16.3 To examine the role of Dpysl3 in cytoskeleton organization of activated microglia

Activation of microglia is associated with changes in cytoskeletal organization. Dpysl3 is shown to regulate the F-actin cytoskeleton causing changes in the migration activity of other cell types such as neurons cells (Rosslenbroich et al., 2005). The regulatory molecules involved in cytoskeletal organization in microglia had not been elucidated. To address this,

- The co-localization of Dpysl3 with F-actin cytoskeleton in activated microglia was confirmed.

- Effects of siRNA-mediated knockdown of Dpysl3 on F-actin bundling and microspike projection in activated microglia were investigated.

1.16.4 To investigate the role of Dpysl3 in Rho GTPases cytoskeletal pathway

Dpysl3 is shown to interact with Rho GTPases (RhoA and Rac1), which are required for cytoskeletal organization for cell migration (Van Aelst and D'Souza-Schorey, 1997; Yoshimura et al., 2005; Villar-Cheda et al., 2012). The RhoA and Rac1 pathways have been shown to regulate inflammatory and oxidative responses in microglia (Van Aelst and D'Souza-Schorey, 1997). The interaction of Dpysl3 with cytoskeletal proteins, RhoA and Rac1 have not been elucidated in microglia. To address this

- Effects of siRNA-mediated knockdown of Dpysl3 on the expression of RhoA and Rac1 in activated microglia were investigated.

The findings of this study will provide novel insights into the regulatory mechanism by which the cytoskeletal proteins contribute to microglia activation in pathological conditions.

Chapter 2

Materials and Methods

2.1 Animals

Wistar rats aged 5, 7, 14 and 28 days were used in this study. The rats were obtained from Laboratory Animal Centre, National University of Singapore. Animal handling and experimental procedures were performed under the guidelines set by Institutional Animal Care and Use Committee (IACUC), National University of Singapore (IACUC 059-11).The numbers of rats used in each experimental group are shown in the Table I.

Table I: Number of rats used for various experimental groups

Age	Number	Experiment
5D	4	Saline injected rats- Immunofluorescence
5D	4	LPS injected rats- Immunofluorescence
28D	4	Saline injected rats- Immunofluorescence
28D	4	LPS injected rats- Immunofluorescence
3D, 5D, 7D, 14D	20	Immunofluorescence
3D	48	Primary culture- Immunofluorescence
Total	84	

2.1.1 Injection of LPS

Wistar rats aged 5- and 28-days received an intraperitoneal (i.p.) injection of 100µl of lipopolysaccharide (LPS) (1mg/kg; Cat. No. L2654, Sigma-Aldrich,

MO, USA) (experimental group) or saline (control group). The rats were sacrificed 6h post injection and used for experiments.

2.2 Perfusion

Prior to perfusion, rats of 3-day, 5-day, 7-day, 14-day and 28-daywere anesthetized by injecting sodium pentobarbital solution (60mg/kg) intraperitoneally (i.p.).

2.2.1 Materials

- 0.1M Phosphate Buffer:

  Solution B

  (178g $Na_2HPO_4.2H_2O$ in 10L of deionized water)

  Solution A

  (69g $Na_2HPO_4.2H_2O$ in 5L of deionized water)

  1 volume of Solution A was mixed with 3 volume of Solution B and pH was adjusted to 7.4
- 2% Paraformaldehyde:

  2g of Paraformaldehyde in 100ml of 0.1M phosphate buffer
- 15% Sucrose:

  15g of Sucrose in 100ml of 0.1M phosphate buffer

2.2.2 Procedure

Two reservoirs was filled with Ringer's solution and 2% Paraformaldehyde respectively. The two reservoirs are connected to a polythene tube interlinked

with an air trap and a 19G needle (Terum Co., Japan) at the end of tube. The air bubbles in the tubes were removed carefully. The heart of rat was exposed by reflecting the thoracic cage and the pericardium using a scissor. Then, the cannula with Ringer‘s solution was inserted to the left ventricle and instantaneously a portion of right atrium was slit in order to let blood flow out. Ringer’s solution was allowed to flow until the lungs and liver were cleared of blood. Subsequently, the rat was perfused with 300ml of 2% Paraformaldehyde. Following perfusion, the brain was dissected out and post-fixed with 2% Paraformaldehyde for 3h and then stored in 15% sucrose overnight at 4°C.

2.2.3 Preparation of frozen sections

The brain tissue was trimmed, then embedded on a metal chuck using Lipshaw M-1 embedding matrix (Pittsburgh, USA) and frozen rapidly in liquid nitrogen. Coronal sections (30µm thick) of forebrain were cut using a cryostat (Model 3050, Leica instruments, Germany). Subsequently, the sections were mounted on gelatin coated slides, and are allowed to dry for 1h at RT then stored at -20°C until use.

2.3 Cell culture

2.3.1 Primary microglial culture

Microglia were isolated from 3-5 day old rat pups for primary culture.

2.3.1.1 Materials

- Fetal bovine serum FBS (Cat. No. SH30070.03, HyClone, UT)

- Non-essential amino acid (Cat. No. M7145, Sigma, USA)
- Antimycotic antibiotic solution (Cat.No.A5955, Sigma, USA)
- Dulbecco's modified eagle medium (Cat. No.SH30022.01, HyClone, UT)
- Insulin (Cat. No. I0516, Sigma, USA)
- Deoxyribonuclease Ⅰ (Cat. No. D4527, Sigma, USA)
- Trypsin-EDTA 10X (Cat. No. 15400-054, Life Technologies, USA)
- 70μm nylon mesh cell strainer (Cat. No. 352350, BD Biosciences, USA)
- Lectin (Cat. No. L0401 ,Sigma, USA,)
- 75cm^2 tissue culture flasks (Corning, USA)

2.3.1.2 Procedure

Rat pups were anesthetized with an i.p. injection of sodium pentobarbital (50 mg/kg). The skin covering the head was cleaned with 70% ethanol and incised and the skull was cut opened. The cortex of brain was transferred to asterile petridish containing ice-cold PBS and cleaned of the meninges. The brain tissue was transferred into 50ml centrifuge tube and dispersed using DMEM containing 1ml of Trypsin-EDTA with 0.5% of Trypsin and 0.2% of EDTA and then 100μl of Deoxyribonuclease Ⅰ solution (50μg/ml). Subsequently, the cell suspension was transferred to a 75cm2 tissue culture flask and shaken in an orbital shaker (200rpm/min) for 15min at 37°C. The cells were then filtered using the 70μm nylon mesh cell strainer to remove the tissue clumps. At last, the cell suspension was centrifuged for 5min at 1000rpm and seeded at a density of 1.2×10^6 cells/ml in a 75cm^2 culture flask containing DMEM supplemented with 10% FBS and

cultured at 37°C incubator in a humidified chamber with 5% CO2 / 95% air. The medium will be replaced with fresh complete media for every 48h until we observe 80-90% confluency of growth, which takes nearly 2 weeks. The heterogenous glial culture were purified by mild trypsinization (Saura et al., 2003).Initially, the glial culture was washed twice with 1X PBS. Then it is incubated for 10min in trypsin solution composed of 1ml of 0.25% trypsin and 20µl of 0.5M EDTA diluted in 40ml of DMEM. The upper cell layer (containing other glial cells) detached was discarded, while the adherent microglial cells were again cultured in DMEM containing 10% FBS overnight. For immunostaining, $2.5_X 10^5$ cells were seeded per well on the poly-L-lysine coated coverslips of a 24-well plate. The purity of microglia were determined by immunofluorescence using Lectin (1:100), which is a marker for microglia.

2.3.2 BV-2 microglial cell culture

BV-2 cells are immortalized murine microglial cell line, was used in the present study (Henn et al., 2009; Stansley et al., 2012).

2.3.2.1 Materials

- Fetal bovine serum FBS (Cat. No. SH30070.03, HyClone, UT)
- Dulbecco's modified eagle medium (Cat. No.SH30022.01, HyClone, UT)
- Trypsin-EDTA (Cat. No. T4174, Sigma, USA)
- Phosphate Buffered Saline, 10XPBS (Cat. No. PB0344-1L, Vivantis, USA)
- $75cm^2$ tissue culture flasks (Corning, USA)

2.3.2.2 Procedure

BV-2 cells were grown in 75cm^2 cell culture flask containing DMEM supplemented with 10% FBS in a humidified chamber filled with 5% CO_2 and 95% air at 37°C for 3-4 day. The cells were passaged every two days and replated in fresh medium. Briefly, the cells were washed with twice of 1X PBS and then treated with 5ml of 1X TE in PBS at 37°C for 5min. The effect of TE was neutralized by addition of 10ml of DMEM containing 10% FBS. The cell suspension was taken in a 50ml centrifuge tube and centrifuged at 1000rpm at 4°C for 5min. The pellet was suspended with 10ml of complete medium and the supernatant was discarded off. Then the cells were seeded in either 24 well plates for immunostaining or in 6 well plates for isolation of RNA isolation.

2.3.3 Treatment of BV-2 cells

2.3.3.1 Material

- Lipopolysaccharide LPS (Cat. No. L2654, Sigma, USA)

2.3.3.2 Procedure

BV-2 cells were cultured in culture dishes in DMEM supplemented with 10% FBS. After 12h, the cells were washed twice with 1X PBS, and then treated with LPS (1μg/ml in DMEM). Following addition of LPS, the cells were incubated for different time points (1h, 3h, 6h) before they were used for various experiments. The basis for selection of time points is for two reasons: first to see whether LPS had time dependent function on inflammation and secondly what is the time at

which Dpysl3 is maximally expressed. This would give an estimate of direct relationship between Dpysl3 and magnitude of inflammation.

2.4 siRNA mediated gene knockdown

2.4.1 Principle

RNA interference technology has shown that level of target gene expression can be effectively silenced by the introduction of short double-stranded RNA oligonucleotides to mammalian cells. The siRNAs are cleaved from double stranded RNAs by DICER (RNase III –like enzyme) (Tauser and Stoica, 2003). This short siRNA pieces (20-25bp) unwind to single stranded RNA and bind with proteins, forming a multi-subunit protein complex termed as RNA-Induced Silencing Complex (RISC). This protein complex guides the siRNAs to its target mRNA sequence, leading to degradation of complementary mRNA sequence with help of endo and exonucleases (Tauser and Stoica, 2003). When the pairing is perfect between native mRNA and siRNA sequence, the native mRNA becomes fragmented, and hence it cannot be translated (Gavrilov and Saltzman, 2012).

2.4.2 Materials

- Predesigned siRNA (Ambion, USA)
- OPTIMEM I reduced serum medium (Cat. No. 31985-070, Life technologies, USA)
- Negative Control siRNA, silencer select, 5nM (Cat. No. 4390843, Ambion, USA).

- Lipofectamine RNA iMAX transfection reagent (Cat. No. 13778150, Life technologies, USA)

The siRNA sequences for Dpysl3 are shown in Table II:

Table II: Dpysl3siRNA construct sequences

Construct	siRNA ID #	Sequence
C1	S75750	Sense: 5'-GAAUCGUCAAUGAUGAUCAtt-3' Anti-sense: 5'UGAUCAUCAUUGACGUCCtc-3'
C2	S75749	Sense: 5'-GAAUAGAUGGAACUCAUUAtt-3' Anti-sense: 5'-UAAUGAGUUCCAUCUAUUCcc-3'
C3	S75748	Sense: 5'-GUGUUUGACUUGACCACCAtt-3' Anti-sense: 5'- UGGUGGUCAAGUCAAACACtg-3'

2.4.3 Procedure

BV-2 cells were plated at a density of $2x10^5$ cells/ml and grown in DMEM containing 10%FBS (2ml) for 24h to achieve maximum confluency. 500µl Opti-MEM with 10µl of predesigned siRNA (50nm) and 4µl of Lipofectamine with 500µl Opti-MEM were incubated for 10min at 37°C in separate tubes. Following incubation, the two solutions were combined and incubated at 37°C for 20min to form siRNA-Lipofectamine complex. After 20min, the BV-2 cells were incubated in Opti-MEM containing siRNA-Lipofectamine complex for 8.5h. After 8h of incubation, the Opti-MEM medium was changed with DMEM containing 10% FBS. For the control, the BV-2 cells transfected with

scrambled (negative control) siRNA were used. The transfected cells were cultured for 48h, after which the knockdown efficiency was determined by qRT-PCR.

2.5 RNA isolation and quantitative reverse transcription-polymerase chain reaction (qRT-PCR)

2.5.1 Principle

The RNA isolation was performed using the RNeasy kit (Qiagen, Germany), which uses micro spin technology. The cell samples are lysed with guanidium isothiocyanate (GITC) buffer by which the RNases are inactivated to extract the RNA. The ethanol is added in order to provide binding conditions for the RNA samples and then added to spin column. In the spin column, RNA longer than 200 bases is adsorbed on a silica-gel membrane based on its selective binding properties and remaining contaminants are discarded. High grade quality RNA is eluted in RNase-free water. Using this protocol, longer RNA molecules of about 200 nucleotides are extracted and shorter RNA nucleotides namely 5S rRNA, tRNAs and 5.8S rRNA, are excluded (Qiagen RNeasy Mini handbook).

Polymerase chain reaction (PCR) is a method that amplifies several copies of specific region of DNA. A PCR reaction consists of 3 major steps: denaturation, annealing and DNA synthesis (repeated for 30-40 cycles). In this process, the double strand DNA (template) is denatured to become a single stranded DNA which then hybridized to a set of 5’ and 3’ primers (20 nucleotides in length and are complementary to a defined sequence of the gene of interest).

Then, DNA polymerase and polynucleotides extend the primers and make a copy of designated DNA sequence. Due to complementary nature of primers with both strands of DNA, the reaction continues to produce more copies of DNA (Belokhvostov, 1995).

The combination of reverse transcription and polymerase chain reaction (RT-PCR) is a powerful method to quantify the levels of mRNA expression. The quantitative RT-PCR using fluorescent probes is extremely sensitive for the quantification of gene expression. This method uses a SYBR green which is a fluorescent dye that binds to the double stranded DNA. During the extension step, increasing amounts of dye bind to newly synthesized hence the double stranded DNA increases its fluorescence signal intensity (Arya et al., 2005). Hence, the measured fluorescent intensity indicates the amount of amplified DNA. Therefore the assessment of $2^{-\Delta\Delta Ct}$ indicate the fold change of target gene expression normalized to endogenous reference gene (Livak and Schmittgen, 2001).

2.5.2 Materials

- RNeasy Mini Kit (Cat. No. 74106, Qiagen, Germany)
- RNase inhibitor RNasin (Cat. No. N2511, Promega, USA)
- Moloney murine leukemia virus reversetanscriptase-5Xbuffer (Cat. No. M531, Promega, USA)
- Moloney murine leukemia virus reverse transcriptase (Cat. No. M1701, Promega, USA)
- Olido(dT) 15 Primer (Cat. No. C1101, Promega, USA)

- 10mM dNTP (Cat. No. U1511, Promega, USA)
- RNase-free water
- Fast SYBR Green Master Mix (Cat.No.4385612, Applied Biosystems, USA)
- TAE buffer (Cat. No.PB09040-1L,Vivantis,USA)
- 100bp DNA ladder (Cat. No. G6951, Promega, USA)
- RT-PCR instrument (Applied Biosystems 7500HT)
- Gene Genius (Syngene, UK)
- Spectrophotometer (Eppendorf, Germany)

2.5.3 RNA extraction

Total RNA was extracted from control and LPS treated BV-2 cells using the RNeasy mini kit. First, the cells were lysed in 650µl of RLT lysis buffer for 10-15min on ice and then scraped. The cell lysate was homogenized and centrifuged at 14000×g for 30s. To the supernatant, 650µl of ethanol was added to clear the cell lysate. The samples were transferred to RNeasy mini spin column and centrifuged at 14000×g for 30s and the flow through was discarded. Then the spin column was washed with RW1 and RPE buffers. Finally, the RNA is eluted by adding 20µl of RNase free water to the spin column. The quality of the extracted RNA was assessed at 260 and 280nm using the Nanodrop (Biophotometer, Eppendorf, Germany). The RNA samples were then stored at -80°C for further use.

2.5.4 cDNA Synthesis

2.5.4.1 Materials

- RNase inhibitor RNasin (Cat.No.N2511, Promega, USA)
- Moloney murine leukemia virus reverse tanscriptase- 5X buffer (Cat. No. M531, Promega, USA)
- Moloney murine leukemia virus reverse transcriptase (Cat. No. M1701, Promega, USA)
- Olido(dT) 15 Primer(Cat. No. C1101, Promega, USA)
- 10mM dNTP (Cat.No.U1511, Promega, USA)
- RNase-free water

2.5.4.2 Procedure

Moloney murine leukemia virus (M-MLV) Reverse Transcriptase is an RNA dependent DNA polymerase enzyme used for synthesis of cDNA from the RNA. 1µl of Oligo (dT)15 primer was added to 2µg of RNA sample in a microcentrifuge tube and heated to 70°C for 5min, following which the tubes were incubated on ice. The reaction mixture containing 1µl of M-MLV RT, 5µl of M-MLV RT 5x buffer, 0.675µl of RNasin inhibitor, 1.2µl of dNTP mix and RNase free water (which makes upto a final volume of 25µl) was added to the tube and incubated at 42°C for 1h. Then, the reaction was stopped by heating for 15min at 70°C and the synthesized cDNA was then stored at -20°C until use.

2.5.5 Quantitative real-time -PCR

Quantitative real time-PCR was carried out on an Applied Biosystems 7900HT. The primer sequences used are tabulated in Table III:

Table III: Primer sequences for RT-PCR

Gene	Primer sequence	Product size
TNFα	Forward primer- 5'-CGTCAGCCGATTTGCTATCT-3' Reverse primer-5'-CGGACTCCGCAAAGTCTAAG-3'	205bp
IL-1β	Forward primer-5'-GCCCATCCTCTGTGACTCAT-3' Reverse primer-5'-AGGCCACAGGTATTTTGTCG-3'	229bp
iNOS	Forward primer-5'-GCTTGTCTCTGGGTCCTCTG-3' Reverse primer-5'- CTCACTGGGACAGCACAGAA-3'	217bp
Dpysl3	Forward primer- 5'-ATCAAGGGAGGGAGAATCGT-3' Reverse primer-5'-TTGTCCCTTGGAAGAAATCG-3'	225bp
RhoA	Forward primer- 5'-GTGGATGGGAAGCAGGTAGA-3' Reverse primer-5'-TTGTTCCCAACCAGGATGAT-3'	212bp
Rac1	Forward primer- 5'-CTGAAGTGCGACACCACTGT-3' Reverse primer-5'-TGTCTTGAGTCCTCGCTGTG-3'	206bp
β-actin	Forward primer- 5'- GGATTCCATACCCAAGAAGGA-3' Reverse primer- 5'- GAAGAGCTATGAGCTGCCTGA-3'	103bp

Each reaction mixture contains 0.5µl of 5mM gene specific primers, 5µl of PCR master mix, 1µl of cDNA and RNase free water (to a final volume of 10µl). The real time PCR was performed in triplicates using the following program 95°C for 15min, followed by 40 cycles of denaturing at 94°C for 15s, annealing at 60°C for 25s and then extension at 72°C for 12s. The results of the PCR were normalized

with the β-actin product and analyzed using the $2^{-\Delta\Delta Ct}$ (Livak and Schmittgen, 2001) method.

2.5.6 Detection of PCR products

2.5.6.1 Materials

- 1% agarose gel:

  Agarose (Vivantis, USA) 1g

  Ethidium Bromide solution (Bio-Rad) 1µl

  1X TAE buffer (Vivantis, USA) 100ml

- 100bp cDNA Ladder (Cat.No.G2101, Promega, USA)

2.5.6.2 Procedure

The PCR products were analyzed on 1% agarose gel using the gel electrophoresis equipment. 1% agarose gel was prepared in 1X TAE buffer and then 1µl of EtBr was mixed with the heated agarose solution and then was poured and solidified in the gel tray. 10µl of PCR product mixed with 2µl of 6x loading dye was added to each lane of the agarose gel and gel was ran on an electrophoresis tank containing 1X TAE buffer at 110V for 30min. The PCR products were visualized and photographed using a gel documentation system.

2.6 Western blotting

2.6.1 Principle

Western blotting is an analytical technique that determines the amount of proteins in samples. In this technique, a complex protein mixture is separated by

electrophoresis based on its molecular size, then transferred to a PVDF or nitrocellulose membranes and detected with specific primary antibodies. Primary antibodies detect only specific protein antigen on the membrane. Antigen-Antibody complexes are detected using secondary antibodies conjugated with horseradish peroxidase (HRP) (Kurien and Scofield, 2006). The chemiluminescence HRP substrate was used to develop the protein expression on X-ray film.

2.6.2 Materials

- Rabbitanti-Dpysl3 (Cat. No. AB5454, Millipore, USA)
- Goat anti-Dpysl3 (Cat. No. SC-27323, Santa Cruz, USA)
- Rabbit anti-TNF-α (Cat. No. AB2148P, Chemicon, USA)
- Rabbit anti-IL-1β (Cat. No.AB1413, Chemicon, USA,)
- Rabbit anti-iNOS(Cat. No. SC-649, Santa Cruz, USA)
- Rabbit anti-NF-κB(Cat. No. SC-372, Santa Cruz, USA)
- Mouse anti-Rac1 (Cat. No. SC05-389, Millipore, USA)
- Mouse anti-RhoA (Cat. No. SC418, Santa Cruz, USA)
- Mouse anti- βactin (Cat. No.55441 , Sigma, USA)
- Goat-anti-Mouse horseradish peroxidase (Cat. No. 31430, Thermo scientific, USA)
- Goat anti-Rabbit horseradish peroxidase (Cat. No. 31460, Thermo scientific, USA)

- Mammalian protein extraction reagent (Cat. No. 88665, Thermo scientific, USA)
- Protein assay kit (Cat. No. 5000002, Bio-Rad, USA)
- Pierce Protease inhibitor (Cat. No. 88665, Thermo scientific, USA)Western blot stripping buffer (Cat. No. 46430, Thermo scientific, USA)
- 6x SDS gel-loading buffer
- 10% Resolving gel:

H_2O	7.9ml
30% Acrylamide mix	6.7ml
1.5M Tris (pH8.8)	5.0ml
10%SDS	0.2ml
10% Ammonium persulfate	0.2ml
TEMED	0.008ml

- 5% Stacking gel:

H_2O	5.5ml
30% Acrylamide mix	1.3ml
1.5M Tris (pH6.8)	1.0ml
10% SDS	0.08ml
10% Ammonium persulfate	0.08ml
TEMED	0.0008ml

- Running buffer: 10X Tris-Glycine-SDS (Cat. No. 161-0732, Bio-Rad, USA)

- Transfer buffer: 10X Tris-Glycine (Cat. No. 161-0734, Bio-Rad, USA)
- 1X TBS:

  Tris base 2.42g

  NaCl 0.8g

  Made upto 1L with deionized water of pH 7.4.
- 1X TBST

  1X TBS 1L

  0.1%Tween 20

2.6.3 Procedure

BV-2 cells (control and experimental groups) cultured in 6 well plates were washed twice with ice cold PBS. 600µl of protein extraction buffer was added per well and incubated for 10min on ice. The cells were then scraped using cell scraper and the cell lysate was centrifuged at 14,000×g at 4°C for 15min. The supernatant containing total protein was collected and stored at -20ºC for further use. A standard curve was plotted using Protein Assay Standard Lyophilized Bovine Serum (1.25mg/ml) protein assay kit. The standard proteins were prepared using BSA with the following concentrations 0.06, 0.12, 0.24, and 0.48mg/ml in a 96-well plate. 200µl of dye reagent was mixed with 10µl of each standard or sample and was added to each well in a 96-well plate. The sample/standard mixtures were incubated for 15min at RT, and its absorbance was examined at 595nm using microplate reader (GENios, Tecan, Switzerland). Then the concentration of samples was calculated based on the standard curve. 20µg of each protein extract was mixed with 1x SDS gel-loading buffer and heated to

95℃ for 5min to denture the proteins. The denatured proteins were subjected to SDS-PAGE and were separated based on its molecular size. Using the semi-dry electrophoretic transfer equipment (Bio-Rad, USA), the separated proteins were transferred to PVDF membrane. The membrane blots were blocked with 5% non-fat milk protein in 1X TBST at RT for 1h and then incubated with primary antibodies at 4ºC overnight. The following primary antibodies were used: rabbit anti-Dpysl3 (1:500) /Goat anti-Dpysl3 (1:250), rabbit anti-TNF-α (1:500), rabbit anti- IL-1β (1:500), rabbit anti- NF-κB (1:250) and mouse anti-actin (1:10000). Following day, the blots were washed thrice with 1X TBST for 15min and incubated with secondary antibody conjugated horseradish peroxidase (HRP) for 1h at RT. The immunoblots were washed thrice with 1X TBST and then developed using chemiluminescence (ECL). The membrane blots were stripped with stripping buffer and reprobed with β-actin as control. The optical density for each protein bands were quantified using the Quantity One software (Bio-Rad, USA).

2.6.4 Cytoplasmic and nuclear protein extraction

The cytoplasmic and nuclear components of the cells were extracted using the nuclear and cytoplasmic extraction kit (Pierce, Thermo Scientific, Catalog no.78833). The BV-2 cells transfected with scrambled siRNA and Dpysl3 siRNA were trypsinized and the cell pellets were washed with thrice with 1X PBS. To the cell pellet, 100µl of (CER-I) cytoplasmic extraction reagent –I was added and vortexed for 15s. The mixture was then incubated in ice for 10min. Following this, 5.5µl of cytoplasmic extraction reagent –II (CER-II) was added to the

mixture and then was incubated for 1min in ice. The mixture was then centrifuged at 16,000 g for 5min and the supernatant containing the cytoplasmic extract was transferred to a separate tube. To the cell pellet 50µl of nuclear extraction reagent was added and then was incubated in ice for 40min and was with vortex for 10min each. The mixture was then centrifuged for 10min at 16,000g and the supernatant containing the nuclear extract was stored at -80°C for further use.

2.7 Immunohistochemistry and Immunofluorescence staining

2.7.1 Principle

Immunohistochemistry (IHC) is highly sensitive technique that helps to visualize the distribution and localization of specific antigens and cellular components within tissues (Hachmeister and Kracht, 1975). In this technique, antigens can be detected using fluorescent probe or chromogen. In immunofluorescence technique, the antibodies are conjugated with a fluorescent dye and the antigen-antibody complex is visualized through a fluorescence microscope (von dem Borne et al., 1978). First, the cell/tissue samples are fixed to retain the cellular and subcellular architecture. This is followed by a blocking step that prevents non-specific binding of primary antibodies. The Immunofluorescence staining comprises of direct and indirect method. In direct staining method, the primary antibody is labeled with fluorescent dye and in indirect method, the secondary antibody is labeled with a flurochrome which recognizes the primary antibody (Beutner, 1961).

2.7.2 Immunofluorescence labeling

2.7.2.1 Materials

- Rabbit anti-Dpysl3 (Cat. No. AB5454, Millipore, USA)
- Goatanti-Dpysl3 ((Cat. No.SC-27323, Santa Cruz, USA)
- Mouse anti-OX-42 (Cat. No. CBL 1512, Chemicon, USA)
- Rabbit anti-TNF-α (Cat. No. AB2148P, Chemicon, USA)
- Rabbit anti-IL-1β (Cat. No.AB1413, Chemicon, USA,)
- Rabbit anti-iNOS (Cat. No. SC-649, Santa Cruz, USA)
- Rabbit anti-NF-κB (Cat. No. SC-372, Santa Cruz, USA)
- Mouse anti-Rac1 (Cat. No. SC05-389, Millipore, USA)
- Mouse anti-RhoA (Cat. No. SC418, Santa Cruz, USA)
- DAPI (Cat. No. D1306, Molecular Probes, USA)
- Lectin (Cat. No. L0401, Sigma, USA)
- Anti-Rabbit Cy3 (Cat. No. C2306, Sigma, USA)
- Anti-Mouse FITC (Cat. No. F9137, Sigma, USA)
- Anti-Rabbit FITC (Cat. No. F6005, Sigma, USA)
- 0.1M phosphate buffer, pH-7.4
- 10X Phosphate buffer saline PBS (Cat. No. PB0344-1L, Vivantis, USA)
- 4% Paraformaldehyde:

  Paraformaldehyde- 4g

  0.1M phosphate buffer - 100ml

2.7.2.2 Brain tissue sections

The tissue sections were rinsed in PBS (thrice for 10min each), and blocked with 5% normal goat serum or normal horse serum for 1h. The sections were incubated with rabbit anti-Dpysl3 (1:500)/Goat anti-Dpysl3 (1:200) and mouse OX-42 (1:50) antibody at 4°C overnight. The following day, the tissue slides were washed thrice with 1X PBS and then incubated with Cy3 or FITC conjugated secondary antibodies for 1h in the dark. Finally, the sections were counterstained with DAPI and mounted using the DAKO fluorescent mounting medium. The tissue sections were visualized using a Confocal microscope (Fluoview, FV1000; Olympus, Tokyo, Japan).

2.7.2.3 BV-2 cells-Poly-lysine coating of coverslips

The sterilized cover slips were plated in each well of 24-well plate. 400µl of poly-L-lysine was added to each coverslips and the plate was incubated for 3h at RT. After the incubation time, the wells were washed thrice with 1X PBS and then theBV-2 cells were seeded.

BV-2 cells (control and experimental groups) were washed thrice with 1X PBS and fixed in 4% PF for 30min at RT. Then the cells were washed and then blocked with 5% normal goat serum for 1h. Following incubation, the cells were incubated with primary antibodies directed against rabbit anti-Dpysl3 (1:500)/Goat anti-Dpysl3 (1:200),or rabbit anti- TNF-α (1:200), or rabbit anti- IL-1β (1:200), or rabbit anti- iNOS (1:200), or rabbit anti-NF-κB (1:200), or mouse anti-RhoA (1:200) and mouse anti-Rac1 (1:200) at 4°C overnight. The following day, the cells were washed thrice with 1X PBS 10min and then incubated with

Cy3/FITC-conjugated secondary antibodies for 1h at RT. Then the cells were stained with Lectin for 30min and counterstained with DAPI for 3min. Finally, the cells were washed with 1X PBS and coverslips were mounted with DAKO fluorescent mounting medium. The slides were visualized using a Confocal microscope.

2.7.2.4 F-actin labeling

2.7.2.4.1 Material

- Phalloidin-Rhodamine (Cat. No. PHDR1, Cytoskeleton Inc., USA)

2.7.2.4.2 Procedure

The actin cytoskeleton in microglia was detected using Phalloidin-Rhodamine (3.5µl:500µl of PBS) dye. BV-2 microglial cells grown on coverslips were fixed with 4% PF for 30min at RT. The BV-2 cells were washed thrice in 1X PBS and then incubated with Phalloidin-Rhodamine (according to the manufacturer's instructions) for 30min at RT. Following incubation, the cells were washed thrice with 1X PBS and the coverslips were mounted using DAKO fluorescent mounting medium onto the slides (Christensen et al., 2006).

2.8 *in vitro* migration assay

2.8.1 Materials

- Polycarbonate membrane transwell inserts, 8µm pore size (Cat. No. 3422, Corning, USA)

- Lipopolysaccharide LPS (Cat. No. L2654, Sigma, USA)

2.8.2 Procedure

The migration of microglia *in vitro* was evaluated using 8µm pore size polycarbonate membrane transwell inserts. The BV-2 cells transfected with scrambled siRNA (negative control) and Dpysl3 siRNA were grown in 6-well plates. To examine chemotactic migration, the transfected BV-2 cells were trypsinized and added at a density of 5×10^4 cells in 200µl of serum-free medium to the upper well of the transwell insert. 500µl of serum free medium with and without LPS was applied to the bottom of transwell insert (Kim et al., 2006a; Karlstetter et al., 2011). The BV-2 cells in transwell insert were incubated for 24h in a humidified incubator filled with 5% CO_2 and 95% air at 37°C. The cells present on the upper layer of the transwell insert were removed with a moist cotton swab, and the transfected cells migrated to the bottom layer of the insert were fixed with methanol for 15min at RT and then stained using 1% crystal violet. The migrated cells on the bottom layer of the transwell insert were quantified and captured using the light microscope (Leica, CLS150X, Germany).

2.9 Phagocytosis

2.9.1 Materials

- 0.8µm latex beads (Cat. No. L398, Sigma, USA)

2.9.2 Procedure

Phagocytosis was assayed using latex beads (Marker et al., 2012). At first, the BV-2 cells transfected with scrambled siRNA and Dpysl3 siRNA for 48h in a 24-well plate. Following transfection, the transfected BV-2 cells were stimulated with LPS (1µg/mL) in DMEM for 1h. To examine the microglial phagocytic activity, 1µl/ml of 0.8µm latex beads (Sigma) were added to each well and then incubated for 2h at 37°C in a humidified chamber filled with 5% CO_2 and 95% air. Following transfection, the transfected BV-2 cells were fixed with 4% PF for 20min and excess beads were removed by washing thrice with ice cold 1X PBS for 10min each. Phagocytic cells were visualized and captured under confocal microscope with phase contrast settings. Phagocytic cells (containing minimum of 10 beads per cell) were counted in each microscopic field (Allen et al., 2002).

2.10 Nitric oxide assay

2.10.1 Principle

Nitric oxide (NO) plays a vital role in immune response, neurotransmission and apoptosis. Nitric oxide is oxidized to nitrite and nitrate to determine NO production. Nitric oxide colorimetric bioassay kit measures NO in a two step process. The first step involves conversion of nitrate to nitrite using the nitrate reductase enzyme. The second step uses Griess reagents that converts nitrite to a purple azo compound (US Biological Nitric Oxide Colorimetric BioAssay Kit handbook).The amount of azo chromophore determines the amount of nitric oxide in samples (Stone et al., 2006).

2.10.2 Materials

- Nitric Oxide Colorimetric BioAssay Kit (Cat. No. 2577-01, US Biological,Massachusetts, USA)

2.10.3 Procedure

The quantity of NO was measured using the colorimetric nitric oxide assay kit with a Griess reagent system. Culture supernatant from the BV-2 cells transfected with scrambled siRNA and Dpysl3 siRNA was collected 1h after LPS treatment. At first, 200µl/well of diluted assay buffer was coated to a 96 well plate, and then 80µl/ well of the supernatants were added to it. Later, 10µl/well of the enzyme cofactor mixture and then 10µl/well of the reconstituted nitrate reductase were added to the wells subsequently. The plates were covered and incubated for 1-4h at RT, then 50µl/well of Griess reagent R1 and 50µl of Griess reagent R2 were added immediately. A colored product developed within 10min at RT and the absorbance was measured at 540nm with EMAX precise microplate reader (Molecular Devices, USA). The NO production of the samples was calculated using standard curve obtained from the nitrate standard using the formula: [Nitrate+Nitrite](µM)=[(A540-Yintercept)/(slope)x(200µl/samplevolume(µl))]xDilution.

2.11 Cell viability assay

2.11.1 Material

- CellTiter 96 Aqueous One Solution Cell Proliferation Assay kit (Cat. No. G3582, Promega, USA)

2.11.2 Procedure

The viability of siRNA transfected BV-2microgliawere measured using CellTiter 96 Aqueous One Solution Cell Proliferation Assay kit. The transfected BV-2 cells were seeded at a density 2.0×10^5 in a 6-well plate and then transfected with scrambled siRNA (negative control) andDpysl3siRNA. 200µl/well of MTS reagent was added toeach seeded well and the plate was incubated for 4h in a humidified chamber of 5% CO_2 and 95% air at 37°C. Following the incubation, the absorbance was measured at 490nm using a microplate reader (GENIOS, Tecan, Switzerland). The absorbance measured is proportional to the number of BV-2 cells seeded in each well at different conditions.

2.12 BrdU assay

2.12.1Principle

Bromodeoxyuridine (BrdU) is a thymidine analog that incorporates into the newly synthesized DNA strands of actively proliferating cells (Rothaeusler and Baumgarth, 2007; Lehner et al., 2011). Anti-BrdU antibodies are used to detect the incorporated BrdU in cellular DNA. The number of BrdU positive cells can be quantified to determine the rate of cell proliferation.

2.12.2 Materials

- Mouse anti-BrdU monoclonal antibody (Cat. No. B2531, Sigma, USA)
- Anti-Mouse Cy3 (Cat. No. C2181, Sigma, USA)
- Lectin (Cat. No. L0401, Sigma, USA)
- Fluorescent Mounting Medium (Cat. No. S302380, Dako Cytomation, Denmark)
- Phosphate Buffered Saline, 10XPBS (Cat. No.PB0344-1L, Vivantis, USA)
- 1X PBS containing 0.1% Triton-X 100 (PBS-TX)
- 4% Paraformaldehyde (PF)

  Paraformaldehyde-4g

  0.1M Phosphate buffer pH-7.4-100ml

2.12.3 Procedure

The transfected BV-2 cells were incubated with BrdU (10µmol/l) for 2h, then the cells were washed with twice of 1X PBS-TX and then fixed with 4% PF for 20min at 4ºC. Next, the fixed cells were treated with 2NHCl at 37ºC for 30min and then washed thrice with 1X PBS-TX. Subsequently, the cells were blocked with 5% normal goat serum for 1h, and incubated with anti-BrdU monoclonal antibody (1:1000) overnight at 4ºC. Further, the cells were washed with twice of 1X PBS and incubated with goat anti-mouse secondary antibody conjugated with Cy3 (1:200) for 1h at RT. Then the cells were counterstained with Lectin (1:300) for 30min and DAPI. Finally, the coverslips were mounted with DAKO mounting medium and visualized in a Confocal microscope. The percentage of BrdU

positive cells was assessed by scoring 5 fields each in control and experimental groups.

2.13 Co-Immunoprecipitation

2.13.1 Principle

Co-immunoprecipitation is a widely used technique to identify protein-protein interactions. Co-immunoprecipitation is based on immunoprecpitation which shares the principle of antigen-antibody interaction (Masters, 2004). In this method, an antibody specific for a target protein forms an immune complex and binds to its target in a cell lysate. This immune complex is precipitated using agarose A/G beads. The agarose beads are immobilized with the antibody binding protein and other proteins that are not precipitated are washed away. Following this step, the purified sample is subject to SDS-PAGE and western blot to identify the antigen.

2.13.2 Materials

- Agarose G beads (Cat. No. 20398, Pierce, USA)
- Control Mouse Isotope IgG (Cat. No. SC2025, Santa Cruz, USA)
- Mouse anti-Rac1 (Cat. No. SC05389, Millipore, USA)
- Mouse anti-RhoA (Cat. No. SC418, Santa Cruz, USA)
- Mouse anti-Dpysl3 (Cat. No. 100323, Santa Cruz, USA)
- RIPA lysis Buffer:

  5M NaCl 500µl

1M Tris pH8.0	2500µl
0.5M EDTA	100 µl
Triton-100	50 µl
Sodium Deoxycholate	0.05g
10% SDS	250µl
1XProteinase inhibitor	5000 µl

- Deionized water make up the volume to 50ml.

2.13.3 Procedure

BV-2 cells are washed twice with ice cold 1X PBS and then incubated with 1ml of RIPA lysis buffer for 10min on ice. The cells were scraped using a cell scraper transferred to a centrifuge tube. The tubes were incubated for 30min in an end-to-end shaker at 4°C. The cells were centrifuged for 13,200 rpm for 10min at 4°C. The protein supernatant was collected and quantified using protein assay kit. The protein sample is mixed withDpysl3 antibody (4µg) and incubated in the shaker overnight at 4°C. For the control, the protein samples were mixed with isotype control mouse IgG antibody and incubated in the shaker at 4°C overnight. The next day, 20µl of agarose G beads are added to the control isotypic and antibody mixed samples and incubated for 1h in the shaker at 4°C. Later, the protein samples are centrifuged at 300rpm for 1min at 4°C, the supernatant was discarded off. The beads were washed thrice with RIPA buffer and centrifuged at 300rpm at 4°C for 1min, and then the protein supernatant was removed without losing the beads. The bead samples are mixed with 20µl of 2x SDS and boiled to 95°C for 5

min, then the samples were spun and the supernatant were collected and loaded on SDS-PAGE.

2.14 Quantitative analysis

The number of Dpysl3-positive microglial cells was counted from at least 5 tissue sections cut through the corpus callosum (30µm thickness) from 3 different brain samples. The percentage of Dpysl3-positive cells was calculated by counting the number of Dpysl3-positive cells in OX42-stained microglial cells and the total number of OX42–positive microglial cells in a specified unit area on each section. The average immunofluorescence intensity of Dpysl3 in BV-2 microglial cells was calculated using the software (Fluoview, FV1000). The Dpysl3 immunofluorescence staining in an individual BV-2 microglial cell was captured using a Confocal microscope. About 15 microglial cells from 3 different slides of each group were selected and outlined, and then the mean value of the Dpysl3 staining intensity of outlined BV-2 microglia was measured. The Fold change was calculated (Lin et al., 2011).

2.15 Statistical analysis

All experiments were performed in triplicates. The difference between experimental and control groups was calculated by one way analysis of variance (ANOVA) followed by Bonferroni test using the graph pad prism5 software. The data are represented as mean ± SD from at least three independent experiments and was considered significant when $p<0.05$.

Chapter 3

Results

3.1 Differential expression of Dpysl3 in the developing rat brain

The amoeboid microglial cells (AMC) have been shown to be predominant in the corpus callosum (CC) region (Fig.1) of the postnatal rat brain (Ling and Wong, 1993). The expression of Dpysl3 in developing rat brains (3, 5, 7 and 14 days) was examined by immunofluorescence technique (Fig 2B-M). Dpysl3 was found to be highly expressed in AMC of 3-day rats and the expression decreased progressively in 5-day and 7-day rats (Fig.2C, F, and I). In 14-day rat pups, the expression of Dpysl3 was hardly detectable in ramified microglia (RMC) (Fig.2L). Quantitative analysis revealed that the percentage of Dpysl3-postive AMC was markedly more in CC of 3-day and 5-day old rat pups when compared to 7-day and 14-day old rat pups (Fig.2N).

3.2 Expression of Dpysl3 is increased in activated microglia

3.2.1 In LPS injected rat brains

The expression of Dpysl3 in activated microglia was examined by immunofluorescence in 5-day old and 28-day old rats treated with LPS. In the CC of 5-day old rats injected with LPS, the expression of Dpysl3 was found to be increased in AMC when compared to the control rats that were injected with saline (Fig.3A-F). Quantitative analysis revealed that the percentage of Dpysl3-positive microglial cells was increased significantly in LPS treated 5-day old rat pups than that of control (Fig.3G). Similarly, the expression of Dpysl3 was increased in CC of 28-day rat brains injected with LPS when compared to the control (Fig.4A-F). Quantitative analysis indicated that the percentage of Dpysl3-

positive microglial cells was increased in CC significantly in LPS-treated 28 day rats when compared to the control (Fig.4G).

3.2.3 Activated microglial cultures

3.2.3.1 Primary microglia

The immunofluorescence expression of Dpysl3 was localized in primary microglia (Fig.5A-F). The expression level of Dpysl3 was increased in activated microglia by LPS (Fig. 5D-F) when compared to the control (Fig.5A-C).

3.2.3.2 Murine microglial cell line, BV-2

The expression of Dpysl3 in mouse microglial cell line, BV-2 was investigated in various time points (1h, 3h, 6h) of LPS administration. The expression of Dpysl3 mRNA was found to be upregulated significantly (~2.8 fold) in BV-2 microglia following LPS treatment for 1h and decline subsequently at 3h and 6h of LPS treatment (Fig.6A, B). Immunofluorescence analysis revealed that the expression of Dpysl3 protein was increased in BV-2 cells following LPS treatment for 1h as compared to control (Fig 6C-F). However, the increase of Dpysl3 expression was not evident in BV-2 cells treated with LPS for 3-6h.The expression level of Dpysl3 protein was examined in LPS activated BV-2 cells by western blot (Fig.6G, H). The Dpysl3 protein level was increased significantly following LPS treatment for 1h in comparison to control cells. This increase was found to be decreased in BV-2 microglia at 3h and 6h of LPS treatment. (Fig.6G, H). The maximal expression of Dpysl3 was evident at 1h post-LPS treatment, the microglia was exposed to LPS for 1h in all the subsequent experiments.

3.3 Distribution of Dpysl3 in activated BV-2 microglia

The F-actin cytoskeleton of microglia was detected by Phalloidin-Rhodamine labeling (Christensen et al., 2006). BV-2 microglia in control medium appeared immotile with cell processes retracted (Fig.7B). In contrast, activated BV-2 microglia cells by LPS showed actin-containing microspikes (Fig.7E). Double staining with Phalloidin-Rhodamine revealed the co-localization of Dpysl3 and F-actin preferentially in actin bundles (Fig.7D-F). This result suggests that Dpysl3 is involved in the cytoskeletal reorganization in microglial motility.

3.4 Dpysl3 regulates the proinflammatory cytokines and neurotoxic mediators in activated microglia through NF-κB signaling pathway

3.4.1 siRNA knockdown of Dpysl3

siRNA-mediated knockdown of Dpysl3 was performed in BV-2 cells in order to understand the function of Dpysl3 in microglia. qRT-PCR analysis showed that the expression of Dpysl3 mRNA was decreased to about 80% in Dpysl3 siRNA transfected cells in comparison to the cells transfected with scrambled siRNA (Negative Control) (Fig.8A). In order to determine if the changes in Dpysl3 mRNA expression following transfection were due to cell death, the cell viability assay was carried out at 48h post transfection. About 90% of the of BV-2 microglia were found to be viable following transfection in comparison to that of non-transfected BV-2 microglia (Fig.8B). The efficient siRNA-mediated knockdown of Dpysl3 was further confirmed by western blot analysis (Fig 8C, D). It was observed that after LPS treatment increased the Dpysl3 expression

level in BV-2 microglia transfected with scrambled siRNA (negative control) whereas, the knockdown of Dpysl3 in BV-2 microglia treated with or without LPS significantly inhibited the Dpysl3 expression (Fig.8C, D).

3.4.2 Knockdown of Dpysl3 decreases the production of TNF-α cytokine by activated microglia

Activated microglia release a number of proinflammatory cytokines namely TNFα, IL-1β and nitric oxide (NO) resulting in cytotoxicity to the neighboring neuronal cells (Smith et al., 2012). To address this, we studied the cytokines level in activated microglial cells following knockdown of Dpysl3 using siRNA.

qRT-PCR analysis showed that the expression level of TNF-α mRNA was significantly increased in scrambled siRNA (negative control) transfected BV-2 microglia cells exposed to LPS in comparison to cells transfected with negative control siRNA. However, following knockdown of Dpysl3, the LPS-induced increase in the expression of TNF-α mRNA was markedly attenuated as compared to the scrambled siRNA control (Fig.9A). Immunofluorescence analysis revealed a similar trend in the expression of TNF-α in LPS activated BV-2 microglia following knockdown of Dpysl3 (Fig.9B-E). The western blot further confirms that knockdown of Dpysl3 prevents the LPS-induced increase in expression of TNF-α protein (Fig.9F, G).

3.4.3 Knockdown of Dpysl3 decreases the production of IL-1β cytokine by activated microglia

qRT-PCR analysis showed that the mRNA expression level of IL-1β was upregulated in scrambled siRNA transfected BV-2 microglial cells exposed to LPS in comparison to negative control siRNA transfected cells. Knockdown of Dpysl3 decreased the expression IL-1β mRNA in LPS activated cells when compared to the control. (Fig.10A). This expression pattern was also observed in the intensity of IL-1β immunofluorescence in LPS activated microglia following knockdown of Dpysl3 (Fig.10B-E). The results of western blot further confirmed that knockdown of Dpysl3 reduced the expression level of IL-1β protein in activated microglia as compared to the scrambled siRNA microglial cells (Fig.10F,G).

3.4.4 Knockdown of Dpysl3 reduces the expression of iNOS expression in activated microglia

qRT-PCR analysis revealed that the mRNA expression of iNOS was increased in LPS treated BV-2 microglia, whereas knockdown of Dpysl3 significantly decreased the mRNA expression of iNOS in activated BV-2 microglial by LPS as compared to scrambled siRNA cells exposed to LPS (Fig.11A). In addition, this result was also confirmed by Dpysl3 immunofluorescence in BV-2 microglia (Fig.11B-E).

3.4.5 Knockdown of Dpysl3 reduces production of nitric oxide in activated microglia

The amount of nitric oxide (NO) produced by microglial cells was measured in the medium obtained from BV-2 microglial cultures subjected to LPS treatment following siRNA transfection. The concentration of NO in scrambled siRNA transfected BV-2 microglial cells was observed to be increased after 1h of LPS stimulation. However, knockdown of Dpysl3 significantly reduced the induction of NO production by activated microglia (Fig.12).

3.4.6 Knockdown of Dpysl3 suppresses NF-κB transcriptional activity

Activation of NF-κB activation is associated with microglial activation. NF-κB is an important transcription factor that regulates genes encoding proinflammatory cytokines, chemokines, and growth factors, thereby contributing to immune and inflammatory reaction (Meffert and Baltimore, 2005). NF-κB was localized in the cytoplasm of BV-2 microglia transfected with scrambled siRNA and Dpysl3 siRNA (Fig.13A, B). In activated BV-2 microglia by LPS, the nuclear translocation of NF-κB was evident (Fig.13C). However, knockdown of Dpysl3 markedly inhibited the NF-κB nuclear translocation in activated BV-2 microglia by LPS (Fig.13D). Western blot analysis using the nuclear protein derived from activated BV-2 microglia by LPS further confirmed that the knockdown of Dpysl3 significantly decreased the NF-κB protein expression as compared to the negative control cells

(Fig.13E, F). The cytoplasmic NFkB shows no obvious change in its protein level as compared with nuclear NFkB (Data not shown).

3.5 Dpysl3 regulates F-actin cytoskeleton, migration, phagocytosis and proliferation of microglia

3.5.1 Knockdown of Dpysl3 alters the structure of F-actin organization

Phalloidin labeling revealed that Dpysl3 colocalizes with F-actin cytoskeleton in BV-2 microglia (Fig 14A-C) and hence the organization of F-actin in BV-2 microglia following knockdown of Dpysl3 was examined. The immunofluorescence staining in BV-2 microglia transfected with scrambled siRNA showed that the expression of Dpysl3 colocalized with F-actin which is associated with an orderly disturbed actin bundles (Fig.14A-C). Activated BV-2 microglia by LPS exhibit microspike projections with intense staining of F-actin with Dpysl3 (Fig.14D-F). The siRNA-mediated knockdown of Dpysl3 drastically reduced the immunoexpression of Dpysl3 in BV-2 microglia (Fig.14G-L). Further, knockdown of Dpysl3 inhibited the formation of microspike projections and reduced the actin staining intensity in activated BV-2 microglia when compared to that of activated microglia transfected with scrambled siRNA (Fig.14J-L). The quantitative analysis showed that the siRNA mediated knockdown of Dpysl3 reduced the expression of Dpysl3 protein in BV-2 microglia, in comparison to that of cells transfected with scrambled siRNA (Fig.14M). This experiment revealed that knockdown of Dpysl3 disturbed the arrangement of F-actin in microglial cells suggesting that Dpysl3 plays an important role in cytoskeletal rearrangement in microglia.

3.5.2 Knockdown of Dpysl3 inhibits migration of microglia

Since Dpysl3 appears to be involved in F-actin cytoskeleton organization, its role in cell migration was assessed by the transwell migration assay. For chemotaxis, LPS was added to the bottom of the chamber (Kim et al., 2006a; Karlstetter et al., 2011) and the optimal time for cells to be activated and to migrate towards LPS in the bottom chamber were determined. Migration of BV-2 microglia transfected with scrambled siRNA was significantly increased towards the lower well containing medium with LPS (Fig.15C) when compared to that of BV-2 microglia transfected with scrambled siRNA or Dpysl3 siRNA (Fig 15A, B). However, siRNA-mediated knockdown of Dpysl3 reduced the chemotactic migrating capability of activated BV-2 microglia (Fig.15D, E). These results indicate that Dpysl3 regulates the migratory ability of microglia.

3.5.3 Knockdown of Dpysl3 inhibits phagocytic ability of microglia

To investigate the role of Dpysl3 in promoting microglial phagocytosis, the uptake of latex beads by microglia was assessed *in vitro* (Marker et al., 2012). The results of this assay showed that in unstimulated BV-2 microglial cells transfected with scrambled siRNA and Dpysl3 siRNA, only a small percentage of cells ingested with latex beads (Fig.16A, B). After LPS stimulation, the number of phagocytic cells laden with latex beads was significantly increased (Fig.16C, E). However in cells transfected with Dpysl3 siRNA treated with LPS significantly inhibited the latex beads adsorption (Fig.16D, E) suggesting that Dpysl3 modulates the phagocytic ability of microglia.

3.5.4 Knockdown of Dpysl3 reduces the proliferation of activated microglia

CRMPs proteins have been shown to affect the proliferation index, and hence the role of Dpysl3 in proliferation of microglia was studied by the BrdU incorporation assay (Lehner et al., 2011). The LPS treatment increased the number of BrdU positive BV-2 microglia transfected with scrambled siRNA (Fig.17D-F) in comparison to that of scrambled siRNA transfected cells (Fig 17A-C). However knockdown of Dpysl3 reduced the proliferation index in activated microglia by LPS (Fig.17J-L, M). In addition to this, the BV-2 cells were labeled with microglia marker lectin (Fig.17A, D, G, J).

3.6 Interaction of Dpysl3with Rho GTPases

3.6.1 Interaction of Dpysl3 with RhoA

Studies have reported that Dpysl3 interacts with Rho GTPases (namely, RhoA and Rac1)(Alabed et al., 2007)which are necessary for cytoskeletal organization and help in the process of cell migration (Van Aelst and D'Souza-Schorey, 1997; Barcia et al., 2012). RhoA pathway plays a prominent role in mediating the inflammatory and oxidative responses in microglia (Villar-Cheda et al., 2012). The interaction of Dpysl3 and RhoA was examined in microglia by co-immunoprecpitation. Western blot result shows the protein expression of Dpysl3 and RhoA in BV-2 microglia before and after precipitation (Fig.18). Dpysl3 and RhoA co-immunoprecpitation was observed in control as well as LPS treated microglia. Microglia immunoprecipitated with isotype G was used as control to validate the specificity of the protein signal obtained.

3.6.1.1 Knockdown of Dpysl3 reduces RhoA in activated microglia

Interaction of Dpysl3 with Rho A has been demonstrated in neurons (Alabed et al., 2007). qRT-PCR results showed that mRNA expression of RhoA was increased upon LPS treatement to BV-2 cells transfected with scrambled siRNA. However in cells transfected with Dpysl3 siRNA treated with LPS, the RhoA expression was significantly attenuated in BV-2 microglial cells transfected with Dpysl3 siRNA (Fig.19A). A similar pattern of decreased intensity of RhoA expression was observed in Dpysl3 siRNA transfected BV-2 cells (Fig.19B-E). The western blot result also confirmed a significant reduction in RhoA protein expression in LPS-activated BV-2 microglia transfected with Dpysl3 siRNA as compared to negative control (Fig.19 F, G).

3.6.2 Interaction of Dpysl3 with Rac1

Rac1 signaling in microglia promotes NADPH oxidase for the formation of reactive oxygen species (Gao et al., 2003; Zhang et al., 2012). Rac1 activation promotes microglial phagocytosis (Wilkinson et al., 2006). The interaction of Dpysl3 and Rac1 was observed in microglia by co-immunoprecpitation. Western blot result indicates the protein expression of Dpysl3 and Rac1 in BV-2 microglia before and after precipitation (Fig.20). Dpysl3 and Rac1 co-immunoprecpitation was detected in both control and LPS treated microglial cells. The microglia immunoprecipitated with isotype G was used as control for confirmation.

3.6.2.1 Knockdown of Dpysl3 reduces the Rac1 in activated microglia

Dpysl3 interaction with Rac1 was confirmed by co-immunoprecpitation. The Rac1 expression was also examined in BV-2 cells transfected with Dpysl3 siRNA. qRT-PCR results showed a significant decrease in mRNA expression of Rac1 upon LPS treatement to the cells transfected with Dpysl3 siRNA compared to that of activated microglia transfected with scrambled siRNA (negative control) (Fig.21A). Immunofluorescence analysis also showed the similar pattern of intensity of Rac1expression in activated BV-2 microglia transfected with Dpysl3 siRNA (Fig.21B-E). The western blot results further confirmed that the protein expression of Rac1 was significantly reduced in activated BV-2 microglia transfected with Dpysl3 siRNA compared to that of scrambled siRNA transfected cells (Fig.21F, G).

Chapter 4

Discussion

Activation of microglia is characterized with altered morphology extensive proliferation, chemotaxis, migratory behavior, and phagocytic ability in several neurodegenerative disorders and neuropathological conditions (Chamak and Mallat, 1991; Nolte et al., 1996; Guillemin and Brew, 2004; Dheen et al., 2007). Many of these processes in activated microglia are interrelated and involve dynamic reorganization of the actin cytoskeleton (Cross and Woodroofe, 1999; Martin et al., 2003), morphological changes, and lamellipodia projections which are important in the initiation of cell migration (Lauffenburger and Horwitz, 1996; Mitchison and Cramer, 1996). In addition, it has been reported that activated microglia in neonatal rats following hypoxia mediate the release of pro-inflammatory cytokines, nitric oxide and free radicals (Deng et al., 2008). Controlling or inhibiting microglial activation is considered to be the primary therapeutic option in neurodegenerative disorders. Understanding the role of a cytoskeletal gene, Dpysl3 in regulating the function of activated microglia was the primary focus of this present study.

4.1 Dpysl3 is developmentally regulated in microglia

The function of Dpysl3 is well documented in neurogenesis and regeneration mediated by Semaphorin 3A / PlexinA signaling (Goshima et al., 1995; Nacher et al., 2002; Alabed et al., 2007). However the expression and role of Dpysl3 in microglia has remained unexplored. The present study convincingly demonstrated that Dpysl3 is developmentally regulated in microglia as it was found to be expressed in amoeboid microglial cells in postnatal rat brain from 3-day to 5-day and was hardly detected in ramified microglia in the brain of 14 day rats. The

microglial cells in the developing brain have been reported to phagocytose apoptotic cells, cellular debris and dying neurons (Eyo and Dailey, 2013). The high expression of Dpysl3 in amoeboid microglia in early postnatal rat brain may be associated in rearrangement of microglial cytoskeleton in mediating the process of phagocytosis and migration in the developing brain.

4.2 Dpysl3 expression increases in activated microglia *in vitro* and *in vivo*

Activated microglial cells are involved in inflammatory processes in the CNS and have been described in several neurodegenerative disorders. The microglial activation in response to neurological diseases namely Alzheimer's , Parkinson's disease or LPS has been shown to be associated with excessive production of pro-inflammatory cytokines including IL-1β, TNF-α, IL-6 (Lund et al., 2006a) and neurotoxic mediators such as NO and ROS.

LPS has been widely shown to activate microglia and mediate neurotoxic effects in both *in vitro* and *in vivo* system (Nakamura et al., 1999; Tanaka et al., 2006). In macrophages and microglia, studies have described that binding of LPS to TLR4 receptors triggers the signaling cascades resulting in phosphorylation of NF-κB thereby play a key role in mediating inflammation in these cells (Sakurai et al., 1999). In this study, Dpysl3 expression was found to be induced in LPS-activated microglia, suggesting its role in the inflammation response of microglia.

4.3 Dpysl3 knockdown attenuated the production of proinflammatory cytokines and inflammatory mediators in activated BV-2 microglia

Microglial activation is necessary for host defense and over activation of microglia is neurotoxic as reported in several neurodegenerative disorders (McGeer et al., 2005). Therefore, we have studied the effect of knockdown of Dpysl3on proinflammatory cytokines and neurotoxic mediators generated by activated microglial cells. Neuroinflammation occurs in response to injury or infection or noxious stimuli in the CNS thereby leading to multiple neurodegenerative diseases (Wilms et al., 2007). Microglia, as the resident innate immune cells in the brain, actively monitor the microenvironment in the brain and are activated in response to diverse cues to produce proinflammatory cytokines namely TNF-α and IL-1β (Sawada et al., 1989) cytotoxic molecules such as reactive oxygen/nitrogen intermediates including ROS (Colton and Gilbert, 1987) and NO (Liu et al., 2002). In the present study, knockdown of Dpysl3 in BV-2 microglia significantly suppressed the LPS-induced protein levels of proinflammatory cytokines, IL-1β and TNF-α, suggesting that Dpysl3 could be an important mediator for cytokine production in activated microglial cells. The downregulation of Dpysl3 may lead to an effective inhibition of microglial activation and cytokine production.

iNOS catalyzes the production of nitric oxide (NO) which, acts as a neurotransmitter in the CNS and has protective functions in anti-inflammatory pathways (Possel et al., 2000). However, high concentrations of NO results in cell death and can therefore potentially be neurotoxic (Chao et al., 1992). In the

present study, Dpysl3 knockdown resulted in decreased iNOS expression and NO production in activated microglial cells. In the light of this, it is suggested that Dpysl3 is linked to increased iNOS expression and subsequent NO release in microglia.

4.4 NF-κB pathway is involved in Dpysl3 mediated microglial activation

NF-κB is an important transcription factor shown to regulate genes involved in diverse functions including inflammation and immune responses. Under normal conditions, NF-κB is in an inactive state and is localized in the cytoplasm (Rhoads et al., 2010; Schuster et al., 2013). The NF-κB in pathological conditions is phosphorylated and translocates to the nucleus whereby it mediates the expression and regulation of pro-inflammatory genes (namely TNF-α and IL-1β), chemokines and growth factors in activated microglia (Viatour et al., 2005). In activated microglia, the NF-kB is transcriptionally activated and translocated to nucleus mediating the inflammatory response (Meffert and Baltimore, 2005; Shen et al., 2005; Baker et al., 2011).The present study demonstrated that knockdown of Dpysl3 significantly inhibits the LPS-induced transcriptional activity of NF-κB in BV-2 microglia, suggesting that Dpysl3 regulates NF-κB activity which may alter the inflammatory response of activated microglia. The present study shows that NF-κB as one of the downstream pathways involved in Dpysl3-induced production of inflammatory mediators. Overall, these results suggest that downregulation of Dpysl3 inhibits microglial activation and subsequent inflammation by preventing the production of proinflammatory cytokines and the neurotoxic mediator, NO.

4.5 Dpysl3 regulates cytoskeletal dynamics in activated microglia

The process of migration is regulated by changes in the organization of actin and tubulin cytoskeletal proteins in microglia (Eugenin et al., 2005; Stricker et al., 2010; Vincent et al., 2012). The cytoskeletal architecture consists of microtubules in central domain and F-actin in the peripheral domain. During the migration, the tubules invade from central to peripheral domain along with the actin rich lamellar region (Chhabra and Higgs, 2007) thereby mediating the cell movement.

LPS not only activates genes responsible for production of cytokines but it also causes marked changes in the morphological and cytoskeletal organization of microglia (abd-el-Basset and Fedoroff, 1995). Activation of microglia includes changes in cell shape, proliferation, migration and phagocytosis and is regulated by the organization of F-actin cytoskeleton. Regulation of F-actin dynamics is important for the cell motility processes (Lambrechts et al., 2004; Lippman et al., 2008). Actin polymerization and depolymerization is involved in maintaining cell morphology and cell survival (Friedl, 2004). Dpysl3 has been widely shown to regulate cytoskeletal dynamics and F-actin bundling, which is essential for the cell motility process (Rosslenbroich et al., 2005). In neurons, overexpression of Dpysl3 has been shown to result in the extension of filopodia and neurite branches (Alabed et al., 2007). In the present study, Dpysl3 was localized with F-actin and its expression was increased along the microspike projections of activated microglia. In addition, the knockdown of Dpysl3 appeared to inhibit the formation of microspike projection in activated microglia, suggesting the

importance of Dpysl3 in regulating actin cytoskeleton in microglia and their migration when activated.

4.6 Dpysl3 knockdown reduces microglial migration

Activated microglia migrate to the site of injury or infection in the CNS (Blinzinger and Kreutzberg, 1968; Banati et al., 1993) and their migration process is regulated by organization of actin cytoskeleton (Stence et al., 2001; Saraswathy et al., 2006).The present study has also shown that knockdown of Dpysl3 significantly perturbed the actin dynamics and the migration ability of activated microglia indicating that Dpysl3 promotes migration of activated microglia by regulating their cytoskeletal dynamics. This finding is significant as it may provide a functional basis for designing specific therapeutic strategy to delay or control migration of microglia to the site of injury or infection.

4.7 Dpysl3 knockdown reduces microglial proliferation

Microglia have the capacity to increase their cell numbers upon injury in CNS and in neurological diseases (Kettenmann et al., 2011). The microglial proliferation contributes to brain repair and functional recovery through inflammatory response and phagocytosis. However, excessive proliferation has been shown to be detrimental in chronic neurodegenerative disease producing cytotoxic molecules. . Dpysl3 has been shown to be associated with proliferation in neurons (Lin and Hsueh, 2008). However, the present study demonstrated that Dpysl3 is involved in the proliferation of microglia showing that knockdown of Dpysl3 resulted in significant reduction in the proliferation of activated microglia.

4.8 Dpysl3 knockdown reduces the phagocytic activity of activated microglia

In addition to motility and migration, actin remodeling has been shown to be critical for efficacy of phagocytosis and antigen presentation in immune cells (Abd-el-Basset and Fedoroff, 1994; Smith et al., 1998). Phagocytosis is a process which is initiated by attachment of particle bound ligands to phagocytic cell surface receptors (Guzman-Beltran et al., 2012). These receptors trigger signaling proteins at the particle binding site resulting in reorganization of actin cytoskeleton for particle ingestion (Gitik et al., 2010). Activated microglia show enhanced phagocytic function *in vitro* and *in vivo* (Smith et al., 1998; Neher et al., 2011)and have been shown to engulf substances, including latex beads, *E.coli*, α2 macro-globulin, fluorescent labeled liposomes, zymosan *in vitro* (Smith, 2001; Kaur et al., 2004). It is possible that Dpysl3 mediates phagocytosis ability of microglia as it regulates actin dynamics.

In the present study, the Dpysl3 knockdown significantly inhibited the phagocytic ability of activated microglia, thus strengthening the notion that Dpysl3 mediates phagocytic activity of the microglia by regulating the cytoskeletal dynamics. It should be noted that phagocytic function of microglia is not only regulated by Dpysl3 but also by pro-inflammatory cytokines such as TNF-α, IL-1β and Il-6 (Cannella and Raine, 1995) and NO (Tumer et al., 2007). It is also possible that Dpysl3 may influence the phagocytic function of activated microglia by altering the production of proinflammatory cytokines and neurotoxic mediators such as NO.

The molecular mechanisms involved in microglial phagocytosis are largely unknown. Recent studies have indicated the importance of Rho-GTP binding proteins in phagocytosis activity (Caron and Hall, 1998; Coleman and Olson, 2002; Niedergang and Chavrier, 2005).

4.9 Rho GTPases: RhoA and Rac1 pathways are involved in Dpysl3 mediated microglial activation

The reorganization of actin cytoskeleton is essential for morphogenesis, phagocytosis and cell movement. It has been shown that actin remodeling is regulated by Rho family of small GTPases (Hall, 1998). Rho GTPases regulate several cellular events such as cytoskeletal organization, intracellular signaling and membrane trafficking in macrophages (Allen et al., 1997). These proteins have also been shown to be involved in mediating immune response by regulating phagocytosis, cytokine release, and production of ROS in leukocytes (Bokoch, 2005, 2009; Sprague and Khalil, 2009). In the present study, knockdown of Dpysl3 markedly perturbed the actin cytoskeleton of microglia, indicating that the impairment of actin reorganization in microglia by Dpysl3 knockdown may be mediated *via* Rho GTPase signaling.

4.9.1 RhoA in Dpysl3 mediated microglial activation

RhoA pathway is involved in mediating the inflammatory and oxidative responses in microglia (Villar-Cheda et al., 2012). It has been shown that interaction of Dpysl3 with RhoA mediates inhibition of neurite outgrowth, thereby inducing changes in the formation of focal adhesion and actin contractility (Alabed et al.,

2007). The present study showed that Dpysl3 interacts with RhoA in microglia and further knockdown of Dpysl3 decreases the mRNA and protein expression of RhoA in activated microglia. This inhibition of RhoA appears to be associated with impaired actin reorganization and migratory behavior of microglia. Overall, the present study suggests that interaction of Dpysl3 with RhoA regulates the cytoskeletal organization and migration of activated microglia.

4.9.2 Rac1in Dpysl3 mediated microglial activation

Rac1 is a member of Rho family small G-proteins, acts as a multifunctional molecular switch for generation of radicals, actin cytoskeleton and activation of transcription factors (Kitamura et al., 2003; Saraswathy et al., 2006; Grommes et al., 2008). Activation of Rac1 is known to promote lamellipodia and membrane ruffles (Ohsawa et al., 2000). Rac1 is shown to be involved in reorganization of actin cytoskeleton and plays a key role in microglial activation (Chung et al., 2000). In addition, Rac1 signaling induces NADPH oxidase resulting in the formation of iNOS and ROS (Apolloni et al., 2013) and also induces microglial phagocytosis (Grommes et al., 2008). The present study showed that Rac1 interacts with Dpysl3and knockdown of Dpysl3 in activated microglia reduced the expression of Rac1. The lack of Rac1 activation could result in attenuation of phagocytic activity and production of iNOS and ROS in activated microglia as observed after Dpysl3 knockdown.

Overall, the present study demonstrated the mechanism by which Dpysl3 regulates the inflammatory response of activated microglia. Dpysl3 is

developmentally regulated in microglia specifically expressed in the amoeboid microglia of the early postnatal rat brain and its expression is increased in activated microglial cells. Dpysl3is colocalized with F-actin cytoskeleton which is reorganized by the knockdown of Dpysl3. Further, Dpysl3 knockdown altered the expression of proinflammatory cytokines namely TNF-α and IL-1β and inflammatory mediators including iNOS and NO and the migratory and phagocytic capability of activated microglia, possibly by regulating NF-κB and Rho GTPases signaling pathways. From the present findings, it is suggested that Dpysl3 could be considered as a potential therapeutic target that may limit the neuroinflammatory response of microglia in neurodegenerative diseases.

Chapter 5

Conclusion and

Scope for future studies

5.1 Conclusion

Neuroinflammation, which is a process by which the CNS responds to injury, infection and ischemia, has been shown to have both beneficial and detrimental effects on the CNS. However, chronic neuroinflammation is deleterious to neurological functions, leading to the pathogenesis of neurological diseases such as AD, PD, ALS, prion disease, epilepsy etc (Eikelenboom et al., 2006; Whitton, 2007). But, the mechanisms by which it contributes to these pathological processes remain to be elucidated. It has been widely established that microglia, are the immune cells present in the CNS which respond to neuroinflammation and contribute to the disease processes. Hence it is clear that the study of microglial functions would provide new insights into neuroinflammation and pathogenesis of various neurological disorders.

In CNS inflammation and diseases, microglia becomes activated, engulfing pathogens, dead cells, misfolded proteins and damaged synapses. Microglial activation is associated with its rapid proliferation, migration, phagocytic ability and morphological transformation and has been shown to be regulated by several intrinsic and extrinsic factors (Parakalan et al., 2012; Kierdorf and Prinz, 2013). Dysregulation of these factors may induce severe functional changes in the microglia, which could potentially result in neuropathological changes in the CNS.

Recent transcriptome profiling studies revealed that several signaling molecules and transcription factors are differentially expressed in amoeboid and

resting microglia indicating that these cells are functionally distinct (Parakalan et al., 2012). Further, several groups including our group have shown that microglial activation in neuropathological condition is regulated by several signaling molecules such as NF-κB, MAPKs, and SphK1 and transcription factors such as Runx1 and is inhibited by several drugs and factors including dexamethasone, retinoic acid, melatonin, N,N-dimethylsphingosine (DMS) etc (Dheen et al., 2005; Zhou et al., 2007; Gao et al., 2010a; Nayak et al., 2010; Huo et al., 2011). However, these drugs and factors not only target microglia, but also target various other cell types, leading to unwanted side effects. Hence identification of factors regulating the microglial activation is of paramount importance.

Dihydropyrimidinase-like protein 3 (Dpysl3) has been shown to play important roles in neuronal differentiation, axonal outgrowth and neuronal regeneration (Goshima et al., 1995) and also involved in axon injury (Alabed et al., 2007). Interestingly, our studies revealed that Dpysl3 is highly expressed in amoeboid microglia and its expression is induced in activated microglia (Parakalan et al., 2012; Manivannan et al., 2013). Further, it appears to play an important role in microglia-mediated neuroinflammation by altering microglial cell proliferation, migration, phagocytic ability, secretory activity and morphology through NF-κB and Rho GTPase pathways and actin cytoskeleton derangement (Figure IV).

Overall, these findings provide a functional basis for designing specific therapeutic strategy to control microglial migration to the injured site and subsequently to inhibit microglia-mediated neuroinflammation. Moreover, this

study describes that Dpysl3 not only functions as a cytoskeletal gene but also acts as a novel regulator for inflammatory response, migration and phagocytosis of activated microglia.

Although this study demonstrates the potential function of Dpysl3 in activated microglia, further studies using *in vivo* animal models such as Dpysl3 knockout mice, AD mice and TBI mice, would be required to understand its functions in neuropathological conditions.

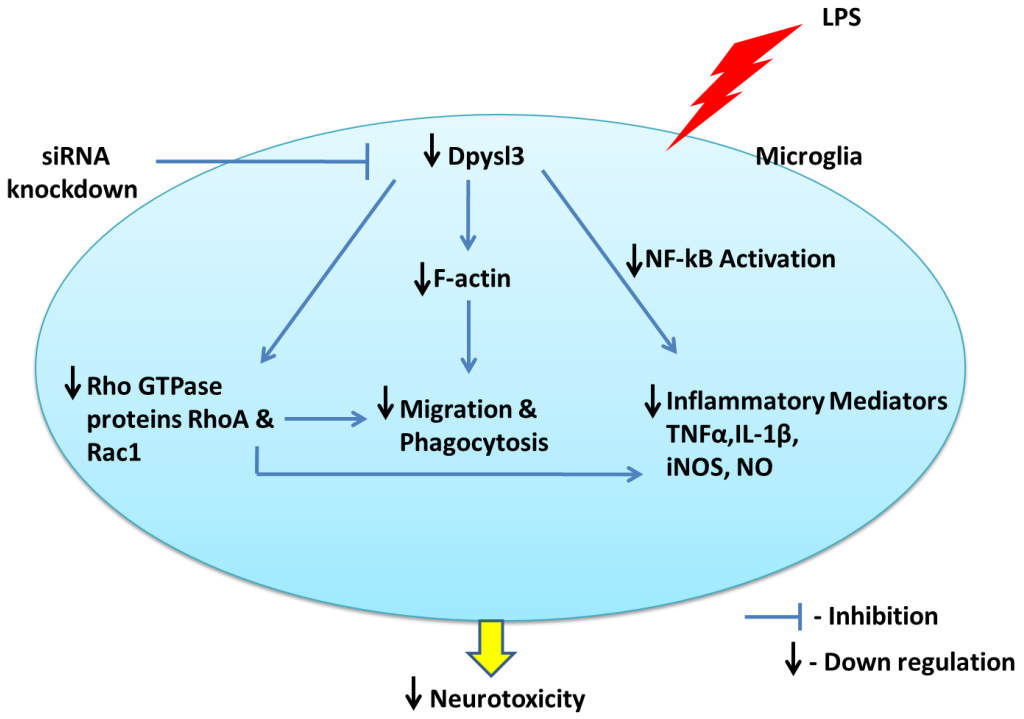

Figure IV: *An illustration demonstrates the functional events of Dihydropyrimidinaselike-3 in activated microglia. siRNA knockdown of Dpysl3inhibits microglial activation, migration, proliferation and phagocytic capability by suppressing the release of proinflammatory mediators via NF-κB signaling. Further Dpysl3 knockdown alters the F-actin structure and decreases the* Rho GTPase *proteins namely RhoA and Rac1 in activated microglia.*

5.2 Scope for future studies

1. Activation of microglia has been associated with various neurodegenerative diseases. Hence, suppression of microglia-mediated inflammation is considered to be therapeutic strategy in several neurodegenerative disorders.While majority of studies have focused on the regulation of the production of cytokines and neurotoxic mediators by activated microglia,the study on regulation of cytoskeleton organization inactivated microglia is only minimal. Therefore there is good scope for further investigations to validate the Dpysl3 role on cytoskeletal reorganization in activated microglia using the Dpysl3 knockout mice model.

2. In order to investigate Dpysl3 as a therapeutic target, future studies using transgenic/ knockout animal models of Dpysl3 will be required to elucidate the exact mechanisms which Dpysl3 inhibit ablate toxic functions (such as excessive production of pro-inflammatory cytokines) while retaining protective functions (such as migration to the injury site and phagocytic clearance of cell debris) of activated microglia in neuropathological conditions.

3. Recently, miRNA-132 has been shown to regulate the Dpysl3 in schizophrenic patients (Miller et al., 2012) and to promote inflammation by targeting NF-κB. Future study can investigate if miRNA-132 is expressed in microglia and if it modulates microglia-mediated inflammatory response by regulating Dpysl3. Moreover, epigenetic regulation of Dpysl3 in activated microglia may also be investigated in detail.

4. The present study has investigated the effects of Dpysl3 knockdown on microglial activation. Dpysl3 functions in activated microglia can be further established by overexpressing this gene in microglia.

5. This study has investigated the role of Dpysl3 in microglia after LPS-induced inflammation in the rat pups. There is a tremendous scope to extend similar studies in animal models of neurological disorders such as AD, PD, TBI, etc., to understand the functional significance of this gene in microglia-mediated neuroinflammation.

References

abd-el-Basset E, Fedoroff S (1995) Effect of bacterial wall lipopolysaccharide (LPS) on morphology, motility, and cytoskeletal organization of microglia in cultures. J Neurosci Res 41:222-237.

Abd-el-Basset EM, Fedoroff S (1994) Dynamics of actin filaments in microglia during Fc receptor-mediated phagocytosis. Acta Neuropathol 88:527-537.

Aggarwal S, Gollapudi S, Yel L, Gupta AS, Gupta S (2000) TNF-alpha-induced apoptosis in neonatal lymphocytes: TNFRp55 expression and downstream pathways of apoptosis. Genes and immunity 1:271-279.

Akiyama H, Tooyama I, Kondo H, Ikeda K, Kimura H, McGeer EG, McGeer PL (1994) Early response of brain resident microglia to kainic acid-induced hippocampal lesions. Brain Res 635:257-268.

Alabed YZ, Pool M, Ong Tone S, Fournier AE (2007) Identification of CRMP4 as a convergent regulator of axon outgrowth inhibition. The Journal of neuroscience : the official journal of the Society for Neuroscience 27:1702-1711.

Allen LA, Yang C, Pessin JE (2002) Rate and extent of phagocytosis in macrophages lacking vamp3. J Leukoc Biol 72:217-221.

Allen WE, Jones GE, Pollard JW, Ridley AJ (1997) Rho, Rac and Cdc42 regulate actin organization and cell adhesion in macrophages. Journal of cell science 110 (Pt 6):707-720.

Aloisi F (2001) Immune function of microglia. Glia 36:165-179.

Apolloni S, Parisi C, Pesaresi MG, Rossi S, Carri MT, Cozzolino M, Volonte C, D'Ambrosi N (2013) The NADPH oxidase pathway is dysregulated by the P2X7 receptor in the SOD1-G93A microglia model of amyotrophic lateral sclerosis. J Immunol 190:5187-5195.

Arimoto T, Bing G (2003) Up-regulation of inducible nitric oxide synthase in the substantia nigra by lipopolysaccharide causes microglial activation and neurodegeneration. Neurobiol Dis 12:35-45.

Arimura N, Menager C, Kawano Y, Yoshimura T, Kawabata S, Hattori A, Fukata Y, Amano M, Goshima Y, Inagaki M, Morone N, Usukura J, Kaibuchi K (2005)

Phosphorylation by Rho kinase regulates CRMP-2 activity in growth cones. Mol Cell Biol 25:9973-9984.

Arya M, Shergill IS, Williamson M, Gommersall L, Arya N, Patel HR (2005) Basic principles of real-time quantitative PCR. Expert Rev Mol Diagn 5:209-219.

Aylsworth A, Jiang SX, Desbois A, Hou ST (2009) Characterization of the role of full-length CRMP3 and its calpain-cleaved product in inhibiting microtubule polymerization and neurite outgrowth. Exp Cell Res 315:2856-2868.

Bachstetter AD, Xing B, de Almeida L, Dimayuga ER, Watterson DM, Van Eldik LJ (2011) Microglial p38alpha MAPK is a key regulator of proinflammatory cytokine up-regulation induced by toll-like receptor (TLR) ligands or beta-amyloid (Abeta). Journal of neuroinflammation 8:79.

Bachstetter AD, Rowe RK, Kaneko M, Goulding D, Lifshitz J, Van Eldik LJ (2013) The p38alpha MAPK regulates microglial responsiveness to diffuse traumatic brain injury. The Journal of neuroscience : the official journal of the Society for Neuroscience 33:6143-6153.

Baker RG, Hayden MS, Ghosh S (2011) NF-kappaB, inflammation, and metabolic disease. Cell metabolism 13:11-22.

Bal-Price A, Brown GC (2001) Inflammatory neurodegeneration mediated by nitric oxide from activated glia-inhibiting neuronal respiration, causing glutamate release and excitotoxicity. The Journal of neuroscience : the official journal of the Society for Neuroscience 21:6480-6491.

Bamberger ME, Landreth GE (2001) Microglial interaction with beta-amyloid: implications for the pathogenesis of Alzheimer's disease. Microscopy research and technique 54:59-70.

Banati RB, Gehrmann J, Schubert P, Kreutzberg GW (1993) Cytotoxicity of microglia. Glia 7:111-118.

Barcia C, Ros CM, Annese V, Carrillo-de Sauvage MA, Ros-Bernal F, Gomez A, Yuste JE, Campuzano CM, de Pablos V, Fernandez-Villalba E, Herrero MT (2012) ROCK/Cdc42-mediated microglial motility and gliapse formation lead to phagocytosis of degenerating dopaminergic neurons in vivo. Sci Rep 2:809.

Beckman JS, Koppenol WH (1996) Nitric oxide, superoxide, and peroxynitrite: the good, the bad, and ugly. Am J Physiol 271:C1424-1437.

Belokhvostov AS (1995) [Polymerase chain reaction and ligase reactions. Principles, traditional methods, and innovations]. Mol Gen Mikrobiol Virusol:21-26.

Beutner EH (1961) Immunofluorescent Staining: The Fluorescent Antibody Method. Bacteriol Rev 25:49-76.

Biber K, Vinet J, Boddeke HW (2008) Neuron-microglia signaling: chemokines as versatile messengers. Journal of neuroimmunology 198:69-74.

Blinzinger K, Kreutzberg G (1968) Displacement of synaptic terminals from regenerating motoneurons by microglial cells. Z Zellforsch Mikrosk Anat 85:145-157.

Block ML, Hong JS (2005) Microglia and inflammation-mediated neurodegeneration: multiple triggers with a common mechanism. Progress in neurobiology 76:77-98.

Block ML, Hong JS (2007) Chronic microglial activation and progressive dopaminergic neurotoxicity. Biochemical Society transactions 35:1127-1132.

Boje KM, Arora PK (1992) Microglial-produced nitric oxide and reactive nitrogen oxides mediate neuronal cell death. Brain Res 587:250-256.

Bokoch GM (2005) Regulation of innate immunity by Rho GTPases. Trends in cell biology 15:163-171.

Bokoch GM (2009) NADPH oxidases in innate immunity. Journal of innate immunity 1:507-508.

Brot S, Rogemond V, Perrot V, Chounlamountri N, Auger C, Honnorat J, Moradi-Ameli M (2010) CRMP5 interacts with tubulin to inhibit neurite outgrowth, thereby modulating the function of CRMP2. The Journal of neuroscience : the official journal of the Society for Neuroscience 30:10639-10654.

Brown GC (2007) Mechanisms of inflammatory neurodegeneration: iNOS and NADPH oxidase. Biochemical Society transactions 35:1119-1121.

Brown GC, Cooper CE (1994) Nanomolar concentrations of nitric oxide reversibly inhibit synaptosomal respiration by competing with oxygen at cytochrome oxidase. FEBS letters 356:295-298.

Brown GC, Neher JJ (2010) Inflammatory neurodegeneration and mechanisms of microglial killing of neurons. Molecular neurobiology 41:242-247.

Bustelo XR, Sauzeau V, Berenjeno IM (2007) GTP-binding proteins of the Rho/Rac family: regulation, effectors and functions in vivo. Bioessays 29:356-370.

Byk T, Dobransky T, Cifuentes-Diaz C, Sobel A (1996) Identification and molecular characterization of Unc-33-like phosphoprotein (Ulip), a putative mammalian homolog of the axonal guidance-associated unc-33 gene product. The Journal of neuroscience : the official journal of the Society for Neuroscience 16:688-701.

Caamano J, Hunter CA (2002) NF-kappaB family of transcription factors: central regulators of innate and adaptive immune functions. Clin Microbiol Rev 15:414-429.

Cacci E, Claasen JH, Kokaia Z (2005) Microglia-derived tumor necrosis factor-alpha exaggerates death of newborn hippocampal progenitor cells in vitro. J Neurosci Res 80:789-797.

Cannella B, Raine CS (1995) The adhesion molecule and cytokine profile of multiple sclerosis lesions. Ann Neurol 37:424-435.

Carnevale D, De Simone R, Minghetti L (2007) Microglia-neuron interaction in inflammatory and degenerative diseases: role of cholinergic and noradrenergic systems. CNS Neurol Disord Drug Targets 6:388-397.

Caron E, Hall A (1998) Identification of two distinct mechanisms of phagocytosis controlled by different Rho GTPases. Science 282:1717-1721.

Chamak B, Mallat M (1991) Fibronectin and laminin regulate the in vitro differentiation of microglial cells. Neuroscience 45:513-527.

Chan WY, Kohsaka S, Rezaie P (2007) The origin and cell lineage of microglia: new concepts. Brain research reviews 53:344-354.

Chao CC, Hu S, Molitor TW, Shaskan EG, Peterson PK (1992) Activated microglia mediate neuronal cell injury via a nitric oxide mechanism. Journal of immunology 149:2736-2741.

Charrier E, Reibel S, Rogemond V, Aguera M, Thomasset N, Honnorat J (2003) Collapsin response mediator proteins (CRMPs): involvement in nervous system development and adult neurodegenerative disorders. Molecular neurobiology 28:51-64.

Chhabra ES, Higgs HN (2007) The many faces of actin: matching assembly factors with cellular structures. Nat Cell Biol 9:1110-1121.

Christensen RN, Ha BK, Sun F, Bresnahan JC, Beattie MS (2006) Kainate induces rapid redistribution of the actin cytoskeleton in ameboid microglia. J Neurosci Res 84:170-181.

Chung CY, Lee S, Briscoe C, Ellsworth C, Firtel RA (2000) Role of Rac in controlling the actin cytoskeleton and chemotaxis in motile cells. Proc Natl Acad Sci U S A 97:5225-5230.

Cole AR, Noble W, van Aalten L, Plattner F, Meimaridou R, Hogan D, Taylor M, LaFrancois J, Gunn-Moore F, Verkhratsky A, Oddo S, LaFerla F, Giese KP, Dineley KT, Duff K, Richardson JC, Yan SD, Hanger DP, Allan SM, Sutherland C (2007) Collapsin response mediator protein-2 hyperphosphorylation is an early event in Alzheimer's disease progression. Journal of neurochemistry 103:1132-1144.

Coleman ML, Olson MF (2002) Rho GTPase signalling pathways in the morphological changes associated with apoptosis. Cell Death Differ 9:493-504.

Colton CA, Gilbert DL (1987) Production of superoxide anions by a CNS macrophage, the microglia. FEBS letters 223:284-288.

Couch Y, Anthony DC, Dolgov O, Revischin A, Festoff B, Santos AI, Steinbusch HW, Strekalova T (2013) Microglial activation, increased TNF and SERT expression in the prefrontal cortex define stress-altered behaviour in mice susceptible to anhedonia. Brain Behav Immun 29:136-146.

Crehan H, Hardy J, Pocock J (2012) Microglia, Alzheimer's disease, and complement. International journal of Alzheimer's disease 2012:983640.

Croisier E, Moran LB, Dexter DT, Pearce RK, Graeber MB (2005) Microglial inflammation in the parkinsonian substantia nigra: relationship to alpha-synuclein deposition. Journal of neuroinflammation 2:14.

Cross AK, Woodroofe MN (1999) Chemokines induce migration and changes in actin polymerization in adult rat brain microglia and a human fetal microglial cell line in vitro. J Neurosci Res 55:17-23.

Czech T, Yang JW, Csaszar E, Kappler J, Baumgartner C, Lubec G (2004) Reduction of hippocampal collapsin response mediated protein-2 in patients with mesial temporal lobe epilepsy. Neurochem Res 29:2189-2196.

de Mos M, Laferriere A, Millecamps M, Pilkington M, Sturkenboom MC, Huygen FJ, Coderre TJ (2009) Role of NFkappaB in an animal model of complex regional pain syndrome-type I (CRPS-I). J Pain 10:1161-1169.

Defilippi P, Di Stefano P, Cabodi S (2006) p130Cas: a versatile scaffold in signaling networks. Trends Cell Biol 16:257-263.

Deng Y, Lu J, Sivakumar V, Ling EA, Kaur C (2008) Amoeboid microglia in the periventricular white matter induce oligodendrocyte damage through expression of proinflammatory cytokines via MAP kinase signaling pathway in hypoxic neonatal rats. Brain pathology 18:387-400.

Deng YY, Lu J, Ling EA, Kaur C (2009) Monocyte chemoattractant protein-1 (MCP-1) produced via NF-kappaB signaling pathway mediates migration of amoeboid microglia in the periventricular white matter in hypoxic neonatal rats. Glia 57:604-621.

Deo RC, Schmidt EF, Elhabazi A, Togashi H, Burley SK, Strittmatter SM (2004) Structural bases for CRMP function in plexin-dependent semaphorin3A signaling. EMBO J 23:9-22.

Dheen ST, Kaur C, Ling EA (2007) Microglial activation and its implications in the brain diseases. Curr Med Chem 14:1189-1197.

Dheen ST, Jun Y, Yan Z, Tay SS, Ling EA (2005) Retinoic acid inhibits expression of TNF-alpha and iNOS in activated rat microglia. Glia 50:21-31.

di Penta A, Moreno B, Reix S, Fernandez-Diez B, Villanueva M, Errea O, Escala N, Vandenbroeck K, Comella JX, Villoslada P (2013) Oxidative stress and proinflammatory cytokines contribute to demyelination and axonal damage in a cerebellar culture model of neuroinflammation. PloS one 8:e54722.

Dikmen SS, Corrigan JD, Levin HS, Machamer J, Stiers W, Weisskopf MG (2009) Cognitive outcome following traumatic brain injury. The Journal of head trauma rehabilitation 24:430-438.

Doens D, Fernandez PL (2014) Microglia receptors and their implications in the response to amyloid beta for Alzheimer's disease pathogenesis. Journal of neuroinflammation 11:48.

Doty P, Rudd GD, Stoehr T, Thomas D (2007) Lacosamide. Neurotherapeutics : the journal of the American Society for Experimental NeuroTherapeutics 4:145-148.

Eikelenboom P, Veerhuis R, Scheper W, Rozemuller AJ, van Gool WA, Hoozemans JJ (2006) The significance of neuroinflammation in understanding Alzheimer's disease. J Neural Transm 113:1685-1695.

Ellezam B, Dubreuil C, Winton M, Loy L, Dergham P, Selles-Navarro I, McKerracher L (2002) Inactivation of intracellular Rho to stimulate axon growth and regeneration. Prog Brain Res 137:371-380.

Eugenin EA, Dyer G, Calderon TM, Berman JW (2005) HIV-1 tat protein induces a migratory phenotype in human fetal microglia by a CCL2 (MCP-1)-dependent mechanism: possible role in NeuroAIDS. Glia 49:501-510.

Eyo UB, Dailey ME (2013) Microglia: key elements in neural development, plasticity, and pathology. Journal of neuroimmune pharmacology : the official journal of the Society on NeuroImmune Pharmacology 8:494-509.

Figiel I (2008) Pro-inflammatory cytokine TNF-alpha as a neuroprotective agent in the brain. Acta neurobiologiae experimentalis 68:526-534.

Fleisher-Berkovich S, Filipovich-Rimon T, Ben-Shmuel S, Hulsmann C, Kummer MP, Heneka MT (2010) Distinct modulation of microglial amyloid beta phagocytosis and migration by neuropeptides (i). Journal of neuroinflammation 7:61.

Franken S, Junghans U, Rosslenbroich V, Baader SL, Hoffmann R, Gieselmann V, Viebahn C, Kappler J (2003) Collapsin response mediator proteins of neonatal rat brain interact with chondroitin sulfate. The Journal of biological chemistry 278:3241-3250.

Friedl P (2004) Prespecification and plasticity: shifting mechanisms of cell migration. Current opinion in cell biology 16:14-23.

Fulga TA, Elson-Schwab I, Khurana V, Steinhilb ML, Spires TL, Hyman BT, Feany MB (2007) Abnormal bundling and accumulation of F-actin mediates tau-induced neuronal degeneration in vivo. Nat Cell Biol 9:139-148.

Gao HM, Liu B, Hong JS (2003) Critical role for microglial NADPH oxidase in rotenone-induced degeneration of dopaminergic neurons. The Journal of neuroscience : the official journal of the Society for Neuroscience 23:6181-6187.

Gao Q, Lu J, Huo Y, Baby N, Ling EA, Dheen ST (2010a) NG2, a member of chondroitin sulfate proteoglycans family mediates the inflammatory response of activated microglia. Neuroscience 165:386-394.

Gao X, Pang J, Li LY, Liu WP, Di JM, Sun QP, Fang YQ, Liu XP, Pu XY, He D, Li MT, Su ZL, Li BY (2010b) Expression profiling identifies new function of collapsin response mediator protein 4 as a metastasis-suppressor in prostate cancer. Oncogene 29:4555-4566.

Gavrilov K, Saltzman WM (2012) Therapeutic siRNA: principles, challenges, and strategies. Yale J Biol Med 85:187-200.

Ghosh S, Hayden MS (2008) New regulators of NF-kappaB in inflammation. Nat Rev Immunol 8:837-848.

Gitik M, Reichert F, Rotshenker S (2010) Cytoskeleton plays a dual role of activation and inhibition in myelin and zymosan phagocytosis by microglia. FASEB J 24:2211-2221.

Golde S, Chandran S, Brown GC, Compston A (2002) Different pathways for iNOS-mediated toxicity in vitro dependent on neuronal maturation and NMDA receptor expression. Journal of neurochemistry 82:269-282.

Gomez-Gonzalez B, Escobar A (2010) Prenatal stress alters microglial development and distribution in postnatal rat brain. Acta Neuropathol 119:303-315.

Gomez-Nicola D, Fransen NL, Suzzi S, Perry VH (2013) Regulation of microglial proliferation during chronic neurodegeneration. The Journal of neuroscience : the official journal of the Society for Neuroscience 33:2481-2493.

Good PF, Alapat D, Hsu A, Chu C, Perl D, Wen X, Burstein DE, Kohtz DS (2004) A role for semaphorin 3A signaling in the degeneration of hippocampal neurons during Alzheimer's disease. Journal of neurochemistry 91:716-736.

Goshima Y, Nakamura F, Strittmatter P, Strittmatter SM (1995) Collapsin-induced growth cone collapse mediated by an intracellular protein related to UNC-33. Nature 376:509-514.

Graeber MB, Streit WJ, Kreutzberg GW (1988) The microglial cytoskeleton: vimentin is localized within activated cells in situ. J Neurocytol 17:573-580.

Grommes C, Lee CY, Wilkinson BL, Jiang Q, Koenigsknecht-Talboo JL, Varnum B, Landreth GE (2008) Regulation of microglial phagocytosis and inflammatory gene expression by Gas6 acting on the Axl/Mer family of tyrosine kinases. Journal of neuroimmune pharmacology : the official journal of the Society on NeuroImmune Pharmacology 3:130-140.

Guillemin GJ, Brew BJ (2004) Microglia, macrophages, perivascular macrophages, and pericytes: a review of function and identification. J Leukoc Biol 75:388-397.

Guzman-Beltran S, Perez-Torres A, Coronel-Cruz C, Torres-Guerrero H (2012) Phagocytic receptors on macrophages distinguish between different Sporothrix schenckii morphotypes. Microbes Infect 14:1093-1101.

Hachmeister U, Kracht J (1975) [Basic features in immunohistological technique (author's transl)]. Microsc Acta 77:213-220.

Hall A (1998) Rho GTPases and the actin cytoskeleton. Science 279:509-514.

Hanisch UK (2002) Microglia as a source and target of cytokines. Glia 40:140-155.

Hanisch UK, Kettenmann H (2007) Microglia: active sensor and versatile effector cells in the normal and pathologic brain. Nature neuroscience 10:1387-1394.

Heese K, Fiebich BL, Bauer J, Otten U (1998) NF-kappaB modulates lipopolysaccharide-induced microglial nerve growth factor expression. Glia 22:401-407.

Henn A, Lund S, Hedtjarn M, Schrattenholz A, Porzgen P, Leist M (2009) The suitability of BV2 cells as alternative model system for primary microglia cultures or for animal experiments examining brain inflammation. Altex 26:83-94.

Hensley K, Gabbita SP, Venkova K, Hristov A, Johnson MF, Eslami P, Harris-White ME (2013) A derivative of the brain metabolite lanthionine ketimine improves cognition and diminishes pathology in the 3 x Tg-AD mouse model of Alzheimer disease. Journal of neuropathology and experimental neurology 72:955-969.

Hickman SE, Allison EK, El Khoury J (2008) Microglial dysfunction and defective beta-amyloid clearance pathways in aging Alzheimer's disease mice. The Journal of neuroscience : the official journal of the Society for Neuroscience 28:8354-8360.

Hines DJ, Choi HB, Hines RM, Phillips AG, MacVicar BA (2013) Prevention of LPS-induced microglia activation, cytokine production and sickness behavior with TLR4 receptor interfering peptides. PloS one 8:e60388.

Hinkerohe D, Smikalla D, Schoebel A, Haghikia A, Zoidl G, Haase CG, Schlegel U, Faustmann PM (2010) Dexamethasone prevents LPS-induced microglial activation and astroglial impairment in an experimental bacterial meningitis co-culture model. Brain research 1329:45-54.

Huo Y, Rangarajan P, Ling EA, Dheen ST (2011) Dexamethasone inhibits the Nox-dependent ROS production via suppression of MKP-1-dependent MAPK pathways in activated microglia. BMC Neurosci 12:49.

Inagaki N, Chihara K, Arimura N, Menager C, Kawano Y, Matsuo N, Nishimura T, Amano M, Kaibuchi K (2001) CRMP-2 induces axons in cultured hippocampal neurons. Nature neuroscience 4:781-782.

Inoue M, Sato EF, Nishikawa M, Park AM, Kira Y, Imada I, Utsumi K (2003) Mitochondrial generation of reactive oxygen species and its role in aerobic life. Curr Med Chem 10:2495-2505.

Jang SY, Shin YK, Jung J, Lee SH, Seo SY, Suh DJ, Park HT (2010) Injury-induced CRMP4 expression in adult sensory neurons; a possible target gene for ciliary neurotrophic factor. Neuroscience letters 485:37-42.

Jessen KR, Mirsky R (1980) Glial cells in the enteric nervous system contain glial fibrillary acidic protein. Nature 286:736-737.

Kalil K, Dent EW (2005) Touch and go: guidance cues signal to the growth cone cytoskeleton. Current opinion in neurobiology 15:521-526.

Karlstetter M, Lippe E, Walczak Y, Moehle C, Aslanidis A, Mirza M, Langmann T (2011) Curcumin is a potent modulator of microglial gene expression and migration. Journal of neuroinflammation 8:125.

Kaur C, You Y (2000) Ultrastructure and function of the amoeboid microglial cells in the periventricular white matter in postnatal rat brain following a hypoxic exposure. Neuroscience letters 290:17-20.

Kaur C, Ling EA (2009) Periventricular white matter damage in the hypoxic neonatal brain: role of microglial cells. Progress in neurobiology 87:264-280.

Kaur C, Too HF, Ling EA (2004) Phagocytosis of Escherichia coli by amoeboid microglial cells in the developing brain. Acta neuropathologica 107:204-208.

Kaur C, Hao AJ, Wu CH, Ling EA (2001) Origin of microglia. Microscopy research and technique 54:2-9.

Kettenmann H, Hanisch UK, Noda M, Verkhratsky A (2011) Physiology of microglia. Physiol Rev 91:461-553.

Kierdorf K, Prinz M (2013) Factors regulating microglia activation. Front Cell Neurosci 7:44.

Kim H, Lee E, Shin T, Chung C, An N (1998) Inhibition of the induction of the inducible nitric oxide synthase in murine brain microglial cells by sodium salicylate. Immunology 95:389-394.

Kim JS, Kim JG, Moon MY, Jeon CY, Won HY, Kim HJ, Jeon YJ, Seo JY, Kim JI, Kim J, Lee JY, Kim PH, Park JB (2006a) Transforming growth factor-beta1 regulates macrophage migration via RhoA. Blood 108:1821-1829.

Kim SH, Smith CJ, Van Eldik LJ (2004) Importance of MAPK pathways for microglial pro-inflammatory cytokine IL-1 beta production. Neurobiology of aging 25:431-439.

Kim YJ, Hwang SY, Oh ES, Oh S, Han IO (2006b) IL-1beta, an immediate early protein secreted by activated microglia, induces iNOS/NO in C6 astrocytoma cells through p38 MAPK and NF-kappaB pathways. Journal of neuroscience research 84:1037-1046.

Kitamura Y, Shibagaki K, Takata K, Tsuchiya D, Taniguchi T, Gebicke-Haerter PJ, Miki H, Takenawa T, Shimohama S (2003) Involvement of Wiskott-Aldrich syndrome protein family verprolin-homologous protein (WAVE) and Rac1 in the phagocytosis of amyloid-beta(1-42) in rat microglia. J Pharmacol Sci 92:115-123.

Kitano K, Usui S, Ootsuji H, Takashima S, Kobayashi D, Murai H, Furusho H, Nomura A, Kaneko S, Takamura M (2014) Rho-kinase activation in leukocytes plays a pivotal role in myocardial ischemia/reperfusion injury. PloS one 9:e92242.

Klegeris A, McGeer EG, McGeer PL (2007) Therapeutic approaches to inflammation in neurodegenerative disease. Curr Opin Neurol 20:351-357.

Kraft AD, Harry GJ (2011) Features of microglia and neuroinflammation relevant to environmental exposure and neurotoxicity. Int J Environ Res Public Health 8:2980-3018.

Kurien BT, Scofield RH (2006) Western blotting. Methods 38:283-293.

Lambrechts A, Van Troys M, Ampe C (2004) The actin cytoskeleton in normal and pathological cell motility. Int J Biochem Cell Biol 36:1890-1909.

Lauffenburger DA, Horwitz AF (1996) Cell migration: a physically integrated molecular process. Cell 84:359-369.

Lee CY, Landreth GE (2010) The role of microglia in amyloid clearance from the AD brain. J Neural Transm 117:949-960.

Lee JY, Jhun BS, Oh YT, Lee JH, Choe W, Baik HH, Ha J, Yoon KS, Kim SS, Kang I (2006) Activation of adenosine A3 receptor suppresses lipopolysaccharide-induced TNF-alpha production through inhibition of PI 3-kinase/Akt and NF-kappaB activation in murine BV2 microglial cells. Neuroscience letters 396:1-6.

Lee SC, Liu W, Brosnan CF, Dickson DW (1994) GM-CSF promotes proliferation of human fetal and adult microglia in primary cultures. Glia 12:309-318.

Lehner B, Sandner B, Marschallinger J, Lehner C, Furtner T, Couillard-Despres S, Rivera FJ, Brockhoff G, Bauer HC, Weidner N, Aigner L (2011) The dark side of BrdU in neural stem cell biology: detrimental effects on cell cycle, differentiation and survival. Cell Tissue Res 345:313-328.

Lin H, Baby N, Lu J, Kaur C, Zhang C, Xu J, Ling EA, Dheen ST (2011) Expression of sphingosine kinase 1 in amoeboid microglial cells in the corpus callosum of postnatal rats. Journal of neuroinflammation 8:13.

Lin YL, Hsueh YP (2008) Neurofibromin interacts with CRMP-2 and CRMP-4 in rat brain. Biochem Biophys Res Commun 369:747-752.

Ling EA, Wong WC (1993) The origin and nature of ramified and amoeboid microglia: a historical review and current concepts. Glia 7:9-18.

Ling EA, Kaur C, Wong WC (1991) Expression of major histocompatibility complex and leukocyte common antigens in amoeboid microglia in postnatal rats. Journal of anatomy 177:117-126.

Ling EA, Ng YK, Wu CH, Kaur C (2001) Microglia: its development and role as a neuropathology sensor. Prog Brain Res 132:61-79.

Lippman JJ, Lordkipanidze T, Buell ME, Yoon SO, Dunaevsky A (2008) Morphogenesis and regulation of Bergmann glial processes during Purkinje cell dendritic spine ensheathment and synaptogenesis. Glia 56:1463-1477.

Liu B, Hong JS (2003) Role of microglia in inflammation-mediated neurodegenerative diseases: mechanisms and strategies for therapeutic intervention. J Pharmacol Exp Ther 304:1-7.

Liu B, Gao HM, Wang JY, Jeohn GH, Cooper CL, Hong JS (2002) Role of nitric oxide in inflammation-mediated neurodegeneration. Ann N Y Acad Sci 962:318-331.

Liu PC, Yang ZJ, Qiu MH, Zhang LM, Sun FY (2003) Induction of CRMP-4 in striatum of adult rat after transient brain ischemia. Acta Pharmacol Sin 24:1205-1211.

Livak KJ, Schmittgen TD (2001) Analysis of relative gene expression data using real-time quantitative PCR and the 2(-Delta Delta C(T)) Method. Methods 25:402-408.

Lund S, Christensen KV, Hedtjarn M, Mortensen AL, Hagberg H, Falsig J, Hasseldam H, Schrattenholz A, Porzgen P, Leist M (2006a) The dynamics of the LPS triggered inflammatory response of murine microglia under different culture and in vivo conditions. J Neuroimmunol 180:71-87.

Lund S, Christensen KV, Hedtjarn M, Mortensen AL, Hagberg H, Falsig J, Hasseldam H, Schrattenholz A, Porzgen P, Leist M (2006b) The dynamics of the LPS triggered inflammatory response of murine microglia under different culture and in vivo conditions. Journal of neuroimmunology 180:71-87.

Manivannan J, Tay SS, Ling EA, Dheen ST (2013) Dihydropyrimidinase-like 3 regulates the inflammatory response of activated microglia. Neuroscience.

Mannix RC, Whalen MJ (2012) Traumatic brain injury, microglia, and Beta amyloid. International journal of Alzheimer's disease 2012:608732.

Marin-Teva JL, Almendros A, Calvente R, Cuadros MA, Navascues J (1998) Tangential migration of ameboid microglia in the developing quail retina: mechanism of migration and migratory behavior. Glia 22:31-52.

Marker DF, Puccini JM, Mockus TE, Barbieri J, Lu SM, Gelbard HA (2012) LRRK2 kinase inhibition prevents pathological microglial phagocytosis in response to HIV-1 Tat protein. Journal of neuroinflammation 9:261.

Martin S, Vincent JP, Mazella J (2003) Involvement of the neurotensin receptor-3 in the neurotensin-induced migration of human microglia. J Neurosci 23:1198-1205.

Masters SC (2004) Co-immunoprecipitation from transfected cells. Methods in molecular biology 261:337-350.

McGeer EG, Klegeris A, McGeer PL (2005) Inflammation, the complement system and the diseases of aging. Neurobiology of aging 26 Suppl 1:94-97.

Meffert MK, Baltimore D (2005) Physiological functions for brain NF-kappaB. Trends Neurosci 28:37-43.

Miller BA, Crum JM, Tovar CA, Ferguson AR, Bresnahan JC, Beattie MS (2007) Developmental stage of oligodendrocytes determines their response to activated microglia in vitro. Journal of neuroinflammation 4:28.

Miller BH, Zeier Z, Xi L, Lanz TA, Deng S, Strathmann J, Willoughby D, Kenny PJ, Elsworth JD, Lawrence MS, Roth RH, Edbauer D, Kleiman RJ, Wahlestedt C (2012) MicroRNA-132 dysregulation in schizophrenia has implications for both neurodevelopment and adult brain function. Proc Natl Acad Sci U S A 109:3125-3130.

Minturn JE, Geschwind DH, Fryer HJ, Hockfield S (1995a) Early postmitotic neurons transiently express TOAD-64, a neural specific protein. J Comp Neurol 355:369-379.

Minturn JE, Fryer HJ, Geschwind DH, Hockfield S (1995b) TOAD-64, a gene expressed early in neuronal differentiation in the rat, is related to unc-33, a C. elegans gene involved in axon outgrowth. The Journal of neuroscience : the official journal of the Society for Neuroscience 15:6757-6766.

Mitchison TJ, Cramer LP (1996) Actin-based cell motility and cell locomotion. Cell 84:371-379.

Monif M, Reid CA, Powell KL, Smart ML, Williams DA (2009) The P2X7 receptor drives microglial activation and proliferation: a trophic role for P2X7R pore. The Journal of neuroscience : the official journal of the Society for Neuroscience 29:3781-3791.

Moynagh PN (2005) The interleukin-1 signalling pathway in astrocytes: a key contributor to inflammation in the brain. Journal of anatomy 207:265-269.

Mrak RE (2012) Microglia in Alzheimer brain: a neuropathological perspective. International journal of Alzheimer's disease 2012:165021.

Murabe Y, Sano Y (1982) Morphological studies on neuroglia. VI. Postnatal development of microglial cells. Cell Tissue Res 225:469-485.

Nacher J, Rosell DR, McEwen BS (2000) Widespread expression of rat collapsin response-mediated protein 4 in the telencephalon and other areas of the adult rat central nervous system. J Comp Neurol 424:628-639.

Nacher J, Soriano S, Varea E, Molowny A, Ponsoda X, Lopez-Garcia C (2002) CRMP-4 expression in the adult cerebral cortex and other telencephalic areas of the lizard Podarcis hispanica. Brain Res Dev Brain Res 139:285-294.

Nakamura Y, Si QS, Kataoka K (1999) Lipopolysaccharide-induced microglial activation in culture: temporal profiles of morphological change and release of cytokines and nitric oxide. Neurosci Res 35:95-100.

Nayak D, Huo Y, Kwang WX, Pushparaj PN, Kumar SD, Ling EA, Dheen ST (2010) Sphingosine kinase 1 regulates the expression of proinflammatory cytokines and nitric oxide in activated microglia. Neuroscience 166:132-144.

Neher JJ, Neniskyte U, Zhao JW, Bal-Price A, Tolkovsky AM, Brown GC (2011) Inhibition of microglial phagocytosis is sufficient to prevent inflammatory neuronal death. J Immunol 186:4973-4983.

Netea MG, Simon A, van de Veerdonk F, Kullberg BJ, Van der Meer JW, Joosten LA (2010) IL-1beta processing in host defense: beyond the inflammasomes. PLoS Pathog 6:e1000661.

Neumann H, Kotter MR, Franklin RJ (2009) Debris clearance by microglia: an essential link between degeneration and regeneration. Brain : a journal of neurology 132:288-295.

Niedergang F, Chavrier P (2005) Regulation of phagocytosis by Rho GTPases. Curr Top Microbiol Immunol 291:43-60.

Nimmerjahn A, Kirchhoff F, Helmchen F (2005) Resting microglial cells are highly dynamic surveillants of brain parenchyma in vivo. Science 308:1314-1318.

Nolte C, Moller T, Walter T, Kettenmann H (1996) Complement 5a controls motility of murine microglial cells in vitro via activation of an inhibitory G-protein and the rearrangement of the actin cytoskeleton. Neuroscience 73:1091-1107.

Ohsawa K, Imai Y, Kanazawa H, Sasaki Y, Kohsaka S (2000) Involvement of Iba1 in membrane ruffling and phagocytosis of macrophages/microglia. Journal of cell science 113 (Pt 17):3073-3084.

Pang Y, Campbell L, Zheng B, Fan L, Cai Z, Rhodes P (2010) Lipopolysaccharide-activated microglia induce death of oligodendrocyte progenitor cells and impede their development. Neuroscience 166:464-475.

Parakalan R, Jiang B, Nimmi B, Janani M, Jayapal M, Lu J, Tay SS, Ling EA, Dheen ST (2012) Transcriptome analysis of amoeboid and ramified microglia isolated from the corpus callosum of rat brain. BMC Neurosci 13:64.

Park SY, Lee H, Hur J, Kim SY, Kim H, Park JH, Cha S, Kang SS, Cho GJ, Choi WS, Suk K (2002) Hypoxia induces nitric oxide production in mouse microglia via p38 mitogen-activated protein kinase pathway. Brain research Molecular brain research 107:9-16.

Perry VH, Teeling J (2013) Microglia and macrophages of the central nervous system: the contribution of microglia priming and systemic inflammation to chronic neurodegeneration. Seminars in immunopathology 35:601-612.

Pessac B, Godin I, Alliot F (2001) [Microglia: origin and development]. Bulletin de l'Academie nationale de medecine 185:337-346; discussion 346-337.

Peterson LJ, Flood PM (2012) Oxidative stress and microglial cells in Parkinson's disease. Mediators Inflamm 2012:401264.

Petrova TV, Akama KT, Van Eldik LJ (1999) Cyclopentenone prostaglandins suppress activation of microglia: down-regulation of inducible nitric-oxide synthase by 15-deoxy-Delta12,14-prostaglandin J2. Proc Natl Acad Sci U S A 96:4668-4673.

Possel H, Noack H, Putzke J, Wolf G, Sies H (2000) Selective upregulation of inducible nitric oxide synthase (iNOS) by lipopolysaccharide (LPS) and cytokines in microglia: in vitro and in vivo studies. Glia 32:51-59.

Pottler M, Zierler S, Kerschbaum HH (2006) An artificial three-dimensional matrix promotes ramification in the microglial cell-line, BV-2. Neuroscience letters 410:137-140.

Qin L, Crews FT (2012) NADPH oxidase and reactive oxygen species contribute to alcohol-induced microglial activation and neurodegeneration. Journal of neuroinflammation 9:5.

Qu XW, Wang H, De Plaen IG, Rozenfeld RA, Hsueh W (2001) Neuronal nitric oxide synthase (NOS) regulates the expression of inducible NOS in rat small intestine via modulation of nuclear factor kappa B. FASEB J 15:439-446.

Quach TT, Massicotte G, Belin MF, Honnorat J, Glasper ER, Devries AC, Jakeman LB, Baudry M, Duchemin AM, Kolattukudy PE (2008) CRMP3 is required for hippocampal CA1 dendritic organization and plasticity. FASEB J 22:401-409.

Quinn CC, Gray GE, Hockfield S (1999) A family of proteins implicated in axon guidance and outgrowth. Journal of neurobiology 41:158-164.

Quinn CC, Chen E, Kinjo TG, Kelly G, Bell AW, Elliott RC, McPherson PS, Hockfield S (2003) TUC-4b, a novel TUC family variant, regulates neurite outgrowth and associates with vesicles in the growth cone. The Journal of neuroscience : the official journal of the Society for Neuroscience 23:2815-2823.

Ramlackhansingh AF, Brooks DJ, Greenwood RJ, Bose SK, Turkheimer FE, Kinnunen KM, Gentleman S, Heckemann RA, Gunanayagam K, Gelosa G, Sharp DJ (2011) Inflammation after trauma: microglial activation and traumatic brain injury. Ann Neurol 70:374-383.

Rhoads MG, Kandarian SC, Pacelli F, Doglietto GB, Bossola M (2010) Expression of NF-kappaB and IkappaB proteins in skeletal muscle of gastric cancer patients. Eur J Cancer 46:191-197.

Ricard D, Stankoff B, Bagnard D, Aguera M, Rogemond V, Antoine JC, Spassky N, Zalc B, Lubetzki C, Belin MF, Honnorat J (2000) Differential expression of collapsin response mediator proteins (CRMP/ULIP) in subsets of oligodendrocytes in the postnatal rodent brain. Molecular and cellular neurosciences 16:324-337.

Richardson JR, Hossain MM (2013) Microglial ion channels as potential targets for neuroprotection in Parkinson's disease. Neural plasticity 2013:587418.

Ridley AJ (2001) Rho GTPases and cell migration. Journal of cell science 114:2713-2722.

Ridley AJ, Paterson HF, Johnston CL, Diekmann D, Hall A (1992) The small GTP-binding protein rac regulates growth factor-induced membrane ruffling. Cell 70:401-410.

Roepstorff K, Rasmussen I, Sawada M, Cudre-Maroux C, Salmon P, Bokoch G, van Deurs B, Vilhardt F (2008) Stimulus-dependent regulation of the phagocyte NADPH oxidase by a VAV1, Rac1, and PAK1 signaling axis. The Journal of biological chemistry 283:7983-7993.

Rogers J, Mastroeni D, Leonard B, Joyce J, Grover A (2007) Neuroinflammation in Alzheimer's disease and Parkinson's disease: are microglia pathogenic in either disorder? Int Rev Neurobiol 82:235-246.

Rosslenbroich V, Dai L, Baader SL, Noegel AA, Gieselmann V, Kappler J (2005) Collapsin response mediator protein-4 regulates F-actin bundling. Exp Cell Res 310:434-444.

Rothaeusler K, Baumgarth N (2007) Assessment of cell proliferation by 5-bromodeoxyuridine (BrdU) labeling for multicolor flow cytometry. Curr Protoc Cytom Chapter 7:Unit7 31.

Rotshenker S (2003) Microglia and macrophage activation and the regulation of complement-receptor-3 (CR3/MAC-1)-mediated myelin phagocytosis in injury and disease. J Mol Neurosci 21:65-72.

Rubio-Perez JM, Morillas-Ruiz JM (2012) A review: inflammatory process in Alzheimer's disease, role of cytokines. ScientificWorldJournal 2012:756357.

Sakurai H, Chiba H, Miyoshi H, Sugita T, Toriumi W (1999) IkappaB kinases phosphorylate NF-kappaB p65 subunit on serine 536 in the transactivation domain. The Journal of biological chemistry 274:30353-30356.

Salawu FK, Umar JT, Olokoba AB (2011) Alzheimer's disease: a review of recent developments. Annals of African medicine 10:73-79.

Saraswathy S, Wu G, Rao NA (2006) Retinal microglial activation and chemotaxis by docosahexaenoic acid hydroperoxide. Investigative ophthalmology & visual science 47:3656-3663.

Saura J, Tusell JM, Serratosa J (2003) High-yield isolation of murine microglia by mild trypsinization. Glia 44:183-189.

Sawada H, Suzuki H, Nagatsu T, Sawada M (2010) Neuroprotective and neurotoxic phenotypes of activated microglia in neonatal mice with respective MPTP- and ethanol-induced brain injury. Neuro-degenerative diseases 7:64-67.

Sawada M, Kondo N, Suzumura A, Marunouchi T (1989) Production of tumor necrosis factor-alpha by microglia and astrocytes in culture. Brain Res 491:394-397.

Schuster M, Annemann M, Plaza-Sirvent C, Schmitz I (2013) Atypical IkappaB proteins - nuclear modulators of NF-kappaB signaling. Cell Commun Signal 11:23.

Sebire G, Emilie D, Wallon C, Hery C, Devergne O, Delfraissy JF, Galanaud P, Tardieu M (1993) In vitro production of IL-6, IL-1 beta, and tumor necrosis

factor-alpha by human embryonic microglial and neural cells. J Immunol 150:1517-1523.

Shaftel SS, Griffin WS, O'Banion MK (2008) The role of interleukin-1 in neuroinflammation and Alzheimer disease: an evolving perspective. Journal of neuroinflammation 5:7.

Shen S, Yu S, Binek J, Chalimoniuk M, Zhang X, Lo SC, Hannink M, Wu J, Fritsche K, Donato R, Sun GY (2005) Distinct signaling pathways for induction of type II NOS by IFNgamma and LPS in BV-2 microglial cells. Neurochem Int 47:298-307.

Silei V, Fabrizi C, Venturini G, Salmona M, Bugiani O, Tagliavini F, Lauro GM (1999) Activation of microglial cells by PrP and beta-amyloid fragments raises intracellular calcium through L-type voltage sensitive calcium channels. Brain Res 818:168-170.

Smith JA, Das A, Ray SK, Banik NL (2012) Role of pro-inflammatory cytokines released from microglia in neurodegenerative diseases. Brain research bulletin 87:10-20.

Smith ME (2001) Phagocytic properties of microglia in vitro: implications for a role in multiple sclerosis and EAE. Microsc Res Tech 54:81-94.

Smith ME, van der Maesen K, Somera FP (1998) Macrophage and microglial responses to cytokines in vitro: phagocytic activity, proteolytic enzyme release, and free radical production. Journal of neuroscience research 54:68-78.

Solito E, Sastre M (2012) Microglia function in Alzheimer's disease. Frontiers in pharmacology 3:14.

Sprague AH, Khalil RA (2009) Inflammatory cytokines in vascular dysfunction and vascular disease. Biochemical pharmacology 78:539-552.

Sriram K, Matheson JM, Benkovic SA, Miller DB, Luster MI, O'Callaghan JP (2006) Deficiency of TNF receptors suppresses microglial activation and alters the susceptibility of brain regions to MPTP-induced neurotoxicity: role of TNF-alpha. FASEB journal : official publication of the Federation of American Societies for Experimental Biology 20:670-682.

Stansley B, Post J, Hensley K (2012) A comparative review of cell culture systems for the study of microglial biology in Alzheimer's disease. Journal of neuroinflammation 9:115.

Stefano GB, Kim E, Liu Y, Zhu W, Casares F, Mantione K, Jones DA, Cadet P (2004) Nitric oxide modulates microglial activation. Med Sci Monit 10:BR17-22.

Stence N, Waite M, Dailey ME (2001) Dynamics of microglial activation: a confocal time-lapse analysis in hippocampal slices. Glia 33:256-266.

Stone WL, Yang H, Qui M (2006) Assays for nitric oxide expression. Methods in molecular biology 315:245-256.

Streit WJ, Xue QS (2009) Life and death of microglia. Journal of neuroimmune pharmacology : the official journal of the Society on NeuroImmune Pharmacology 4:371-379.

Streit WJ, Walter SA, Pennell NA (1999) Reactive microgliosis. Progress in neurobiology 57:563-581.

Streit WJ, Hurley SD, McGraw TS, Semple-Rowland SL (2000) Comparative evaluation of cytokine profiles and reactive gliosis supports a critical role for interleukin-6 in neuron-glia signaling during regeneration. J Neurosci Res 61:10-20.

Stricker J, Falzone T, Gardel ML (2010) Mechanics of the F-actin cytoskeleton. J Biomech 43:9-14.

Stuart LM, Bell SA, Stewart CR, Silver JM, Richard J, Goss JL, Tseng AA, Zhang A, El Khoury JB, Moore KJ (2007) CD36 signals to the actin cytoskeleton and regulates microglial migration via a p130Cas complex. The Journal of biological chemistry 282:27392-27401.

Su KY, Chien WL, Fu WM, Yu IS, Huang HP, Huang PH, Lin SR, Shih JY, Lin YL, Hsueh YP, Yang PC, Lin SW (2007) Mice deficient in collapsin response mediator protein-1 exhibit impaired long-term potentiation and impaired spatial learning and memory. The Journal of neuroscience : the official journal of the Society for Neuroscience 27:2513-2524.

Su X, Maguire-Zeiss KA, Giuliano R, Prifti L, Venkatesh K, Federoff HJ (2008) Synuclein activates microglia in a model of Parkinson's disease. Neurobiology of aging 29:1690-1701.

Syed MM, Phulwani NK, Kielian T (2007) Tumor necrosis factor-alpha (TNF-alpha) regulates Toll-like receptor 2 (TLR2) expression in microglia. Journal of neurochemistry 103:1461-1471.

Tambuyzer BR, Ponsaerts P, Nouwen EJ (2009) Microglia: gatekeepers of central nervous system immunology. J Leukoc Biol 85:352-370.

Tanaka S, Ide M, Shibutani T, Ohtaki H, Numazawa S, Shioda S, Yoshida T (2006) Lipopolysaccharide-induced microglial activation induces learning and memory deficits without neuronal cell death in rats. J Neurosci Res 83:557-566.

Tauser RG, Stoica O (2003) [Basic principles of the antisense strategy]. Rev Med Chir Soc Med Nat Iasi 107:483-486.

Tran EH, Hardin-Pouzet H, Verge G, Owens T (1997) Astrocytes and microglia express inducible nitric oxide synthase in mice with experimental allergic encephalomyelitis. Journal of neuroimmunology 74:121-129.

Tumer C, Bilgin HM, Obay BD, Diken H, Atmaca M, Kelle M (2007) Effect of nitric oxide on phagocytic activity of lipopolysaccharide-induced macrophages: possible role of exogenous L-arginine. Cell Biol Int 31:565-569.

Uttara B, Singh AV, Zamboni P, Mahajan RT (2009) Oxidative stress and neurodegenerative diseases: a review of upstream and downstream antioxidant therapeutic options. Curr Neuropharmacol 7:65-74.

Van Aelst L, D'Souza-Schorey C (1997) Rho GTPases and signaling networks. Genes Dev 11:2295-2322.

Veroni C, Gabriele L, Canini I, Castiello L, Coccia E, Remoli ME, Columba-Cabezas S, Arico E, Aloisi F, Agresti C (2010) Activation of TNF receptor 2 in microglia promotes induction of anti-inflammatory pathways. Molecular and cellular neurosciences 45:234-244.

Viatour P, Merville MP, Bours V, Chariot A (2005) Phosphorylation of NF-kappaB and IkappaB proteins: implications in cancer and inflammation. Trends Biochem Sci 30:43-52.

Villar-Cheda B, Dominguez-Meijide A, Joglar B, Rodriguez-Perez AI, Guerra MJ, Labandeira-Garcia JL (2012) Involvement of microglial RhoA/Rho-kinase pathway activation in the dopaminergic neuron death. Role of angiotensin via angiotensin type 1 receptors. Neurobiol Dis 47:268-279.

Vincent C, Siddiqui TA, Schlichter LC (2012) Podosomes in migrating microglia: components and matrix degradation. Journal of neuroinflammation 9:190.

von dem Borne AE, Verheugt FW, Oosterhof F, von Riesz E, de la Riviere AB, Engelfriet CP (1978) A simple immunofluorescence test for the detection of platelet antibodies. Br J Haematol 39:195-207.

Vuaillat C, Varrin-Doyer M, Bernard A, Sagardoy I, Cavagna S, Chounlamountri I, Lafon M, Giraudon P (2008) High CRMP2 expression in peripheral T lymphocytes is associated with recruitment to the brain during virus-induced neuroinflammation. Journal of neuroimmunology 193:38-51.

Wang LH, Strittmatter SM (1996) A family of rat CRMP genes is differentially expressed in the nervous system. The Journal of neuroscience : the official journal of the Society for Neuroscience 16:6197-6207.

Whitton PS (2007) Inflammation as a causative factor in the aetiology of Parkinson's disease. Br J Pharmacol 150:963-976.

Wilkinson B, Koenigsknecht-Talboo J, Grommes C, Lee CY, Landreth G (2006) Fibrillar beta-amyloid-stimulated intracellular signaling cascades require Vav for induction of respiratory burst and phagocytosis in monocytes and microglia. The Journal of biological chemistry 281:20842-20850.

Wilkinson BL, Landreth GE (2006) The microglial NADPH oxidase complex as a source of oxidative stress in Alzheimer's disease. Journal of neuroinflammation 3:30.

Wilms H, Zecca L, Rosenstiel P, Sievers J, Deuschl G, Lucius R (2007) Inflammation in Parkinson's diseases and other neurodegenerative diseases: cause and therapeutic implications. Curr Pharm Des 13:1925-1928.

Wilms H, Rosenstiel P, Romero-Ramos M, Arlt A, Schafer H, Seegert D, Kahle PJ, Odoy S, Claasen JH, Holzknecht C, Brandenburg LO, Deuschl G, Schreiber S, Kirik D, Lucius R (2009) Suppression of MAP kinases inhibits microglial activation and attenuates neuronal cell death induced by alpha-synuclein protofibrils. Int J Immunopathol Pharmacol 22:897-909.

Wilt SG, Milward E, Zhou JM, Nagasato K, Patton H, Rusten R, Griffin DE, O'Connor M, Dubois-Dalcq M (1995) In vitro evidence for a dual role of tumor necrosis factor-alpha in human immunodeficiency virus type 1 encephalopathy. Ann Neurol 37:381-394.

Wyss-Coray T (2006) Inflammation in Alzheimer disease: driving force, bystander or beneficial response? Nat Med 12:1005-1015.

Wyss-Coray T, Mucke L (2002) Inflammation in neurodegenerative disease--a double-edged sword. Neuron 35:419-432.

Yoshimura T, Kawano Y, Arimura N, Kawabata S, Kikuchi A, Kaibuchi K (2005) GSK-3beta regulates phosphorylation of CRMP-2 and neuronal polarity. Cell 120:137-149.

Zabel MK, Kirsch WM (2013) From development to dysfunction: Microglia and the complement cascade in CNS homeostasis. Ageing research reviews 12:749-756.

Zhang QG, Laird MD, Han D, Nguyen K, Scott E, Dong Y, Dhandapani KM, Brann DW (2012) Critical role of NADPH oxidase in neuronal oxidative damage and microglia activation following traumatic brain injury. PloS one 7:e34504.

Zhang W, Wang T, Pei Z, Miller DS, Wu X, Block ML, Wilson B, Zhou Y, Hong JS, Zhang J (2005) Aggregated alpha-synuclein activates microglia: a process leading to disease progression in Parkinson's disease. FASEB J 19:533-542.

Zhou Y, Ling EA, Dheen ST (2007) Dexamethasone suppresses monocyte chemoattractant protein-1 production via mitogen activated protein kinase phosphatase-1 dependent inhibition of Jun N-terminal kinase and p38 mitogen-activated protein kinase in activated rat microglia. Journal of neurochemistry 102:667-678.

Zusso M, Methot L, Lo R, Greenhalgh AD, David S, Stifani S (2012) Regulation of postnatal forebrain amoeboid microglial cell proliferation and development by the transcription factor Runx1. The Journal of neuroscience : the official journal of the Society for Neuroscience 32:11285-11298.

Figures and Figure legends

Fig.1.A. Confocal image shows the OX42 (green) microglia in the corpus callosum (CC, within dotted lines) in the postnatal rat brain. B. Confocal image with higher magnification shows the OX42 stained microglia in regions of corpus callosum (CC), lateral ventricle (LV) and subventricular zone (SVZ).

(CX indicates cortex region).

Fig.1

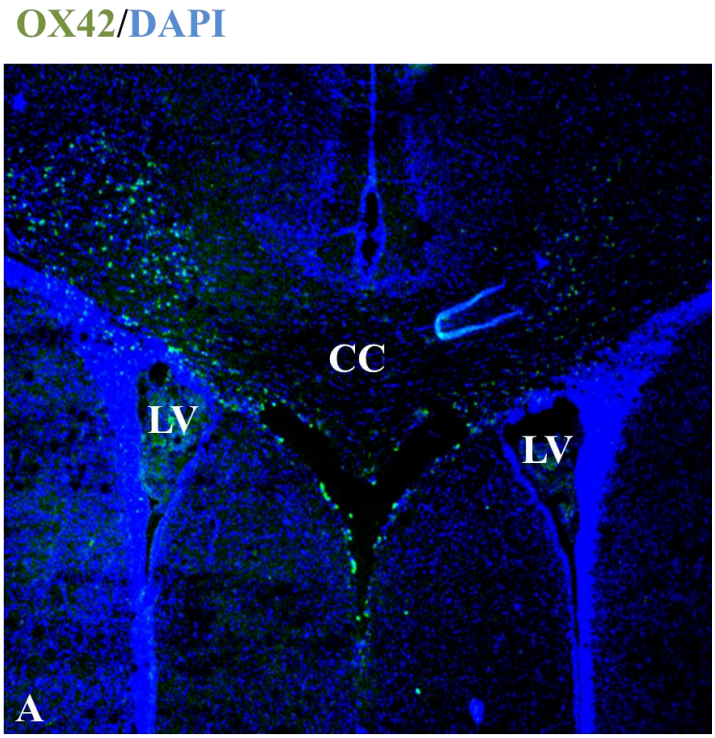

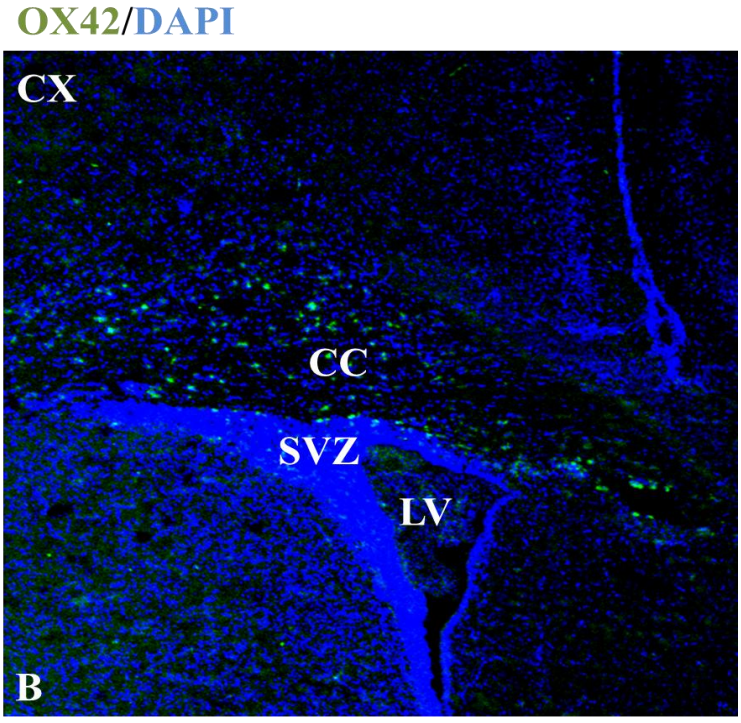

Fig.2. Differential immunoexpression of Dpysl3 in AMC and RMC. A. Confocal image showing the corpus collasum in 5-day postnatal rat brain. (CC- corpus callosum, SVZ- subventricular zone). Confocal images show the immunoexpression of Dpysl3 (red in C, F, I) and OX42 (green in B, E, H) in amoeboid microglial cells (AMC) in the corpus callosum (arrows). Colocalization of OX42 and Dpysl3 is shown in merged images (yellow in D, G, J). Dpysl3 expression is evident at postnatal day 3, 5 and 7-day and is absent in the RMC of postnatal day 14 (red in L). Nuclei are stained with DAPI (blue). Scale bar: 200μm & 50μm. **N)** The quantitative analysis shows that the percentage of Dpysl3-positive microglial cells in the corpus callosum decreases gradually with advancing age. The number of Dpysl3 positive cells decreased in the corpus callosum of 7- and 14-day old rats. Data are presented as mean ± SD (n=3).

Fig.2

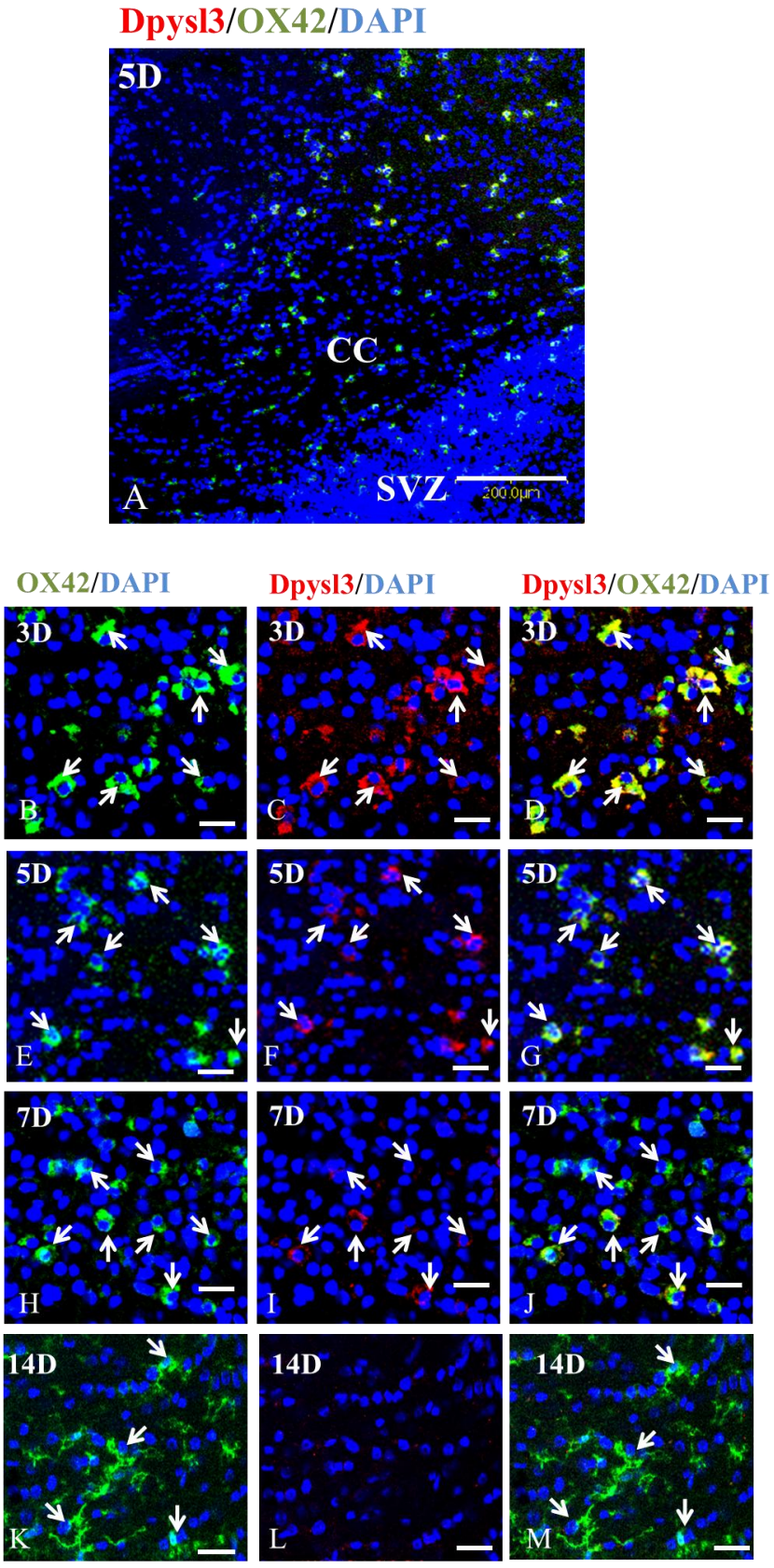
Dpysl3/OX42/DAPI
5D
CC
A
SVZ
200.0μm
OX42/DAPI
Dpysl3/DAPI
Dpysl3/OX42/DAPI
3D
B
3D
C
3D
D
5D
E
5D
F
5D
G
7D
H
7D
I
7D
J
14D
K
14D
L
14D
M

Fig.2

N

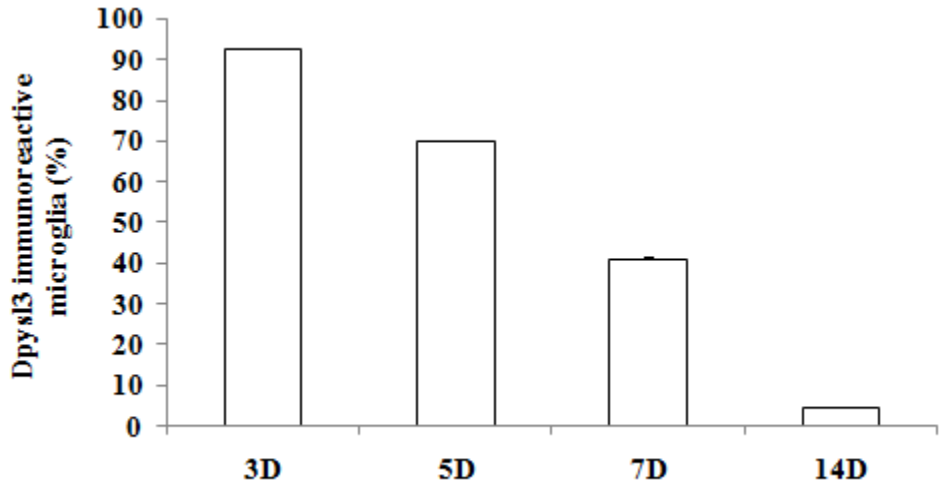
Dpysl3 immunoreactive microglia (%)
100
90
80
70
60
50
40
30
20
10
0
3D
5D
7D
14D

Fig. 3. Co-localization of Dpysl3 and OX42 in the LPS-treated postnatal rat brain by double fluorescence labeling. A–C) In normal postnatal rat brain (5-day old), Dpysl3 expression (red) is localized in OX42-positive microglial cells (green, arrows). **D-F)** Dpysl3 expression (red in E) appears to be increased in OX42 positive microglia (arrows) in the corpus callosum of postnatal rat pups injected with LPS. (CC-corpus callosum, SVZ- subventricular zone). Sections are counterstained with DAPI (blue). Scale bar: 100μm. **G)** The quantitative analysis shows that the percentage of Dpysl3-postive AMC is increased in the corpus callosum of LPS injected 5-day old rats when compared to the control. Data are presented as mean ± SD (n=3), ***p<0.01*.

Fig.3

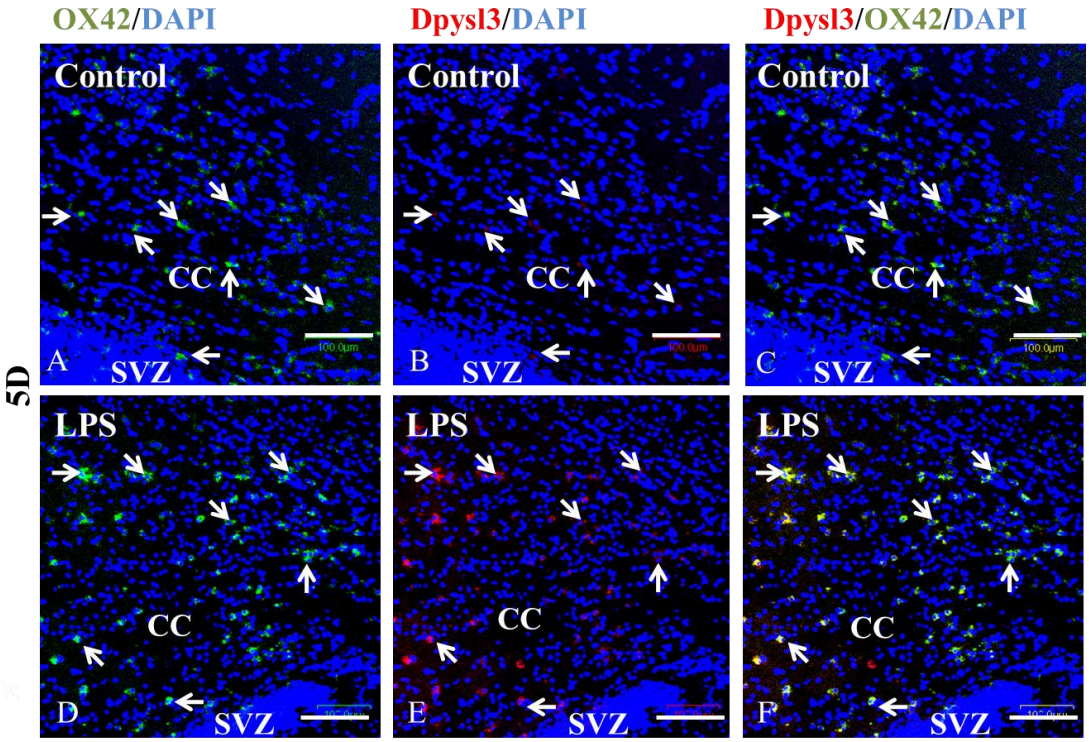
OX42/DAPI
Dpysl3/DAPI
Dpysl3/OX42/DAPI
5D
Control
LPS
CC
SVZ
A
B
C
D
E
F

G

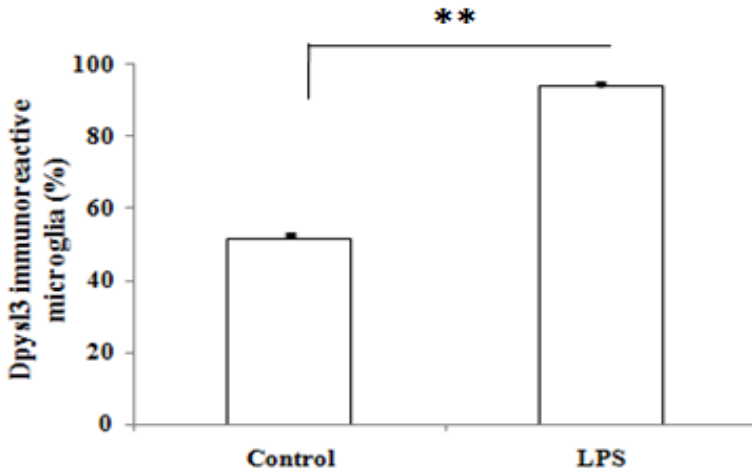
**
Dpysl3 immunoreactive microglia (%)
100
80
60
40
20
0
Control
LPS

Fig.4. Dpysl3 expression in microglial cells of the LPS-treated mature rat brain. A-C) In the normal mature rat brain (28-day old), the expression of Dpysl3 (red in B) is undetectable in OX42-positive (green) microglial cells (arrows in A). D-F) The expression of Dpysl3appears to be induced in OX42-positive microglia (arrows) in the corpus callosum of mature rats after LPS injection. Sections are counterstained with DAPI (blue). Scale bar: 50μm. G) The quantitative analysis shows that the percentage of Dpysl3-postive microglia is significantly increased in the corpus callosum of LPS-injected 28 day rats when compared to the control. Data are presented as mean ± SD (n=3), ***p<0.01*.

Fig.4

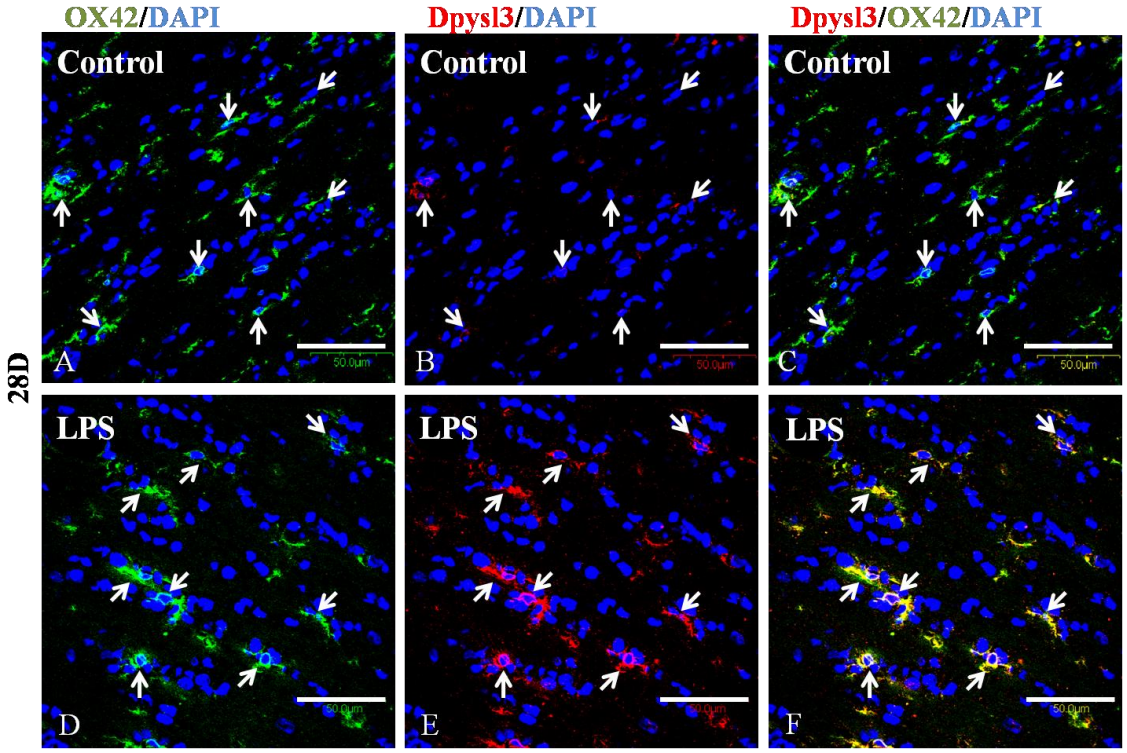
OX42/DAPI
Dpysl3/DAPI
Dpysl3/OX42/DAPI
28D
Control
Control
Control
LPS
LPS
LPS
A
B
C
D
E
F

G

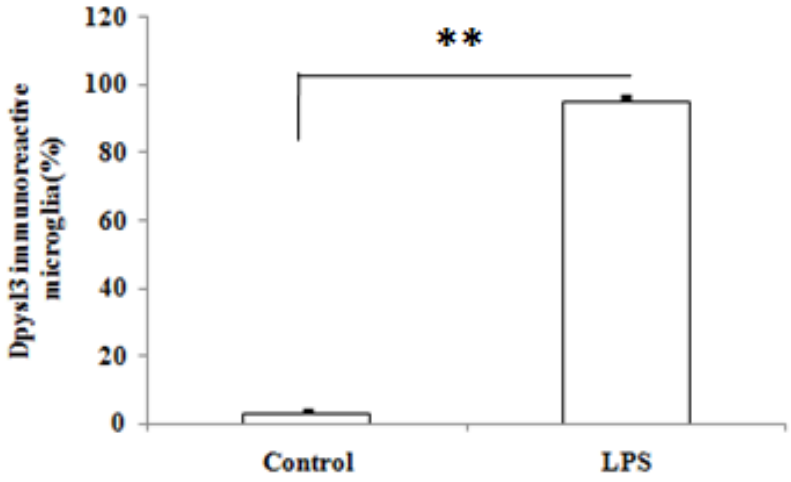
Dpysl3 immunoreactive microglia(%)
120
100
80
60
40
20
0
**
Control
LPS

Fig.5. Expression of Dpysl3 in the rat primary microglia. A-F**)** Confocal images show that the expression of Dpysl3 is highly increased in (red, E) in primary microglia treated with LPS when compared to the control (B). Lectin (green) is used as a marker for microglia. Nucleus is stained with DAPI (blue). Scale bar: 20μm.

Fig.5

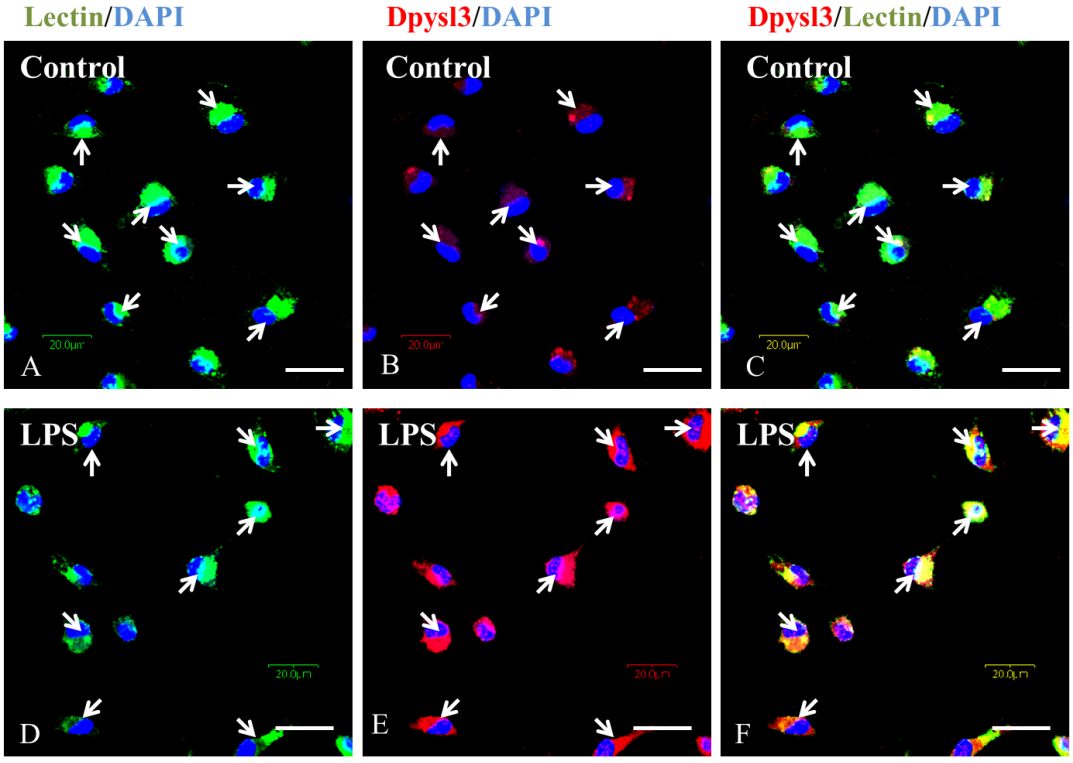
Lectin/DAPI
Dpysl3/DAPI
Dpysl3/Lectin/DAPI
Control
Control
Control
A
B
C
LPS
LPS
LPS
D
E
F

Fig.6. Dpysl3 expression level is increased in BV-2 microglia treated with LPS. A) The quantitative RT-PCR analysis shows that mRNA expression of Dpysl3 was upregulated at 1h after LPS treatment and gradually reduced at 6h after LPS exposure. Data are presented as mean ± SD (n=4), ***p<0.01; *p<0.05*. (B) Gel image showing the size of the amplicons (225bp). C-F) Confocal images show that expression of Dpysl3 (red in D) is increased in BV-2 microglia (arrows) at 1h after LPS treatment and is progressively decreased at 3h and 6h after LPS treatments (red in C, D). Scale bar: 50μm. G**)** Representative western blot showing the expression of Dpysl3 (65kDa) and β-actin (42kDa). H) Quantitative analysis confirms that the expression of Dpysl3 protein peaks at 1h but is reduced to basal level at 3-6h after LPS treatment. Data are represented as mean ± SD (n=5), ***p<0.01; *p<0.05*.

Fig.6

A

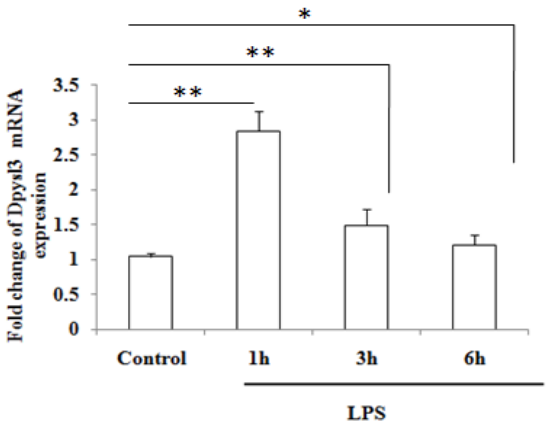
*
**
**
Fold change of Dpysl3 mRNA expression
3.5
3
2.5
2
1.5
1
0.5
0
Control
1h
3h
6h
LPS

B

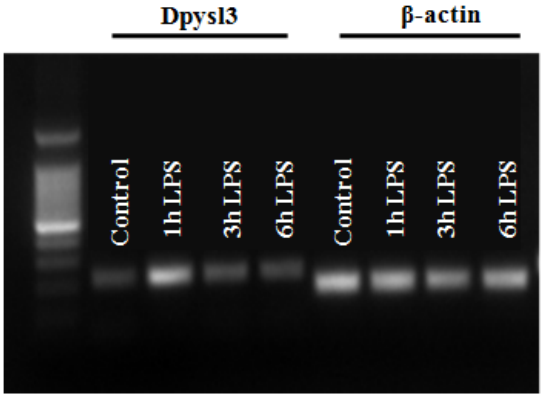
Dpysl3
β-actin
Control
1h LPS
3h LPS
6h LPS
Control
1h LPS
3h LPS
6h LPS

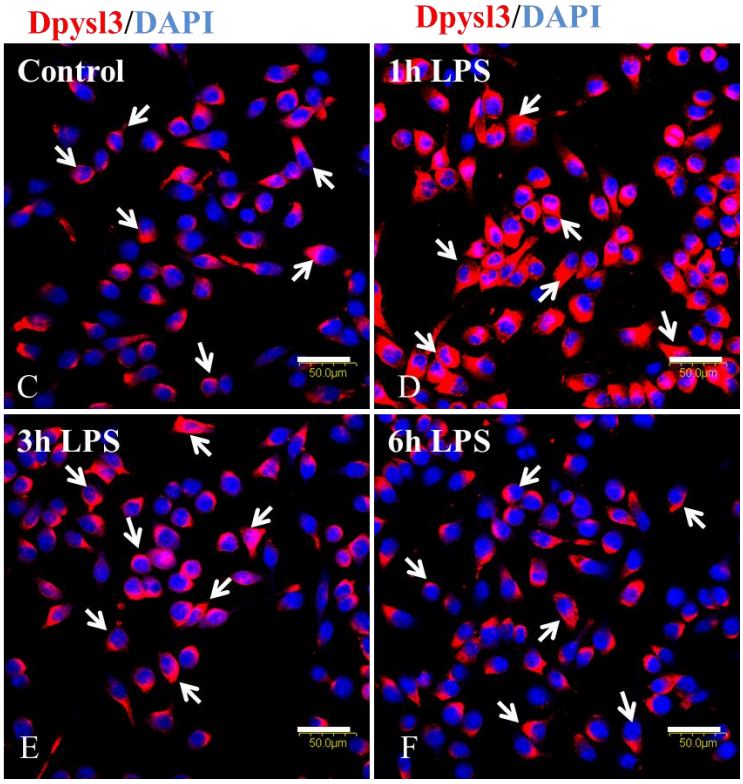
Dpysl3/DAPI
Control
C
50.0μm
Dpysl3/DAPI
1h LPS
D
50.0μm
3h LPS
E
50.0μm
6h LPS
F
50.0μm

Fig.6

G

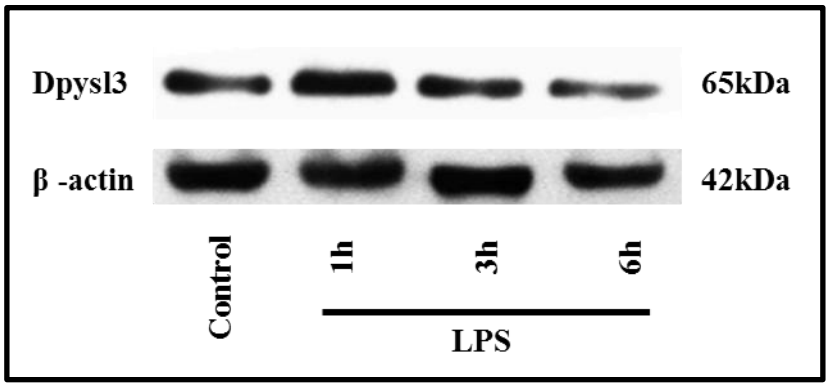
Dpysl3
65kDa
β -actin
42kDa
Control
1h
3h
6h
LPS

H

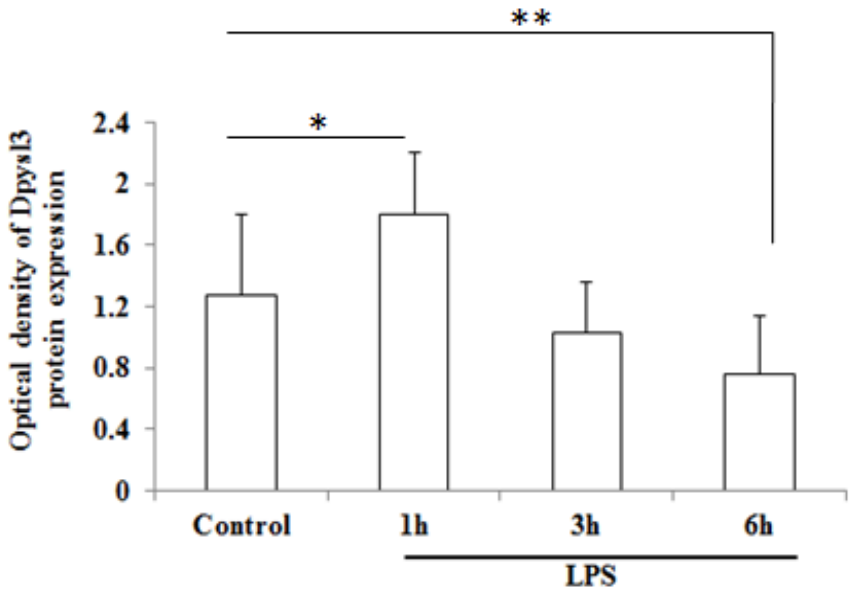
**
*
Optical density of Dpysl3 protein expression
2.4
2
1.6
1.2
0.8
0.4
0
Control
1h
3h
6h
LPS

Fig. 7. Distribution of Dpysl3 and F-actin in control and LPS-treated BV-2 microglial cells. A-C) Confocal images show the colocalization of Dpysl3 with Phalloidin dye (a high-affinity F-actin probe conjugated to the red-fluorescent dye) in untreated and LPS-treated BV-2microglia. D-F) Increased immunostaining of both Dpysl3 (FITC, green) and F-actin (red) is evident in activated microglial cells following 1h of LPS treatement. Scale bar: 20μm.

.

Fig.7

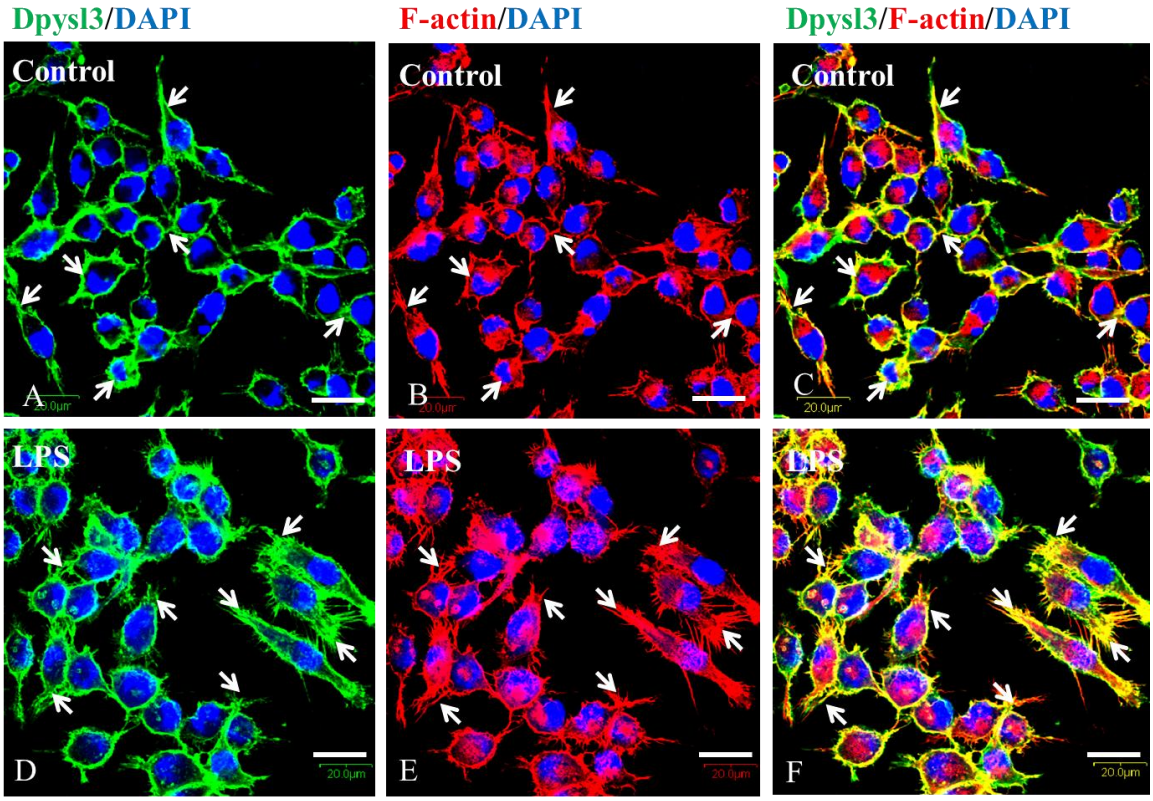
Dpysl3/DAPI
F-actin/DAPI
Dpysl3/F-actin/DAPI
Control
Control
Control
A
B
C
LPS
LPS
LPS
D
E
F
20.0μm

Fig.8. siRNA-mediated knockdown of Dpysl3 gene in BV-2 microglial cells. A) The expression of Dpysl3 mRNA was analyzed in Dpysl3 siRNA-transfected BV-2 cells by RT-PCR. The knockdown efficiency of about 80% was obtained in Dpysl3siRNA transfected cells when compared to cells transfected with negative control (scrambled siRNA-transfected cells). Data are presented as mean ± SD (n=3),*$p<0.05$. B) The viability assay shows that about 87-93% of the cells were viable after siRNA transfection. Data are presented as mean ± SD (n=3). C) Dpysl3 (65kDa) and β-actin (42kDa) immunoreactive bands are shown. D) The quantitative analysis shows the siRNA-mediated knockdown of Dpysl3 reduced the endogenous expression of Dpysl3 protein in BV-2 microglia significantly in comparison to that of cells transfected with scrambled siRNA. Data are presented as mean ± SD (n=5), **$p<0.01$;*$p<0.05$.

Fig.8

A

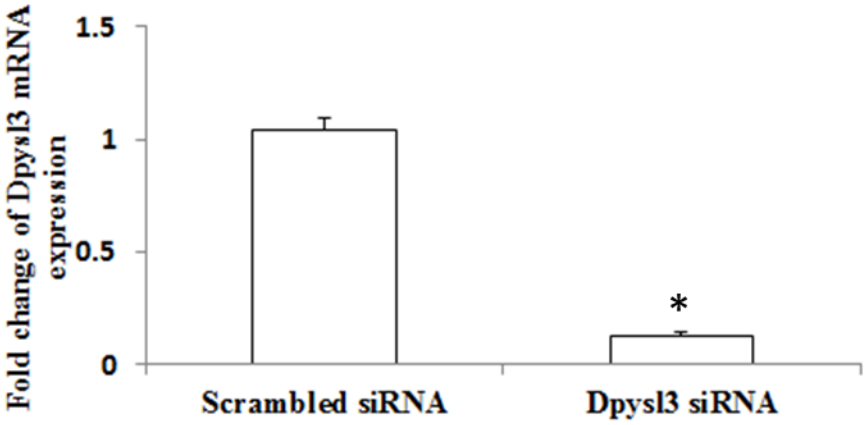
Fold change of Dpysl3 mRNA expression
1.5
1
0.5
0
*
Scrambled siRNA
Dpysl3 siRNA

B

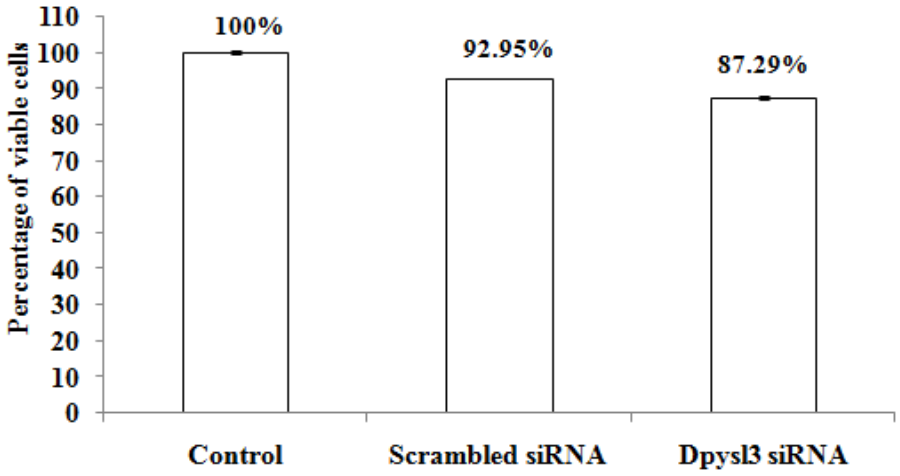
Percentage of viable cells
110
100
90
80
70
60
50
40
30
20
10
0
100%
92.95%
87.29%
Control
Scrambled siRNA
Dpysl3 siRNA

Fig.8

C

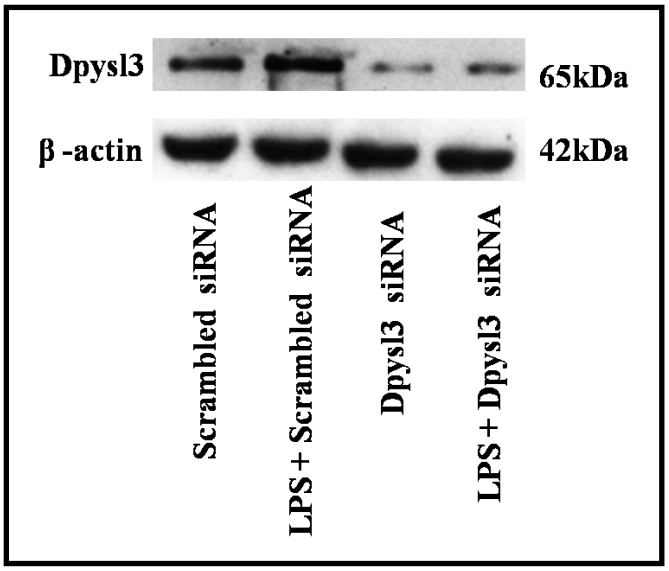
Dpysl3
65kDa
β -actin
42kDa
Scrambled siRNA
LPS + Scrambled siRNA
Dpysl3 siRNA
LPS + Dpysl3 siRNA

D

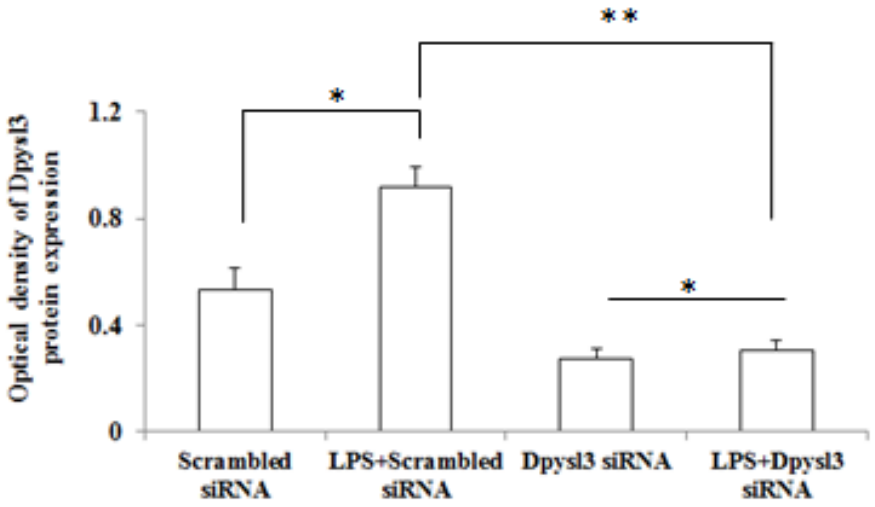
**
*
*
Optical density of Dpysl3 protein expression
1.2
0.8
0.4
0
Scrambled siRNA
LPS+Scrambled siRNA
Dpysl3 siRNA
LPS+Dpysl3 siRNA

Fig. 9. Effect of Dpysl3 knockdown on the production of TNF-α in BV-2 microglia. A**)** RT-PCR analysis shows that knockdown of Dpysl3 inhibits the expression of TNF-α mRNA in activated microglia at 1h LPS treatment, compared with that of negative control. Data are presented as mean ± SD (n=4), ***p<0.01;*p<0.05***.** B-E) Immunofluorescence images show the upregulation in TNF-α expression in BV-2 microglial cells (arrows) treated with LPS while the knockdown of Dpysl3 inhibits the LPS-stimulated increase inDpysl3 expression (red, D, E) Scale bar: 50μm. F) Representative western blots showing the expression of TNF-α (25.6kDa) and β-actin (42kDa) in Dpysl3 knockdown cells. G**)** Quantitative analysis shows that the knockdown of Dpysl3 reduced the expression of TNF-α protein in activated microglia by LPS. Data are presented as mean ± SD (n=6), ***p<0.01;*p<0.05*.

Fig.9

A

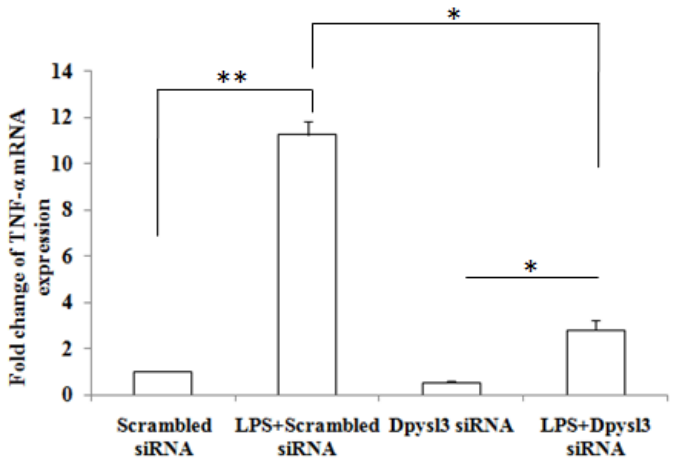
Fold change of TNF-α mRNA expression
14
12
10
8
6
4
2
0
**
*
*
Scrambled siRNA
LPS+Scrambled siRNA
Dpysl3 siRNA
LPS+Dpysl3 siRNA

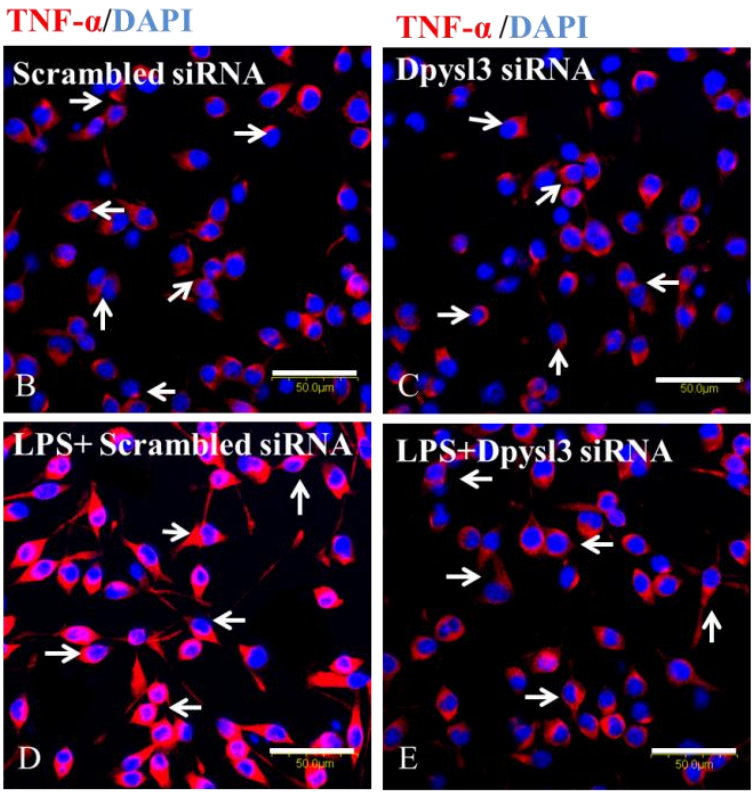
TNF-α/DAPI
Scrambled siRNA
B
TNF-α /DAPI
Dpysl3 siRNA
C
LPS+ Scrambled siRNA
D
LPS+Dpysl3 siRNA
E

Fig.9

F

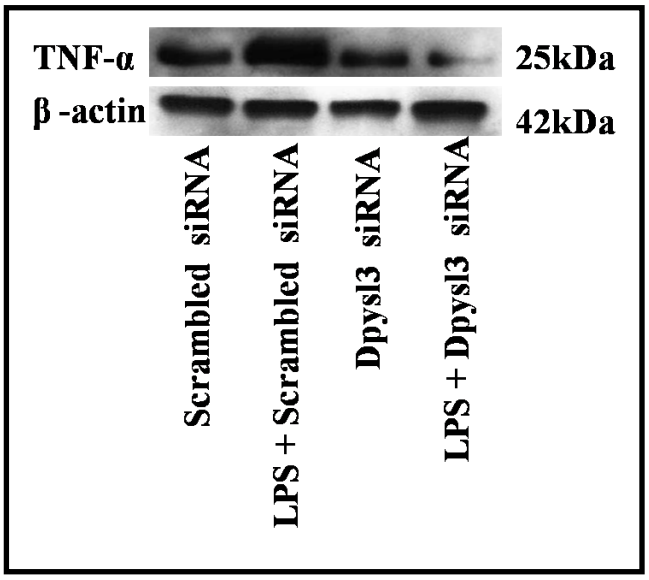
TNF-α
β -actin
25kDa
42kDa
Scrambled siRNA
LPS + Scrambled siRNA
Dpysl3 siRNA
LPS + Dpysl3 siRNA

G

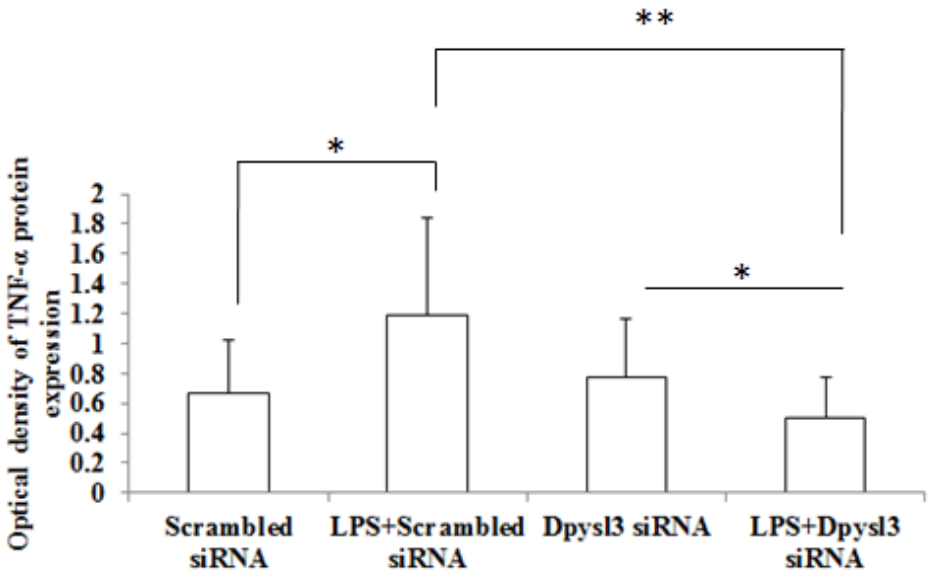
**
*
*
Optical density of TNF-α protein expression
2
1.8
1.6
1.4
1.2
1
0.8
0.6
0.4
0.2
0
Scrambled siRNA
LPS+Scrambled siRNA
Dpysl3 siRNA
LPS+Dpysl3 siRNA

Fig.10. Effect of Dpysl3 knockdown on the production of IL-1β in BV-2 microglia. A) RT-PCR analysis shows that knockdown of Dpysl3 decreases the IL-1β mRNA expression in activated microglia following 1h LPS treatment, compared with that of negative controls. Data are presented as mean ± SD (n=4), ***p<0.01;*p<0.05*. B-E) Immunofluorescence images show the upregulation of IL-1β expression (red, C) in BV-2 microglial cells (arrows) treated with LPS and the knockdown of Dpysl3 inhibits the LPS-stimulated increase of Dpysl3 expression (red, D, E). Scale bar: 50μm. **F)** IL-1β (17kDa) and β-actin (42kDa) immunoreactive bands are shown. G) Histogram shows that knockdown of Dpysl3 reduces the protein expression of IL-1β in BV-2 microglia treated with LPS. Data are presented as mean ± SD (n=6), ***p<0.01; *p<0.05*.

Fig.10

A

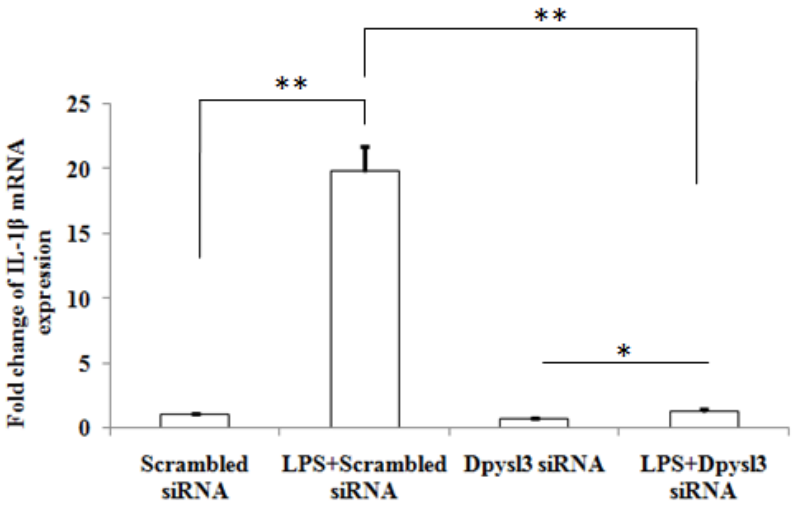
**
**
*
Fold change of IL-1β mRNA expression
25
20
15
10
5
0
Scrambled siRNA
LPS+Scrambled siRNA
Dpysl3 siRNA
LPS+Dpysl3 siRNA

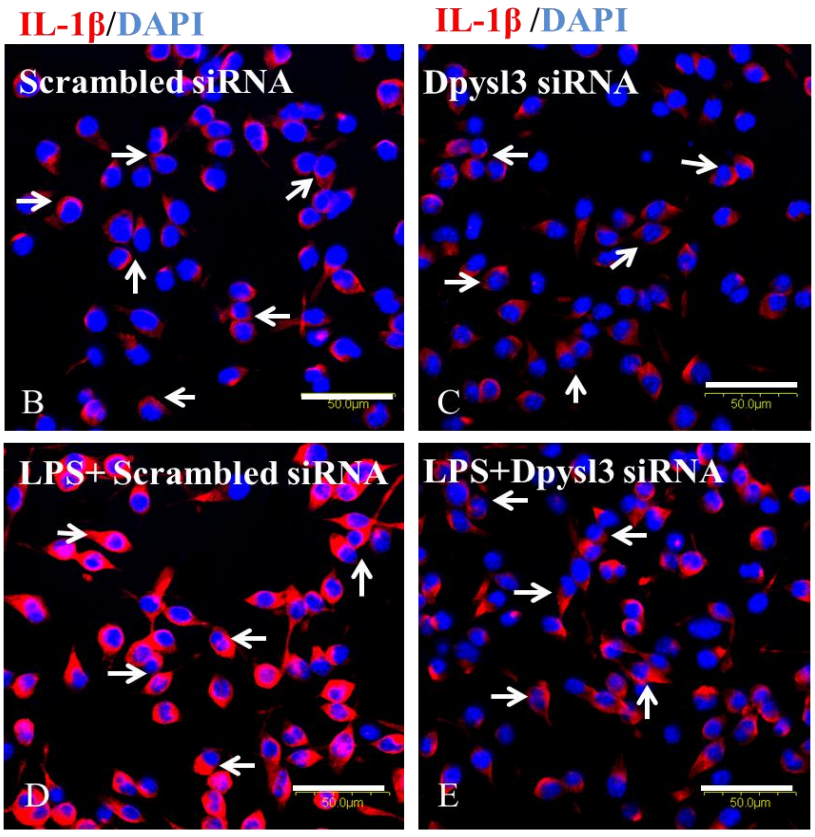
IL-1β/DAPI
IL-1β /DAPI
Scrambled siRNA
Dpysl3 siRNA
LPS+Scrambled siRNA
LPS+Dpysl3 siRNA
B
C
D
E
50.0μm

Fig.10

F

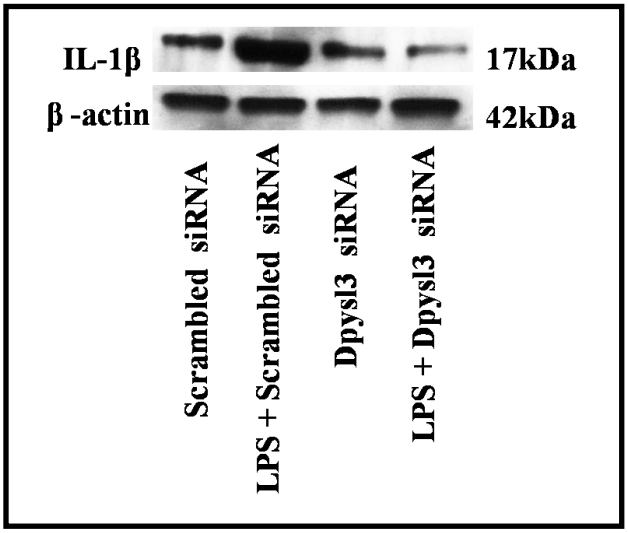
IL-1β
17kDa
β -actin
42kDa
Scrambled siRNA
LPS + Scrambled siRNA
Dpysl3 siRNA
LPS + Dpysl3 siRNA

G

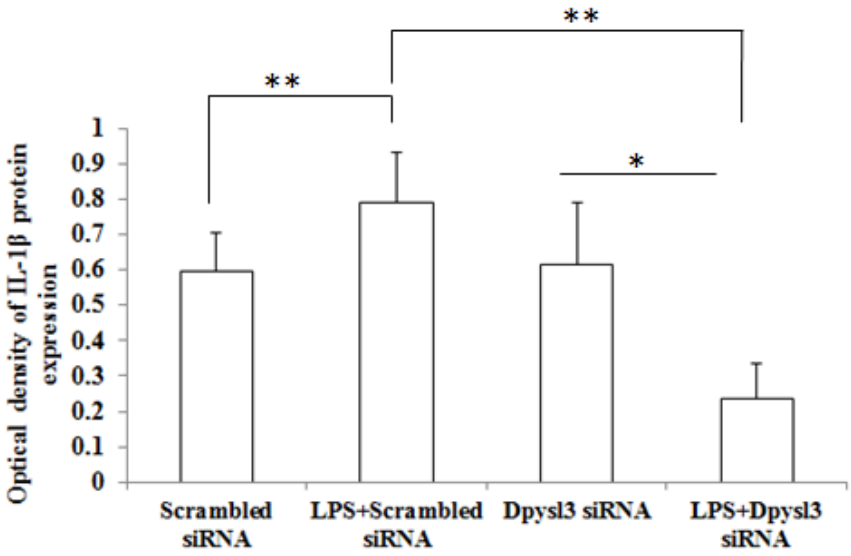
**
**
*
Optical density of IL-1β protein expression
1
0.9
0.8
0.7
0.6
0.5
0.4
0.3
0.2
0.1
0
Scrambled siRNA
LPS+Scrambled siRNA
Dpysl3 siRNA
LPS+Dpysl3 siRNA

Fig. 11. Effect of Dpysl3 knockdown on the mRNA and protein expression of iNOS in activated BV-2 microglia. A) qRT-PCR analysis shows that knockdown of Dpysl3 decreases the induction of iNOS mRNA expression in activated microglia at 1h LPS treatment, compared with that of negative control. Data are presented as mean ± SD (n=4), where $**p<0.01$;$*p<0.05$. B-E) Immunofluorescence images show that the knockdown of Dpysl3 reduced the expression of iNOS (red, E) in activated BV-2 microglia. Scale bar: 50μm.

Fig.11

A

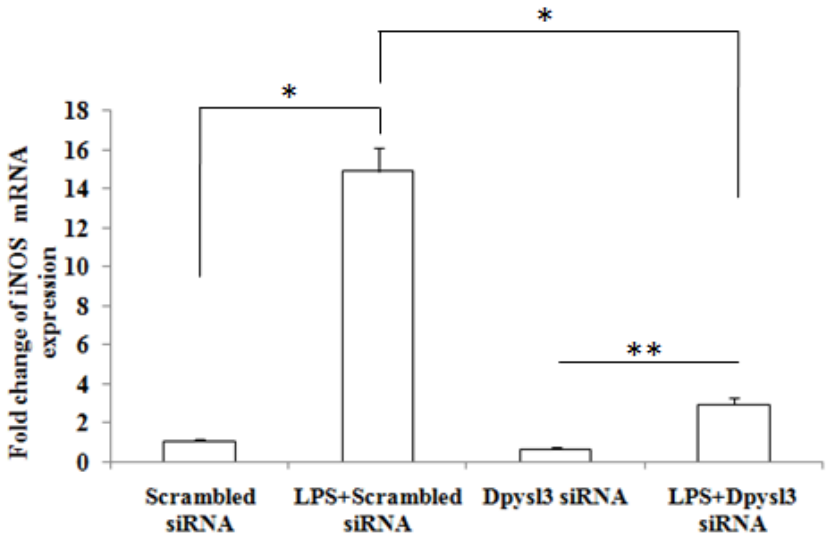
*
*
**
Fold change of iNOS mRNA expression
18
16
14
12
10
8
6
4
2
0
Scrambled siRNA
LPS+Scrambled siRNA
Dpysl3 siRNA
LPS+Dpysl3 siRNA

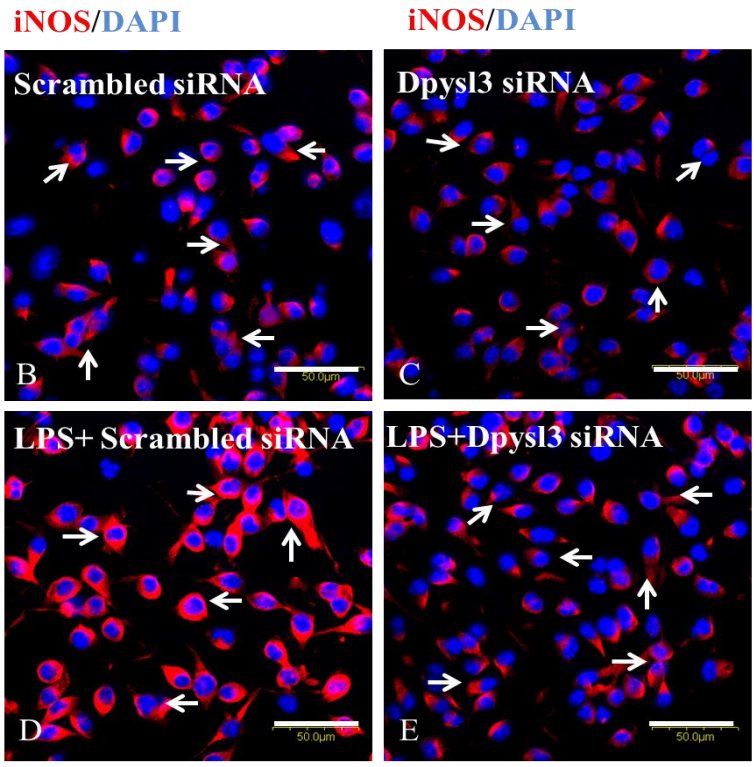
iNOS/DAPI
iNOS/DAPI
Scrambled siRNA
Dpysl3 siRNA
B
C
LPS+ Scrambled siRNA
LPS+Dpysl3 siRNA
D
E
50.0μm

Fig. 12. Effect of knockdown of Dpysl3 on the production of nitric oxide (NO) in activated BV-2 microglia. Bar graph shows that NO release was induced significantly in activated microglia while the knockdown of Dpysl3 inhibited this induction in activated microglia following 1h LPS treatment. Data are presented as mean ± SD (n=3), where ***p<0.01*; **p<0.05*.

Fig.12

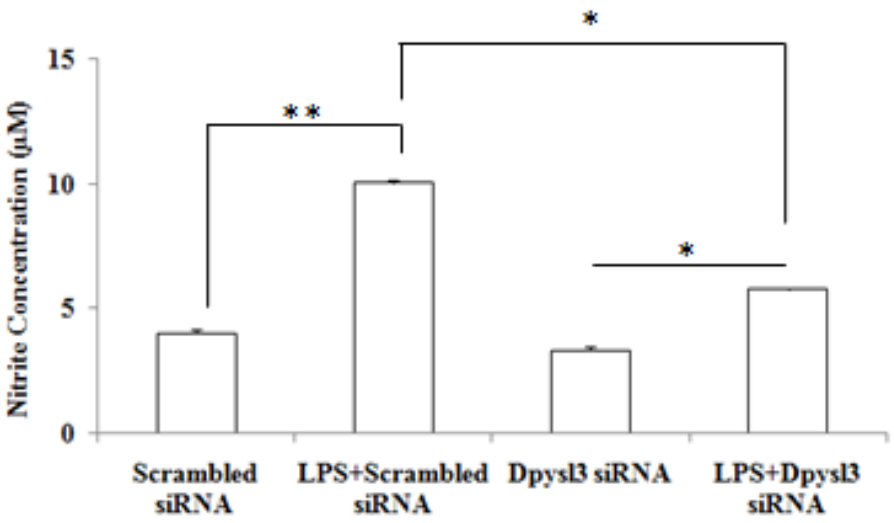
*
**
*
15
10
5
0
Nitrite Concentration (µM)
Scrambled siRNA
LPS+Scrambled siRNA
Dpysl3 siRNA
LPS+Dpysl3 siRNA

Fig.13. Knockdown of Dpysl3 inhibits the nuclear translocation of NF-κB in activated BV-2 microglial cells. A-D) Confocal images of BV-2 microglia transfected with Dpysl3 siRNA or negative control and treated with or without LPS are shown. The nuclear translocation of NF-κB (red, arrows in C) is evident in activated BV-2 microglial cells following 1h LPS treatment. However, majority of the cells transfected with Dpysl3 siRNA did not show nuclear translocation of NF-κB (D). Nuclei are stained with DAPI (blue). Scale bar: 50μm. E) Western blot shows the expression of NF-κB (65kDa) and LaminA (74kDa) in nuclear protein isolated from the various groups of BV-2 microglial cells. F) The quantitative analysis revealed that the expression of nuclear NF-κB protein is increased in BV-2 cells exposed to LPS. However, this increase is not evident in activated BV-2 microglia following knockdown of Dpysl3, indicating a suppression of nuclear translocation of NF-κB protein. Data are presented as mean ± SD (n=4),*$p<0.05$;**$p<0.01$

Fig.13

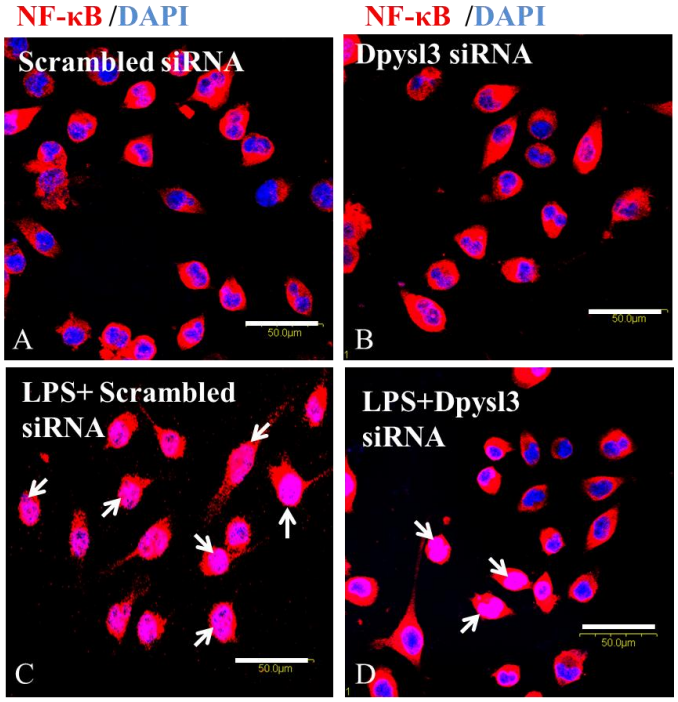
NF-κB /DAPI
Scrambled siRNA
A
NF-κB /DAPI
Dpysl3 siRNA
B
LPS+ Scrambled siRNA
C
LPS+Dpysl3 siRNA
D

E

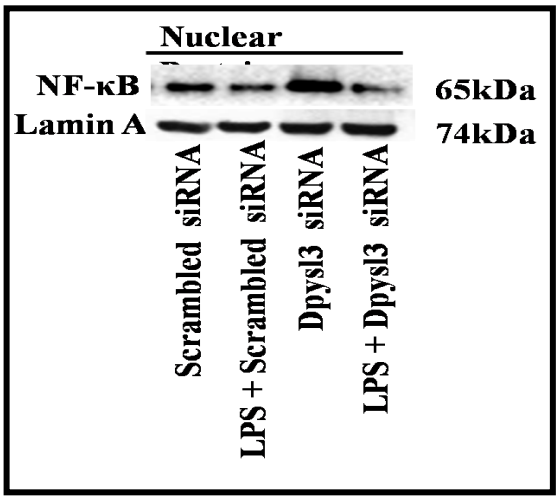
Nuclear
NF-κB
Lamin A
65kDa
74kDa
Scrambled siRNA
LPS + Scrambled siRNA
Dpysl3 siRNA
LPS + Dpysl3 siRNA

F

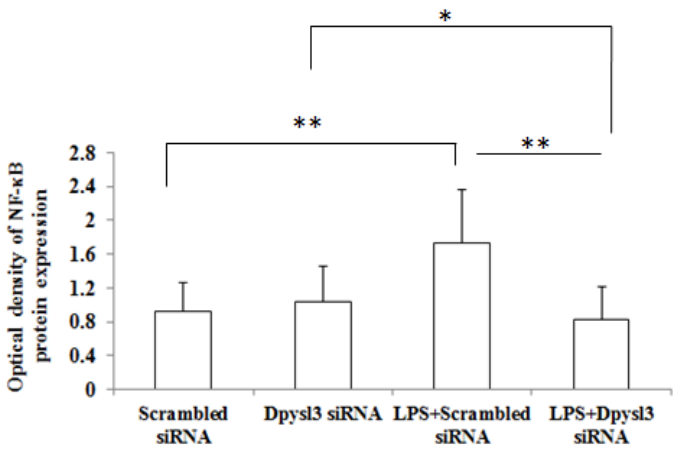
*
**
**
Optical density of NF-κB protein expression
2.8
2.4
2
1.6
1.2
0.8
0.4
0
Scrambled siRNA
Dpysl3 siRNA
LPS+Scrambled siRNA
LPS+Dpysl3 siRNA

Fig. 14. Confocal immunofluorescence images showing the expression of Dpysl3 (FITC, green) with F-actin (TRITC, red) in BV-2 microglial cells transfected with scrambled siRNA (A-F) and Dpysl3 specific siRNA (G-L). A-F) The expression of Dpysl3 which colocalizes with F-actin in negative control transfected BV-2 microglia cells (A-C) appear to be increased when the BV-2 microglial cells were treated with 1h LPS (D-F). Note that microglia treated with LPS exhibit actin microspike projections (D-F); Knockdown of Dpysl3 resulted in reduced actin staining and formation of actin microspike projections (G-I) following LPS treatment compared to negative control (G-L). Scale bar: 20μm.M) Quantitative analysis shows that siRNA-mediated knockdown of Dpysl3 decreased the intensity of Dpysl3 expression in BV-2 microglial cells, compared with that of negative control. Data are presented as mean ± SD (n=3), *$**p<0.01$,$*p<0.05$.*

Fig.14

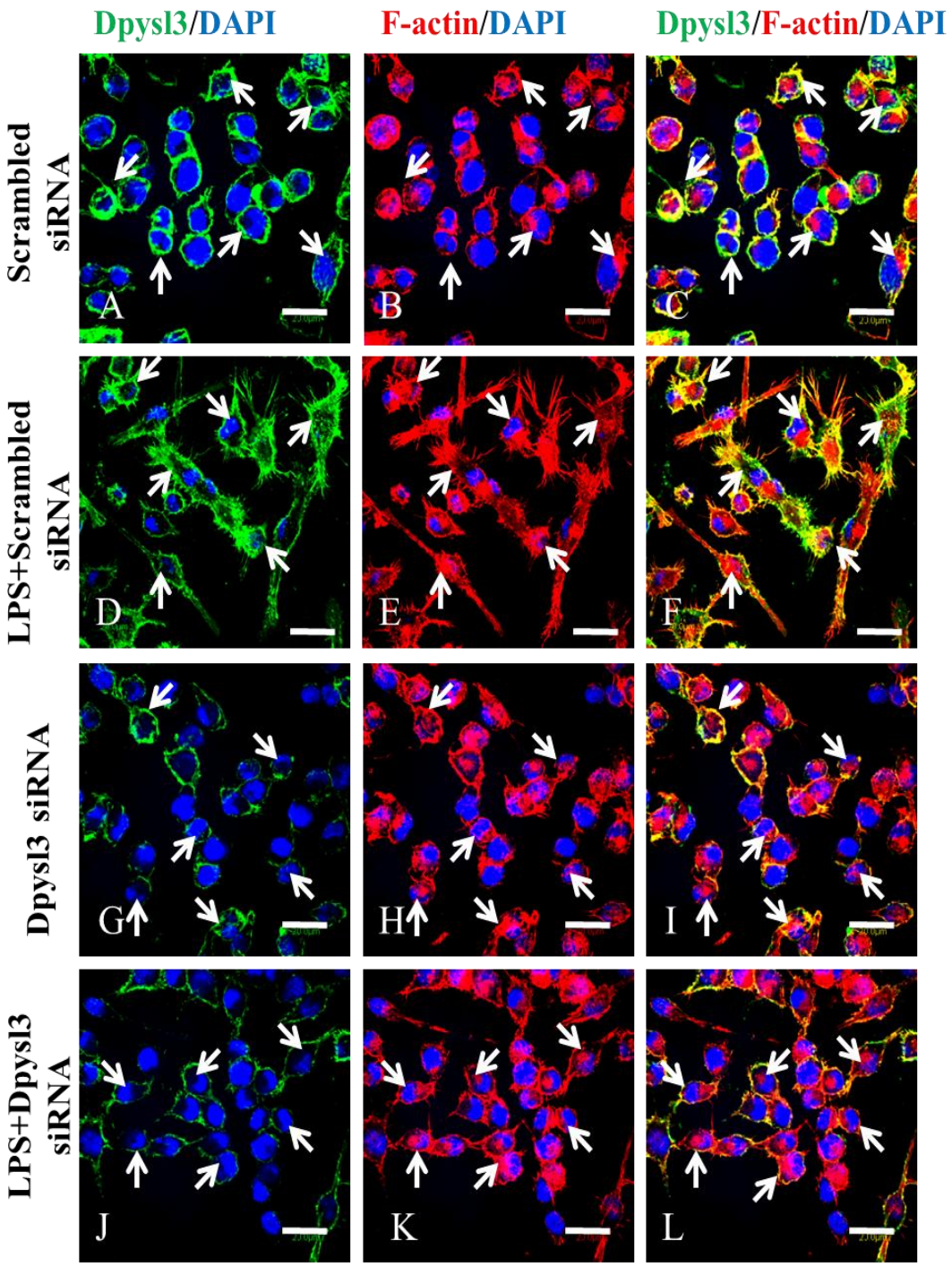
Dpysl3/DAPI
F-actin/DAPI
Dpysl3/F-actin/DAPI
Scrambled siRNA
LPS+Scrambled siRNA
Dpysl3 siRNA
LPS+Dpysl3 siRNA
A
B
C
D
E
F
G
H
I
J
K
L

Fig.14

M

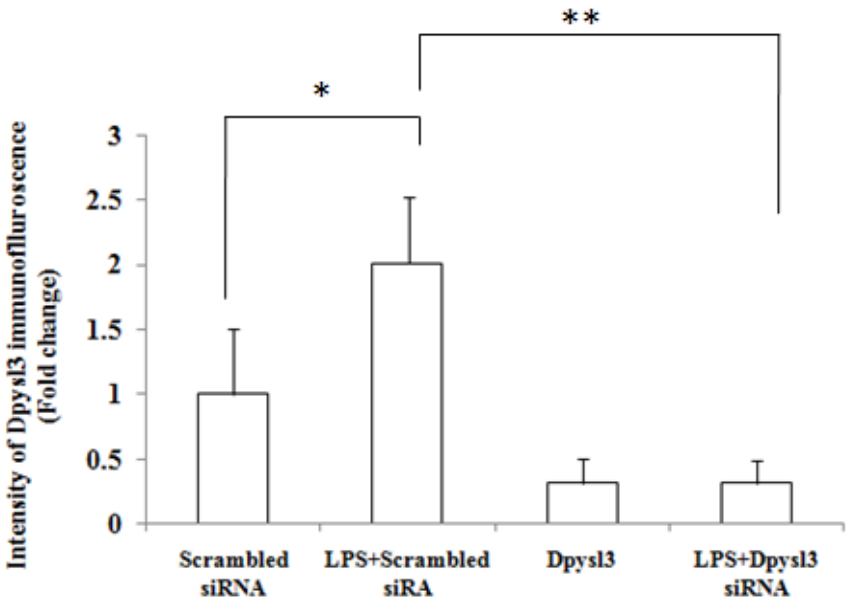
**
*
Intensity of Dpysl3 immunofluroscence (Fold change)
3
2.5
2
1.5
1
0.5
0
Scrambled siRNA
LPS+Scrambled siRA
Dpysl3
LPS+Dpysl3 siRNA

Fig. 15. Transwell migration assay shows that knockdown of Dpysl3 reduces the migration of activated BV-2 microglia. A-D) Light microscopy images of BV-2 cells transfected with Dpysl3 siRNA or negative control and treated with or without LPS in transwell chamber are shown. E) The quantitative analysis revealed an increase in migration of microglia, while knockdown of Dpysl3 reduced the migrating ability of BV-2 microglia. Data are represented as mean ± SD (n=4), ***p<0.01;*p<0.05*. Scale bar: 100μm.

Fig.15

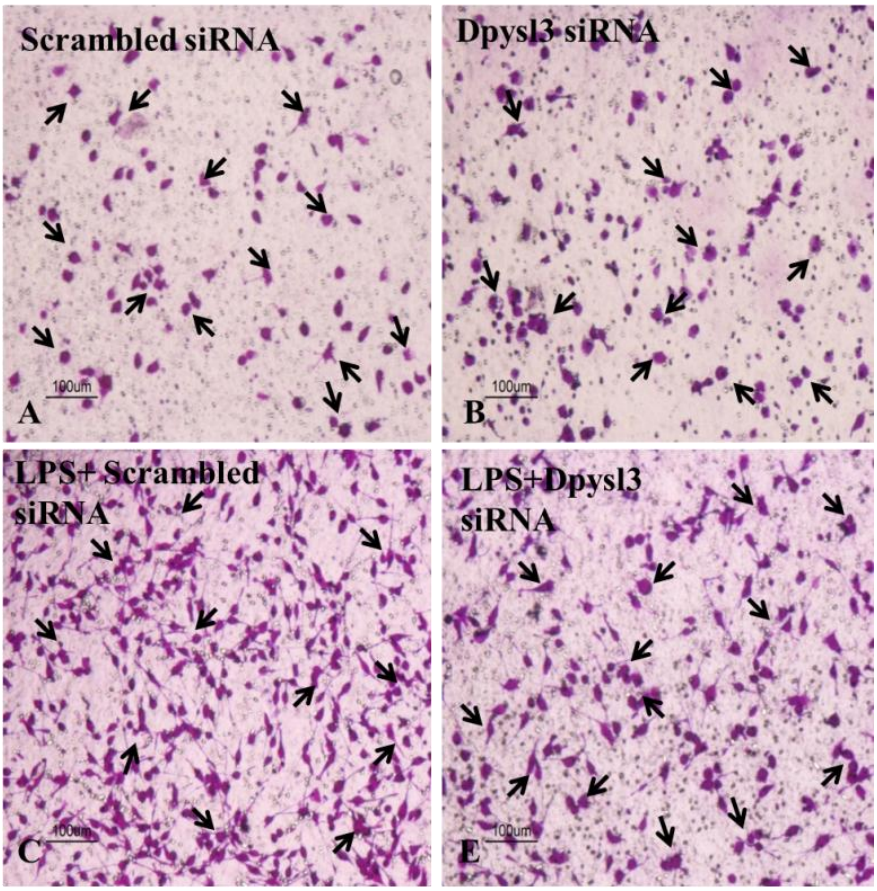
Scrambled siRNA
A
100um
Dpysl3 siRNA
B
100um
LPS+ Scrambled siRNA
C
100um
LPS+Dpysl3 siRNA
E
100um

E

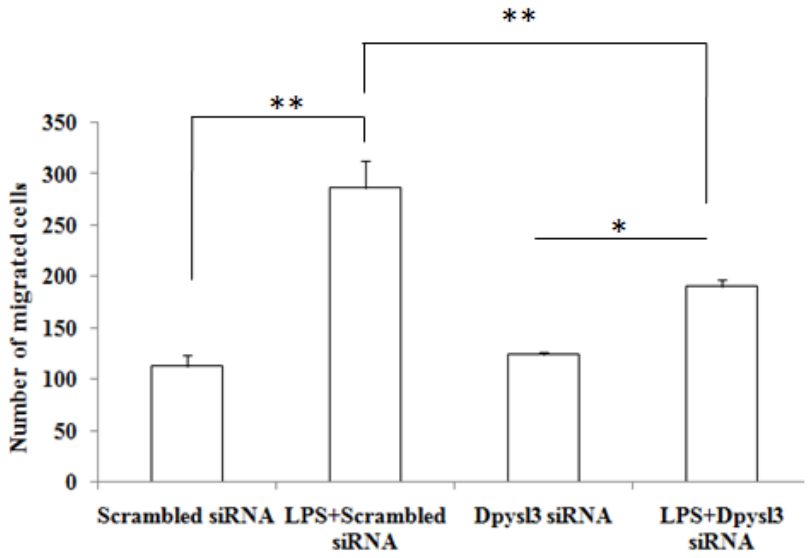
**
**
*
Number of migrated cells
350
300
250
200
150
100
50
0
Scrambled siRNA
LPS+Scrambled siRNA
Dpysl3 siRNA
LPS+Dpysl3 siRNA

Fig. 16.Knockdown of Dpysl3 inhibits the phagocytosis by activated BV-2 microglia. A-D) Confocal images of BV-2 microglial cells transfected with Dpysl3siRNA or negative control and treated with or without LPS are shown. Only a small percentage of unstimulated BV-2 microglial cells transfected either with scrambled or Dpysl3 siRNA, ingested with latex beads. E) The quantitative analysis shows the number of phagocytic cells laden with latex beads increased significantly after 1h LPS stimulation, while knockdown of Dpysl3 appears to inhibit this increase significantly. Data are presented as mean ± SD (n=4), ***p<0.01; *p<0.05*. Scale bar: 20μm.

Fig. 16

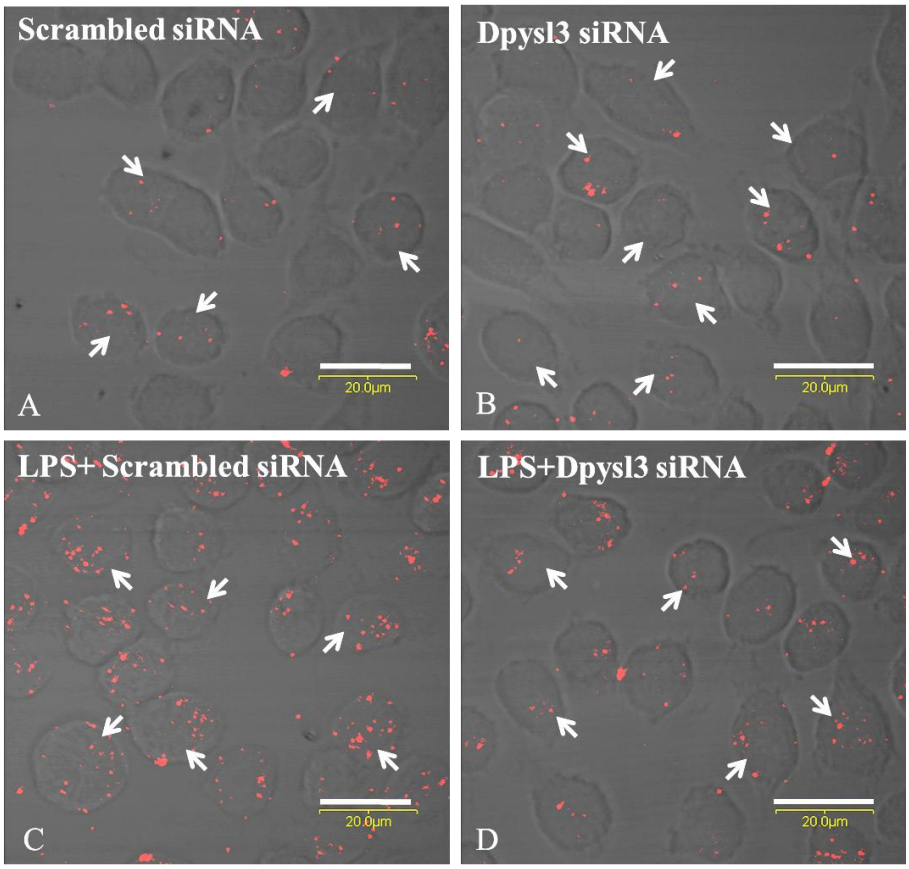
Scrambled siRNA
A
20.0μm
Dpysl3 siRNA
B
20.0μm
LPS+ Scrambled siRNA
C
20.0μm
LPS+Dpysl3 siRNA
D
20.0μm

E

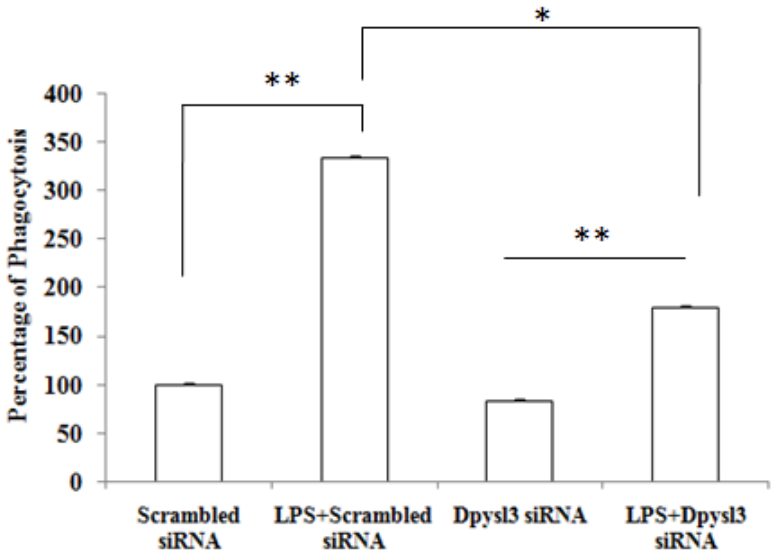
Percentage of Phagocytosis
400
350
300
250
200
150
100
50
0
**
*
**
Scrambled siRNA
LPS+Scrambled siRNA
Dpysl3 siRNA
LPS+Dpysl3 siRNA

Fig. 17. Effect of Dpysl3 knockdown on the proliferation index of BV-2 microglia. A-L) Confocal immunofluorescence images showing the expression of BrdU (red) and lectin (green) in control and LPS-activated BV-2 microglia following transfection of Dpysl3 or scrambled siRNA. M) Quantitative analysis shows that the percentage of BrdU positive cells was significantly increased in scrambled siRNA transfected BV-2 microglial cells following 1h LPS stimulation. Knockdown of Dpysl3 significantly inhibited this increase in activated BV-2 microglial cells. Data are presented as mean ± SD (n=6),*$p<0.05$. Scale bar: 50μm.

Fig.17

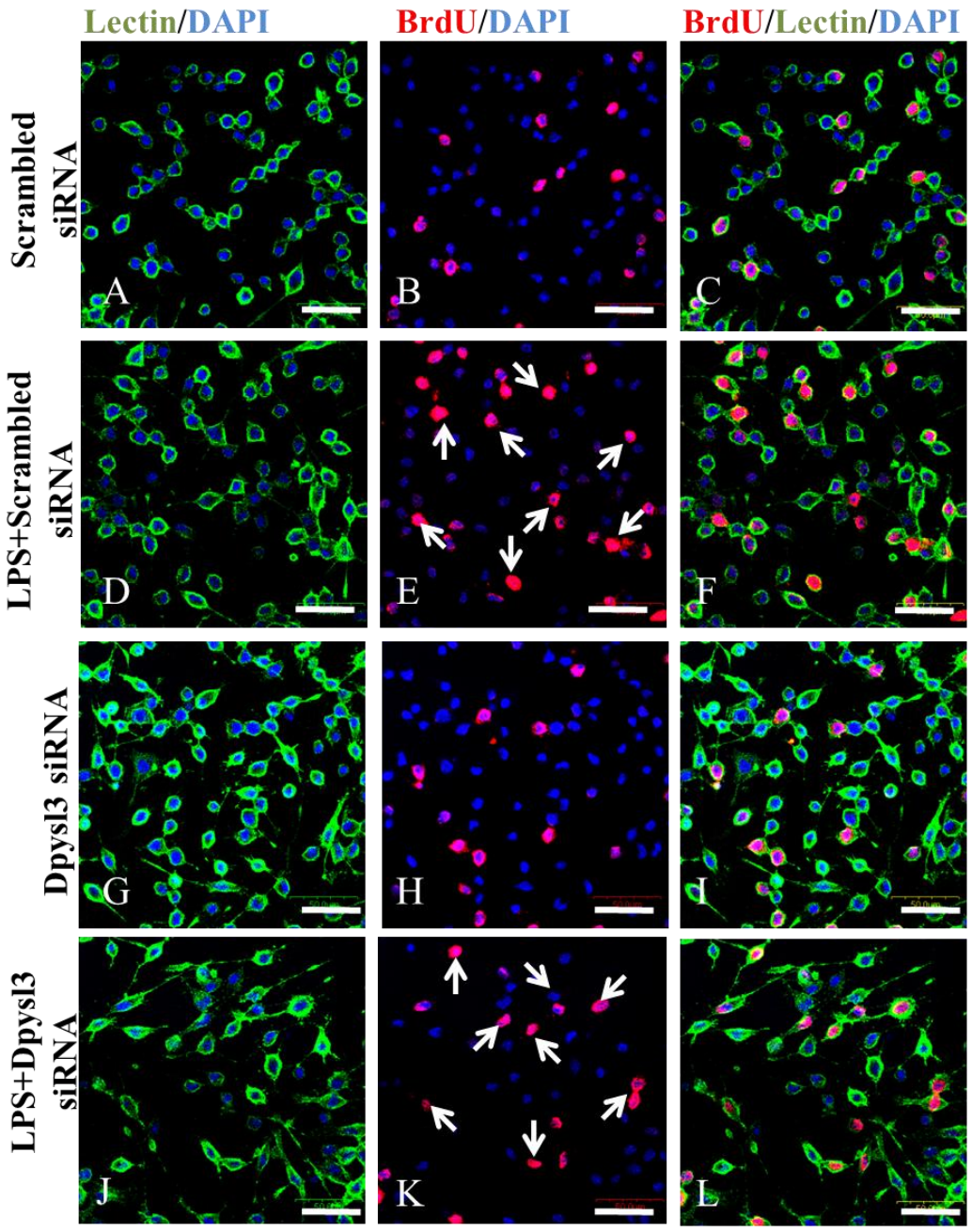
Lectin/DAPI
BrdU/DAPI
BrdU/Lectin/DAPI
Scrambled siRNA
LPS+Scrambled siRNA
Dpysl3 siRNA
LPS+Dpysl3 siRNA
A
B
C
D
E
F
G
H
I
J
K
L

Fig.17

M

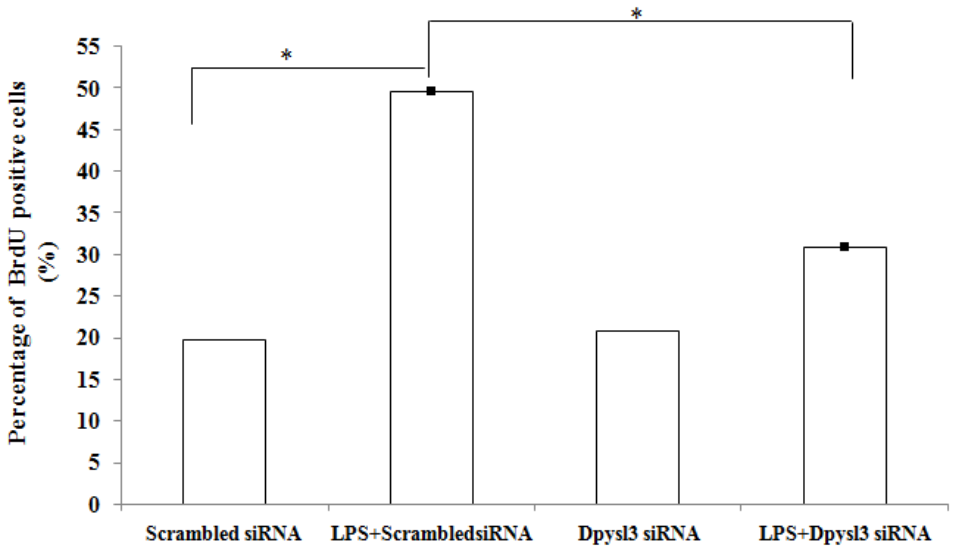
Percentage of BrdU positive cells (%)
55
50
45
40
35
30
25
20
15
10
5
0
*
*
Scrambled siRNA
LPS+ScrambledsiRNA
Dpysl3 siRNA
LPS+Dpysl3 siRNA

Fig.18.Interaction of Dpysl3 and RhoA by co-immunoprecipitation in microglial BV-2 cells. Western blot shows the expression of Dpysl3 and RhoA proteins in BV-2 microglia before and after immunoprecipitation. Dpysl3 (65kDa) and **RhoA** (24kDa) proteins were co-immunoprecipitated from control as well as in 1h LPS treated microglia. Mouse IgG was used as an isotype control. (**Control-Wild type:** Untreated BV-2 cells, **Control- IgG**: IgG pull down from untreated BV-2 cells, **Control- Ab:** Antibody pull down from untreated BV-2cells, **LPS-Wild type:** LPS treated BV-2 cells, **LPS- IgG:** IgG pull down from LPS-treated BV-2 cells, **LPS–Ab**: Antibody pull down from LPS treated BV-2 cells)

Fig.18

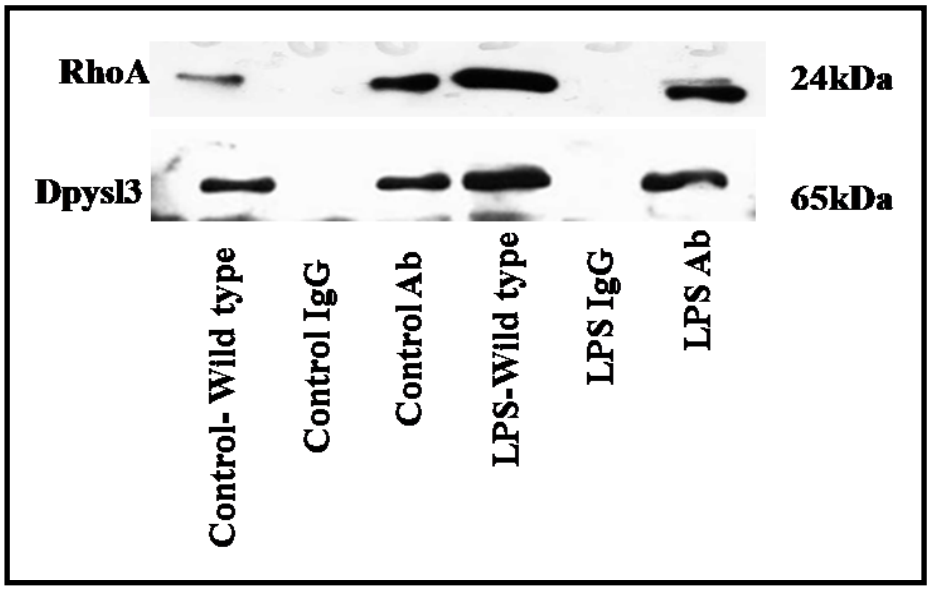
RhoA
24kDa
Dpysl3
65kDa
Control- Wild type
Control IgG
Control Ab
LPS-Wild type
LPS IgG
LPS Ab

Fig.19. **Effect of Dpysl3 knockdown on the production of RhoA in activated BV-2 microglia.** A) RT-PCR analysis shows that knockdown of Dpysl3 inhibits the expression of RhoA mRNA activated microglia at 1h LPS treatment, compared with that of negative control. Data are presented as mean ± SD (n=4), ***p<0.01*. B-E) Immunofluorescence images show the upregulation of RhoA expression in BV-2 microglial cells treated with LPS, while the knockdown of Dpysl3 inhibits the LPS-stimulated increase in RhoA expression (red, E), Scale bar: 50μm. F) Representative western blot shows the expression of RhoA (24kDa) and β-actin (42kDa) proteins in scrambled or Dpysl3 siRNA transfected BV-2 microglial cells. G**)** Quantitative analysis shows that knockdown of Dpysl3 reduced the protein expression of RhoA in microglia treated with LPS. Data are presented as mean ± SD (n=6), ***p<0.01;*p<0.05*.

\

Fig.19

A

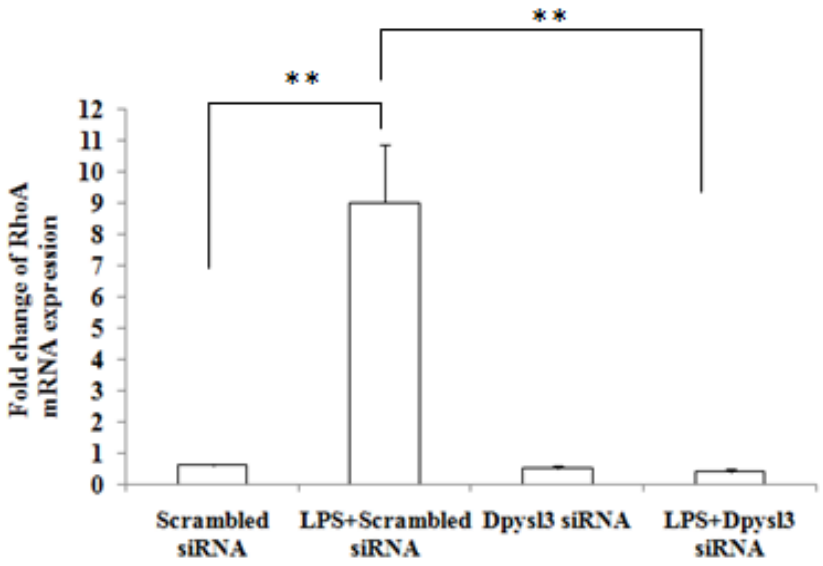
**
**
Fold change of RhoA mRNA expression
12
11
10
9
8
7
6
5
4
3
2
1
0
Scrambled siRNA
LPS+Scrambled siRNA
Dpysl3 siRNA
LPS+Dpysl3 siRNA

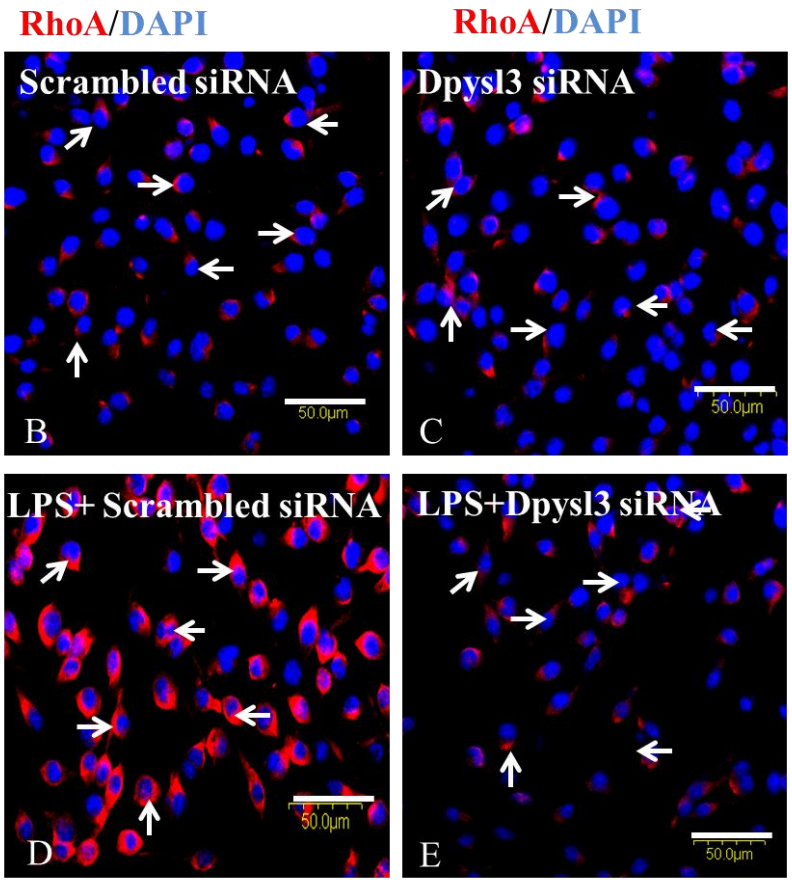
RhoA/DAPI
Scrambled siRNA
B
50.0μm
RhoA/DAPI
Dpysl3 siRNA
C
50.0μm
LPS+ Scrambled siRNA
D
50.0μm
LPS+Dpysl3 siRNA
E
50.0μm

Fig.19

F

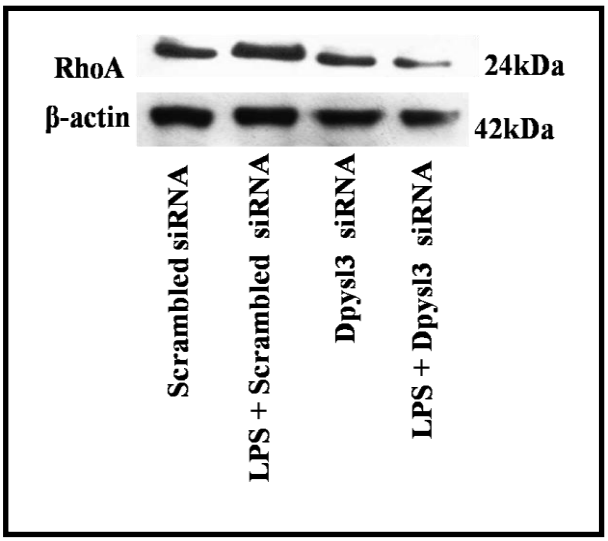
RhoA
β-actin
24kDa
42kDa
Scrambled siRNA
LPS + Scrambled siRNA
Dpysl3 siRNA
LPS + Dpysl3 siRNA

G

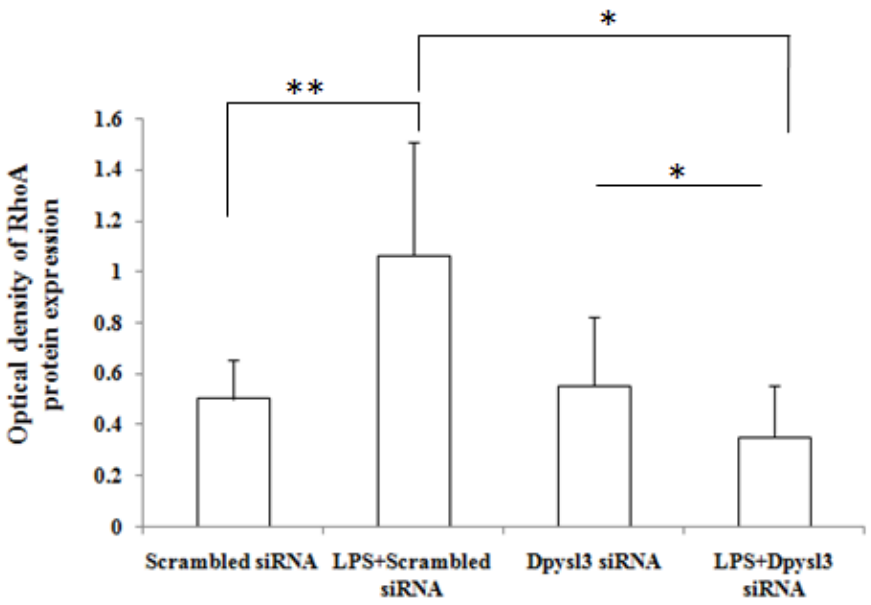
**
*
*
Optical density of RhoA protein expression
1.6
1.4
1.2
1
0.8
0.6
0.4
0.2
0
Scrambled siRNA
LPS+Scrambled siRNA
Dpysl3 siRNA
LPS+Dpysl3 siRNA

Fig. 20. Interaction of Dpysl3 and Rac1 by co-immunoprecipitation in microglial BV-2 cells. Western blot shows the expression of Dpysl3 and Rac1 proteins in BV-2 microglia before and after immunoprecpitation. Dpysl3 and Rac1 proteins were co-immunoprecipitated from the control as well as in 1h LPS treated microglia. Mouse IgG was used as an isotype control. (**Control-Wild type:** Untreated BV-2 cells, **Control- IgG**: IgG pull down from untreated BV-2 cells , **Control- Ab:** Antibody pull down from Untreated BV-2 cells, **LPS- Wild type:**LPS treated BV-2 cells, **LPS- IgG:** IgG pull down from LPS treated BV-2 cells, **LPS –Ab**: Antibody pull down from LPS treated BV-2 cells).

.

Fig.20

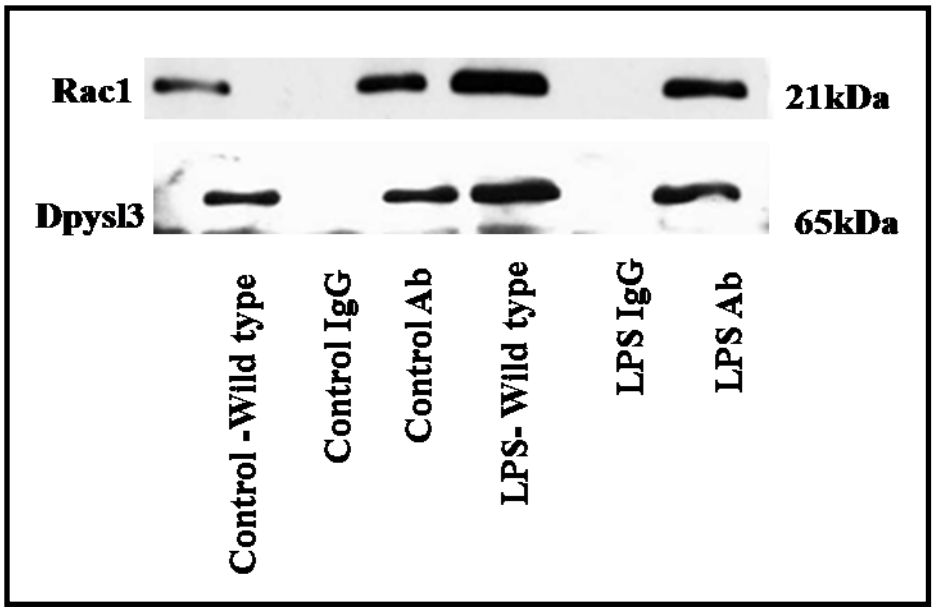
Rac1
21kDa
Dpysl3
65kDa
Control -Wild type
Control IgG
Control Ab
LPS- Wild type
LPS IgG
LPS Ab

Fig. 21.**Effect of Dpysl3 knockdown on the production of Rac1 in activated microglia. A)** RT-PCR analysis shows that knockdown of Dpysl3 inhibits the expression of Rac1 mRNA activated microglia following 1h LPS treatement, compared with that of negative control. Data are presented as mean ± SD (n=4), ***p<0.01*. B-E) Immunofluorescence images show the upregulation of Rac1 expression in BV-2 microglial cells treated with LPS, while the knockdown of Dpysl3 inhibits the LPS-stimulated increase in RhoA expression (red, E), Scale bar: 50μm. F) Representative western blot shows the expression of Rac1 (21kDa) and β-actin (42kDa) proteins in scrambled or Dpysl3 siRNA transfected BV-2 microglial cells. G) Quantitative analysis shows that knockdown of Dpysl3 reduced the protein expression of Rac1 in microglia treated with LPS. Data are presented as mean ± SD (n=6), ***p<0.01;*p<0.05*.

Fig.21

A

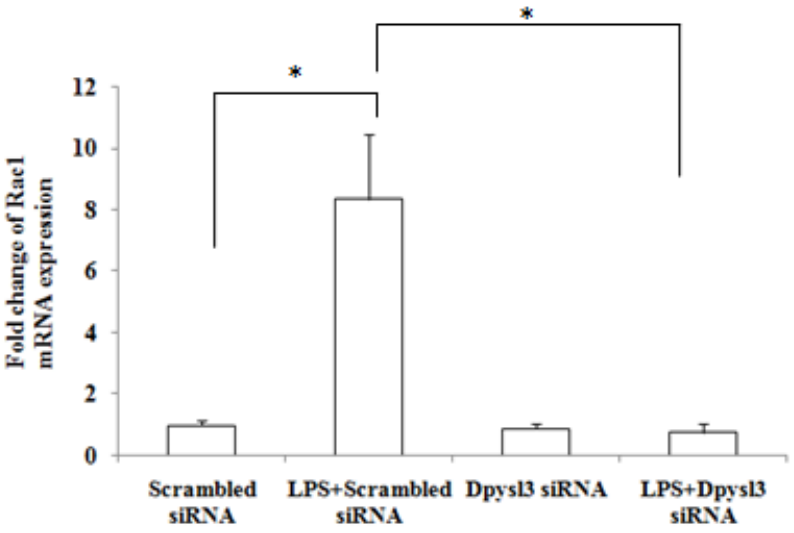
*
*
12
10
8
6
4
2
0
Fold change of Rac1 mRNA expression
Scrambled siRNA
LPS+Scrambled siRNA
Dpysl3 siRNA
LPS+Dpysl3 siRNA

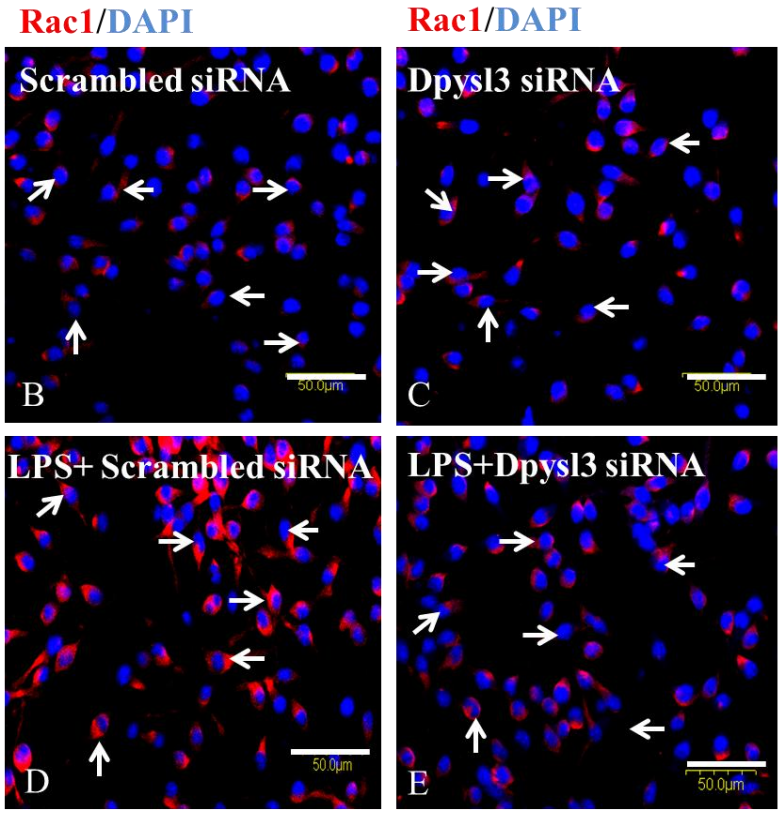
Rac1/DAPI
Rac1/DAPI
Scrambled siRNA
Dpysl3 siRNA
B
C
50.0μm
50.0μm
LPS+ Scrambled siRNA
LPS+Dpysl3 siRNA
D
E
50.0μm
50.0μm

Fig.21

F

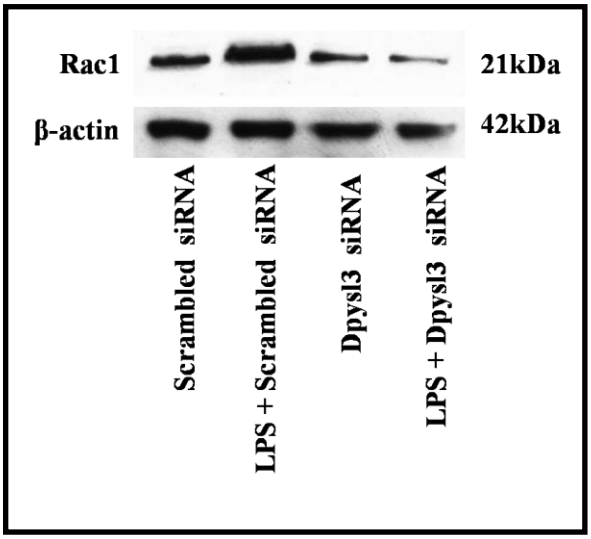
Rac1
21kDa
β-actin
42kDa
Scrambled siRNA
LPS + Scrambled siRNA
Dpysl3 siRNA
LPS + Dpysl3 siRNA

G

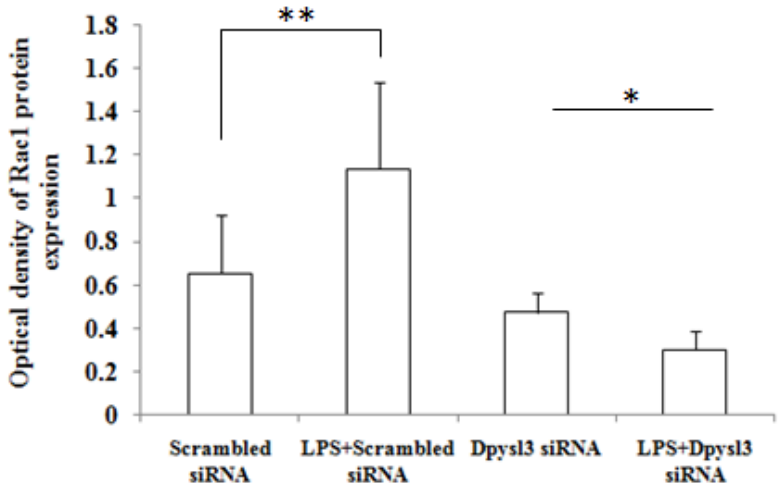
Optical density of Rac1 protein expression
1.8
1.6
1.4
1.2
1
0.8
0.6
0.4
0.2
0
**
*
Scrambled siRNA
LPS+Scrambled siRNA
Dpysl3 siRNA
LPS+Dpysl3 siRNA